Journal of Human Evolution 122 (2018) 38–69

Contents lists available at ScienceDirect

Journal of Human Evolution

journal homepage: www.elsevier.com/locate/jhevol

Evolution of the modern baboon (*Papio hamadryas*): A reassessment of the African Plio-Pleistocene record

Christopher C. Gilbert [a, b, c, d, *], Stephen R. Frost [d, e], Kelsey D. Pugh [b, c], Monya Anderson [e], Eric Delson [b, c, d, f, g, h]

[a] Department of Anthropology, Hunter College of the City University of New York, 695 Park Avenue, New York, NY 10065, USA
[b] PhD Program in Anthropology, Graduate Center of the City University of New York, 365 Fifth Avenue, NY 10016, USA
[c] New York Consortium in Evolutionary Primatology (NYCEP), USA
[d] NYCEP Morphometrics Group, USA
[e] Department of Anthropology, University of Oregon, Eugene, OR 97403-1218, USA
[f] Department of Anthropology, Lehman College of the City University of New York, 250 Bedford Park Boulevard West, New York, NY 10468, USA
[g] Department of Vertebrate Paleontology, American Museum of Natural History, 200 Central Park West, New York, NY 10024, USA
[h] Institut Català de Paleontologia Miquel Crusafont, Universitat Autònoma de Barcelona. Edifici ICTA-ICP, Carrer de les Columnes s/n, Campus de La UAB, Cerdanyola Del Vallès, Barcelona 08193, Spain

ARTICLE INFO

Article history:
Received 31 August 2017
Accepted 24 April 2018
Available online 25 June 2018

Keywords:
Cercopithecoid
Papionin
Crania
Postcrania
Baboons
Plio-pleistocene

ABSTRACT

Baboons (*Papio hamadryas)* are among the most successful extant primates, with a minimum of six distinctive forms throughout Sub-Saharan Africa. However, their presence in the fossil record is unclear. Three early fossil taxa are generally recognized, all from South Africa: *Papio izodi*, *Papio robinsoni* and *Papio angusticeps.* Because of their derived appearance, *P. angusticeps* and *P. robinsoni* have sometimes been considered subspecies of *P. hamadryas* and have been used as biochronological markers for the Plio-Pleistocene hominin sites where they are found.

We reexamined fossil *Papio* forms from across Africa with an emphasis on their distinguishing features and distribution. We find that *P. robinsoni* and *P. angusticeps* are distinct from each other in several cranial features, but overlap extensively in dental size. Contrary to previous assessments, no diagnostic cranio-mandibular material suggests these two forms co-occur, and dental variation at each site is comparable to that within *P. h. ursinus*, suggesting that only one form is present in each case. *P izodi,* however, may co-occur with *P. robinsoni,* or another *Papio* form, at Sterkfontein Member 4.

P izodi appears more primitive than *P. robinsoni* and *P. angusticeps*. *P. robinsoni* is slightly distinct from *P. hamadryas* subspecies in its combination of features while *P. angusticeps* might be included within one of the modern *P. hamadryas* varieties (i.e., *P. h. angusticeps*). No definitive *Papio* fossils are currently documented in eastern Africa until the Middle Pleistocene, pointing to southern Africa as the geographic place of origin for the genus. These results have implications for Plio-Pleistocene biochronology and baboon evolution.

1. Introduction

The savannah baboons of the genus *Papio* are among the most well-known and successful extant primates, with a minimum of six recognizable populations distributed throughout Africa outside of the central forest area, as well as in southern Arabia (Thorington and Groves, 1970; Szalay and Delson, 1979; Jolly, 1993, 2001; Groves, 2001; Frost et al., 2003; Grubb et al., 2003; Fleagle, 2013; see Fig. 1). Despite their evolutionary success and wide distribution across modern African ecological communities, the origins of the genus in the fossil record are not clear. Current molecular and morphological evidence suggests that, among living African papionins, *Papio* is closely related to *Theropithecus*, *Lophocebus*, and *Rungwecebus* (Disotell et al., 1992; Disotell, 1994, 2000; Harris and Disotell, 1998; Fleagle and McGraw, 1999, 2002; Tosi et al., 1999, 2003; Davenport et al., 2006; Gilbert, 2007, 2013; Olson et al., 2008; Burrell et al., 2009; Zinner et al., 2009; Gilbert et al., 2009a, 2011; Roberts et al., 2010), and

* Corresponding author.
E-mail address: cgilbert@hunter.cuny.edu (C.C. Gilbert).

https://doi.org/10.1016/j.jhevol.2018.04.012
0047-2484/

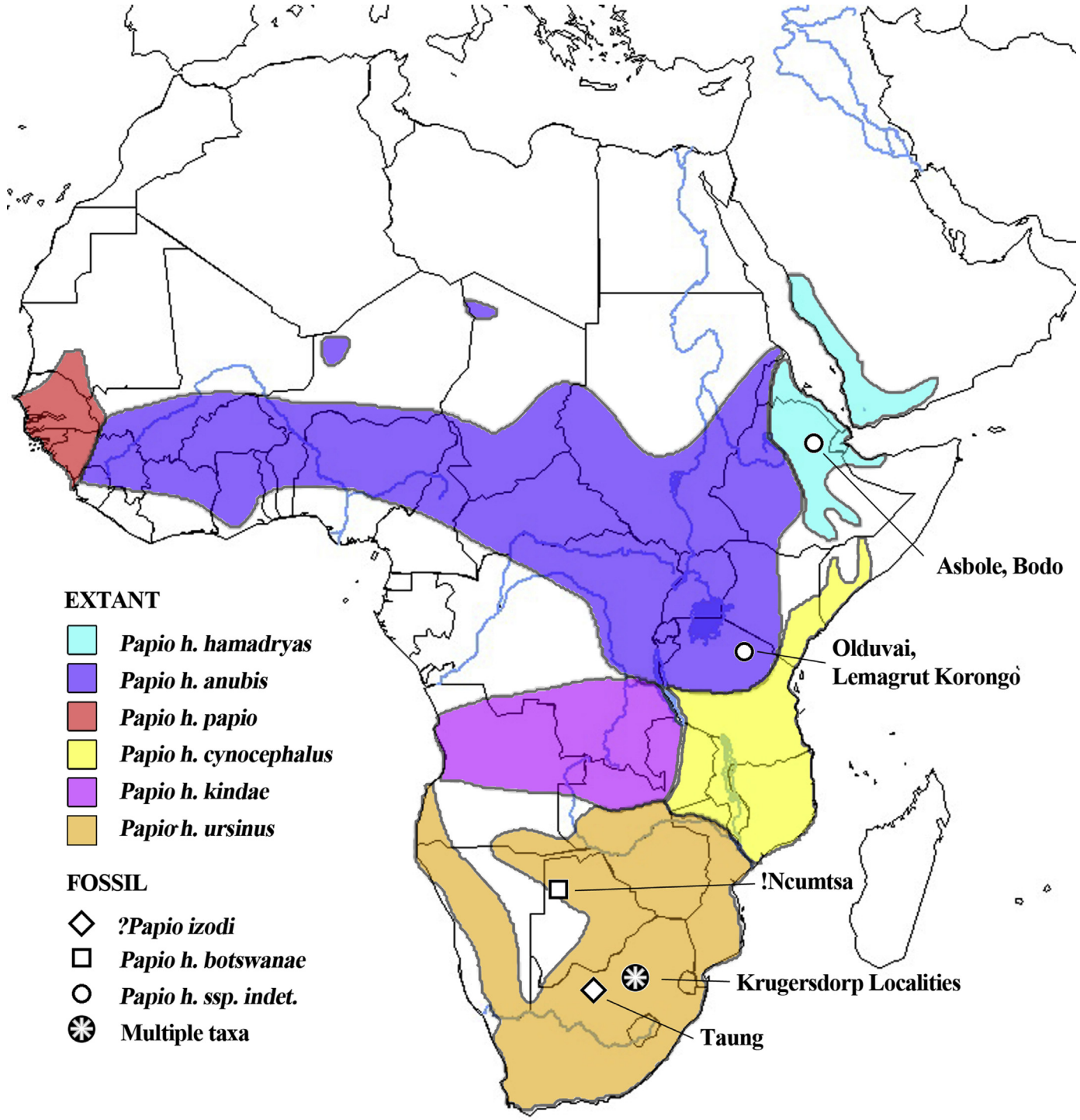

Figure 1. Map of Africa illustrating the geographic distribution of extant and fossil *Papio* populations. Krugersdorp localities include Sterkfontein, Swartkrans, Kromdraai, Bolt's Farm, Cooper's A-D, Gladysvale, Drimolen, Malapa, Haasgat, and Skurweberg.

within this group, the most recent analyses suggest a closer relationship between *Papio* and *Lophocebus,* with *Theropithecus* at the base of this clade (Perelman et al., 2011; Springer et al., 2012; Guevara and Steiper, 2014; Pugh and Gilbert, in press). The position of *Rungwecebus* is controversial, being most recently reconstructed as the sister taxon to *Papio* in molecular studies (Davenport et al., 2006; Olson et al., 2008; Burrell et al., 2009; Zinner et al., 2009; Roberts et al., 2010), yet most similar to *Lophocebus* in morphological comparisons (Jones et al., 2005; Davenport et al., 2006; Singleton, 2009; Singleton et al., 2010; Gilbert et al., 2011a; Gilbert, 2013). Thus, the combination of these data sources implies a close relationship among these three taxa pending additional data.

While *Rungwecebus* is unknown in the fossil record, the earliest specimens of *Theropithecus* are dated to at least 4.2 Ma (Frost, 2001a; Harris et al., 2003; Jablonski et al., 2008; Frost et al., 2014; Frost et al., in revision; Gilbert and Frost, personal obs.). Undoubted *Lophocebus* specimens first appear in the fossil record

by approximately 2.0 Ma (Leakey and Leakey, 1976; Frost, 2001a; Jablonski et al., 2008; Gilbert, 2013) and possibly as early as 3.5 Ma (Harrison and Harris, 1996). Therefore, fossil specimens attributable to the genus *Papio* should also be present in the fossil record by at least 2.0 Ma, and potentially well into the Pliocene.

In fact, numerous taxa in the African Plio-Pleistocene have been assigned to the genus *Papio* over the last century, but many of them have proven to be more properly assigned to other genera such as *Parapapio*, *Theropithecus*, *Soromandrillus* and *Gorgopithecus* (see Szalay and Delson, 1979; Eck and Jablonski, 1984, 1987; Delson and Dean, 1993; Jablonski, 2002; Jablonski and Frost, 2010; Gilbert, 2013; Gilbert et al., 2016a). Currently, there are at least four named and widely recognized fossil *Papio* taxa (*Papio izodi*, *Papio [hamadryas] angusticeps*, *Papio [hamadryas] robinsoni*, and *Papio hamadryas botswanae*) from the African Plio-Pleistocene record, with other specimens placed in *Papio* sp. indet. that may represent one or more additional taxa. In this paper, we review the complicated and confused taxonomy and fossil record of *Papio* with particular focus on South Africa and, based on updated morphological analyses, propose a revised taxonomy of the genus.

1.1. *History of* Papio *fossil record*

Baboons are distinct and iconic primates that have been familiar to humans for centuries (Morris, 2013). Perhaps because of their distinctiveness, large, generalized monkeys with long rostra have been referred to as “baboons” for much of the last 150 years (e.g., see Szalay and Delson, 1979; Jablonski, 2002; and references therein). With increasing resolution of papionin systematics, it is now clear that there are several large-bodied, long-faced papionin genera. Their taxonomy has a complex history with interpretations varying from author to author (e.g., Haughton, 1925; Remane, 1925; Gear, 1926; Broom, 1936, 1940; Dietrich, 1942; Freedman, 1957; Jolly, 1965, 1967; Hill, 1967; Leakey, 1969; Szalay and Delson, 1979; Iwamoto, 1982; Delson, 1984; Eck and Jablonski, 1984, 1987; McKee, 1993; Delson and Dean, 1993; Frost, 2001a, 2007a; 2007b; Frost and Delson, 2002; Jablonski et al., 2008; Williams et al., 2012; Gilbert, 2013).

As there is little agreement on the taxonomy of extant *Papio* populations (see Thorington and Groves, 1970; Jolly and Brett, 1973; Szalay and Delson, 1979; Jolly, 1993, 2003; Groves, 2001; Grubb et al., 2003; Frost et al., 2003; Zinner et al., 2013), a brief explanation of the taxonomy used in this paper is warranted. Even though there is a significant amount of morphological and behavioral variation within and between the various populations of extant *Papio*, for the purposes of this paper we favor recognizing the six commonly recognized populations at the subspecies level within a single species, *Papio hamadryas* (i.e., *P. h. ursinus, P. h. cynocephalus, P. h. kindae, P. h. anubis, P. h. hamadryas, P. h. papio*). Given the clinal pattern of cranial variation (e.g., Frost et al., 2003), the clinal pattern of mtDNA variation (e.g., Newman et al., 2004; Burrell, 2008; Zinner et al., 2009, 2011), and the extensive hybridization between populations observed in the wild (e.g., Jolly et al., 2011), using the Biological Species Concept (BSC) it seems that a single species is warranted. Furthermore, there is little doubt that many of the extant subspecies display an overall level of craniodental similarity that would be difficult to distinguish at the species level in the fossil record (e.g., Jolly, 1993). Most relevant for the current discussion, from a paleontological view, this taxonomic scheme also has the advantage of easily distinguishing between modern forms of *Papio* (i.e., *P. hamadryas* subspecies) and more distinctive fossil forms which can be recognized more readily at the species level.

On the other hand, at least two of us (CCG, KDP) prefer the Phylogenetic Species Concept (PSC), which is more widely accepted in current primate studies (e.g., see Groves, 2001, 2014; Fleagle, 2014; Jolly, 2014; Louis and Lei, 2014; Rylands and Mittermeier, 2014; Silcox, 2014; Tattersall, 2014; Yoder, 2014; Zimmerman and Radespiel, 2014; Zinner and Roos, 2014) and has the advantage of relying on consistent phenotypic (in this case, morphological) differences rather than reproductive isolation as a criterion of separation. Given the widespread documentation of hybridization among commonly recognized primate species (e.g., see Tung and Barreiro, 2017 and references therein), some even representing different genera (most relevant in this case, *Papio* x *Rungwecebus* and *Papio* x *Theropithecus*; see Davenport et al., 2006; Olson et al., 2008; Burrell et al., 2009; Zinner et al., 2009, 2018; Roberts et al., 2010; Tung and Barreiro, 2017), it seems more and more difficult to rely on reproductive isolation as the defining characteristic of a species or evolutionary coherent lineage/population. More directly relevant from a paleontological perspective, it is impossible to know whether one fossil population was reproductively isolated from another, making any paleontologist reliant on morphological features to diagnose species anyway. Thus, for those who prefer the PSC in the study of *Papio* taxonomy, each extant baboon population is recognized as its own distinct species: *Papio anubis, Papio cynocephalus, P. hamadryas, Papio kindae, P. papio*, and *Papio ursinus*. In the fossil record, under the PSC scheme, a fossil baboon that is considered a part of the modern radiation would still be ranked at the species level, while under the BSC scheme it would simply be another subspecies of *P. hamadryas*.

A brief breakdown of the morphological features and current distribution of named fossil *Papio* species is as follows (see also Figs. 2–4):

1.1.1. *Papio izodi*

P. izodi was first named by Gear (1926) based on material from Taung. For the next three decades, this and subsequent material from Taung was variously assigned to *Papio* and *Parapapio* and for a short time even synonymized with *Parapapio antiquus* (Broom, 1936, 1940). Freedman (1957, 1963, 1965) reviewed the material from Taung and allocated all specimens with a perceived anteorbital drop to *P. izodi*, an approach that has generally been followed ever since. A more detailed discussion of *P. izodi* early taxonomic history is given by Freedman (1957). Currently, *P. izodi* is recognized from the Plio-Pleistocene sites of Taung (e.g., Gear, 1926; Freedman, 1957; Szalay and Delson, 1979; Delson, 1984, 1988; Gilbert, 2013) and Sterkfontein Members 2 and 4 (e.g., Eisenhart, 1974; Delson, 1984, 1988; McKee, 1993; Pickering et al., 2004; Heaton, 2006; Gilbert, 2013).

Relative to other *Papio* taxa, *P. izodi* is small-to-medium sized and displays molars and orbits that are large relative to cranial size, a relatively short (anteroposteriorly) and broad snout, a relatively dorso-ventrally short neurocranium, and a relatively dorso-ventrally short malar region (Figs. 2–4; Freedman, 1957; Delson, 1988; McKee, 1993; Gilbert, 2013; Gilbert et al., 2015). In addition, this taxon displays shallow maxillary fossae, a variable anteorbital drop, weak to absent mandibular corpus fossae, and weak development of the maxillary ridges (in males and females) compared to most other *Papio* taxa (Figs. 2–4; Freedman, 1957; McKee, 1993; Gilbert, 2013; Gilbert et al., 2015). Similar to other *Papio* species, *P. izodi* specimens typically exhibit a prominent glabella, pinched temporal lines, downturned nuchal lines, a moderate supraorbital torus, and a moderate ophryonic groove or post-glabellar depression (Figs. 2–4; Freedman, 1957; Gilbert, 2007, 2013).

In a recent phylogenetic analysis, Gilbert (2013) hypothesized that *P. izodi* may in fact be a stem African papionin, largely based on the distinctive and primitive characters listed above (e.g., shallow facial fossae, weak development of maxillary ridges in males, weak to absent mandibular corpus fossae, and variable anteorbital drop). Therefore, *P. izodi* may warrant generic separation from the other

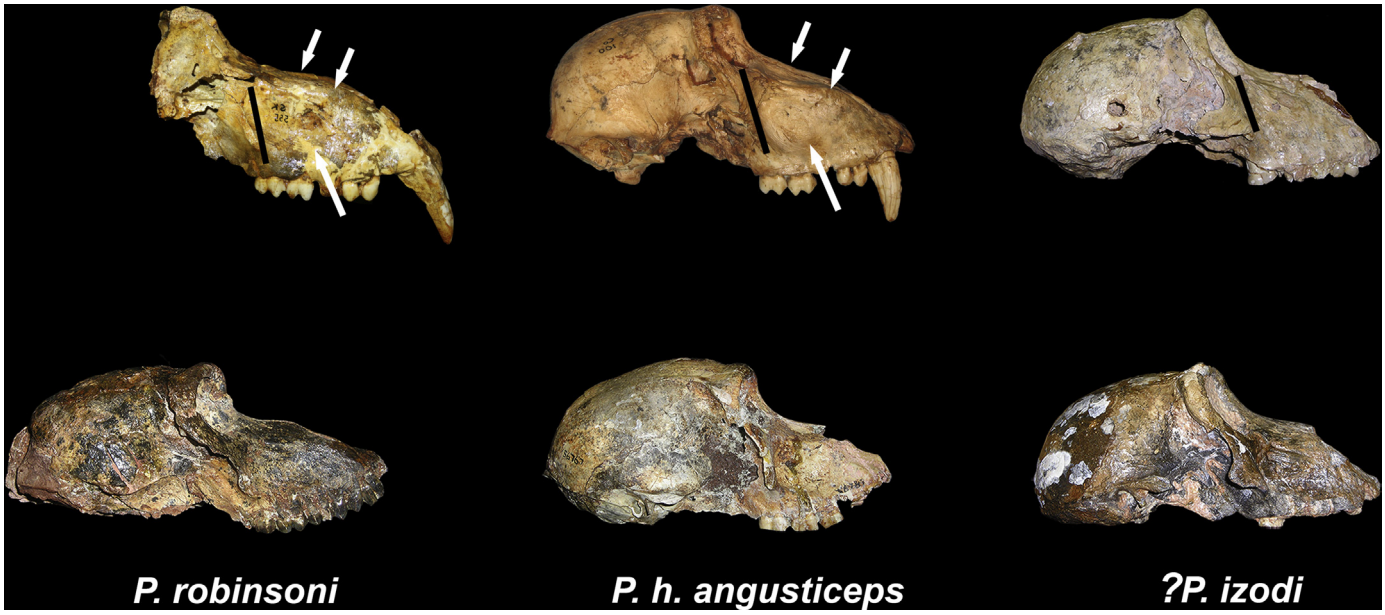

Figure 2. Major morphological differences between specimens of *P. robinsoni* (left), *P. h. angusticeps* (center), and *?P. izodi* (right) in lateral view. Top row = male specimens, bottom row = female specimens. *P. robinsoni* males represented by SK 555; *P. h. angusticeps* males represented by CO 100; and *?P. izodi* represented by SWP Uncatalogued Cranium from Member 2. *P. robinsoni* females represented by UCMP 56797; *P. h. angusticeps* represented by UCMP 56767; and *?P. izodi* represented by TP-10 (ex-UCMP 56605). Specimens are approximately to scale. Differences between taxa are most obvious among male specimens. In males, note the difference in the height of the nasals above the maxillary ridges (white arrows), the development of the maxillary ridges and of the maxillary fossae (white arrows), and relative malar height (black bars). In contrast to *P. robinsoni* and *P. h. angusticeps*, *?P. izodi* males do not possess definitive maxillary ridges or maxillary fossae. Many of the same differences are also seen to a lesser extent among the female specimens.

Papio taxa, and we formally recognize this uncertainty from this point forward with the taxonomic convention *?P. izodi*.

1.1.2. *Papio robinsoni* Freedman (1957) named a large series of partial crania, jaws and more fragmentary material from Swartkrans, Swartkrans II, Cooper's, Kromdraai, Bolt's Farm, Gladysvale and Skurweberg as a new species *Papio robinsoni*. This taxon has been described from a number of sites including Swartkrans Members 1-3, Swartkrans II, Skurweberg, Cooper's A, Kromdraai A, Bolt's Farm, Drimolen Main Quarry, and possibly Sterkfontein Member 4 (Freedman, 1957; Eisenhart, 1974; Szalay and Delson, 1979; Delson, 1984, 1988; McKee et al., 1995; Keyser, 2000; Adams et al., 2016). Dentally and cranially, *P. robinsoni* is most similar in size to modern *P. hamadryas ursinus* and *P. hamadryas anubis*, but Freedman (1957) differentiated *P. robinsoni* from modern *P. hamadryas* ssp. by features such as a more flattened muzzle dorsum with nasals lying inferior to the maxillary ridges in lateral view, a high frequency of the maxillae meeting in the midline and covering the nasal bones in males, a relatively shorter snout, relatively large P^4s, more rounded maxillary ridges and definitive, but shallow-moderate depth (i.e., weaker) facial fossae (Figs. 2–4). Like other *Papio* taxa, *P. robinsoni* exhibits a definitive anteorbital drop, flattened muzzle dorsum, a prominent glabellar/supraorbital region, pinched temporal lines, downturned nuchal lines, and an ophryonic groove or depression behind the orbits (Figs. 2–4). Delson (Szalay and Delson, 1979, 1984, 1988) has argued that the distinctive features displayed by *P. robinsoni* can be found within the large amount of variation encompassing the extant *Papio hamadryas* subspecies, albeit in different frequencies, and on this basis preferred to recognize the taxon as *P. h. robinsoni*, an arrangement followed by Frost (2007a,b), Williams et al. (2012), and Gilbert (2013). In this paper, we use the *P. robinsoni* convention, and evaluate its morphological distinctiveness from *P. hamadryas* in the analyses below.

1.1.3. *Papio angusticeps* On the basis of a partial cranium and other material from Kromdraai A, Broom (1940) originally described this series as a new species of *Parapapio*. Freedman (1957) transferred the type material along with additional specimens from Kromdraai, Cooper's, and Minaar's Cave to the genus *Papio* based on the clear presence of an anteorbital drop and muzzle morphology. While all subsequent authors have agreed that this material belongs in the genus *Papio* there has been debate about its specific distinction from *?P. izodi* (Szalay and Delson, 1979; Jablonski, 2002; Heaton, 2006; Gilbert, 2008; Jablonski and Frost, 2010). Others have noted shared similarities between the *P. angusticeps* material and modern *P. hamadryas*, especially the small-bodied *P. h. kindae,* and therefore separated it from *?P. izodi* (Delson, 1984, 1988; McKee, 1993; Williams et al., 2012; Gilbert, 2013; Gilbert et al., 2015). In fact, some have recognized it as a subspecies of *P. hamadryas* (implied by Delson, 1984, 1988; and Frost, 2007a,b; first formalized by Williams et al., 2012; Gilbert et al., 2015), a decision we follow here from this point forward. For a more detailed discussion of the early taxonomic history of *P. h. angusticeps*, see Freedman (1957).

P. h. angusticeps (Broom, 1940) has been recognized at Kromdraai A, Kromdraai B, Cooper's A, Haasgat, Gladysvale, and Malapa (e.g., Freedman, 1957; Szalay and Delson, 1979; Delson, 1984, 1988; McKee and Keyser, 1994; McKee et al., 1995; Gilbert, 2013; Gilbert et al., 2015). As discussed above, in most respects, *P. h. angusticeps* is extremely similar to modern *P. hamadryas* sspp., possessing a definitive anteorbital drop, moderate-to-deep maxillary fossae, maxillary ridges in males and females, a long and narrow muzzle, a relatively tall malar region, a prominent glabella and supraorbital region, pinched temporal lines, downturned nuchal lines, and a moderate ophryonic groove/post-glabellar depression (Figs. 2–4; Freedman, 1957; Delson, 1984, 1988; McKee, 1993; Gilbert, 2013; Gilbert et al., 2015). Freedman (1957) suggested that it possesses weaker maxillary ridges than extant *P. hamadryas*, but we disagree.

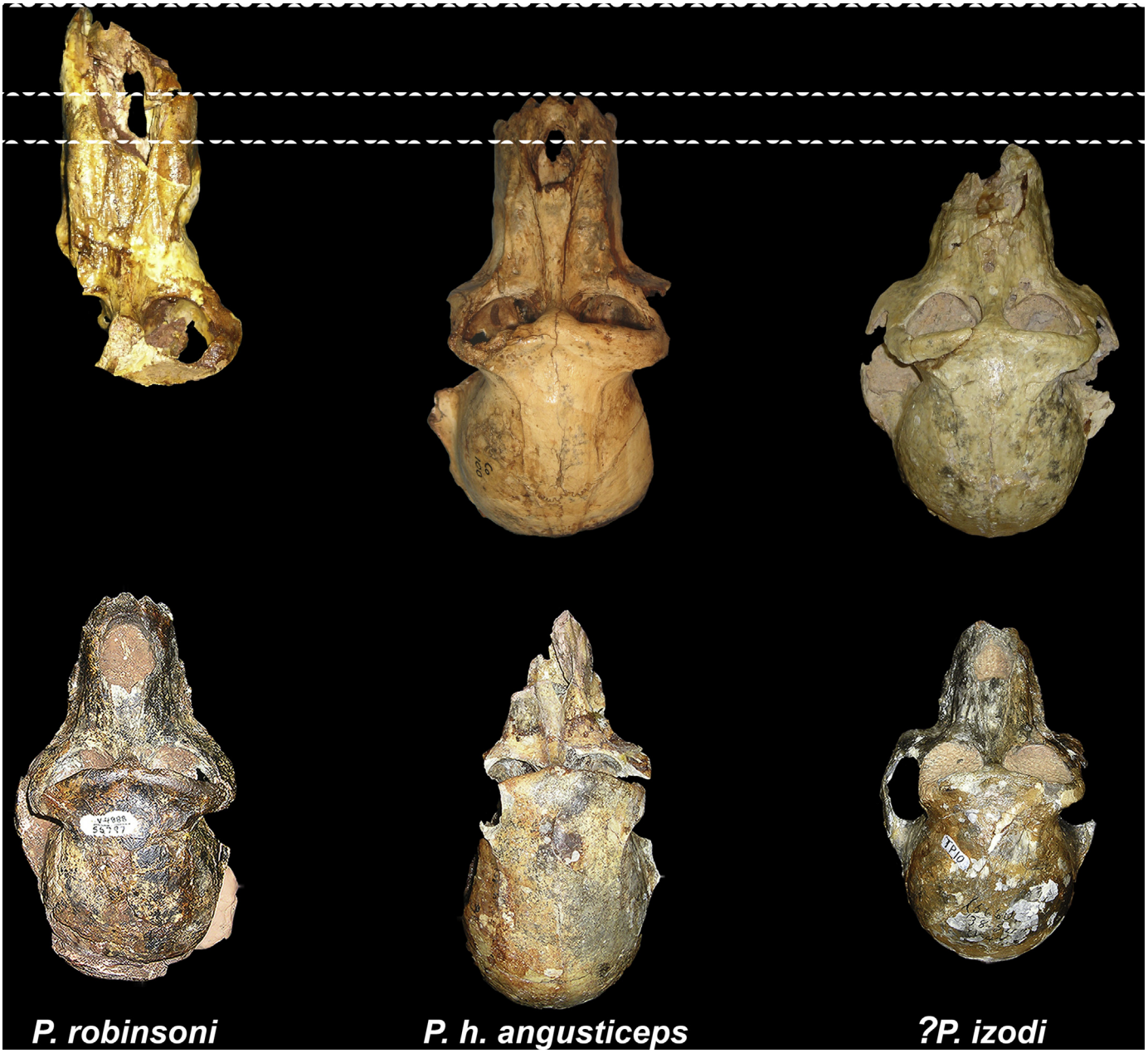

Figure 3. Major morphological differences between specimens of *P. robinsoni* (left), *P. h. angusticeps* (center), and *?P. izodi* (right) in dorsal view. Top row = male specimens, bottom row = female specimens. *P. robinsoni* males represented by SK 555; *P. h. angusticeps* males represented by CO 100; and *?P. izodi* represented by SWP Uncatalogued Cranium from Member 2. *P. robinsoni* females represented by UCMP 56797; *P. h. angusticeps* represented by UCMP 56767; and *?P. izodi* represented by TP-10 (ex-UCMP 56605). Specimens are approximately to scale. Differences between taxa are most obvious among male specimens. In males, note the difference in the relative breadth and length of the snout (length from orbitale inferior to [estimated] prosthion highlighted for each species with dotted lines). *?P. izodi* males have relatively shorter and broader snouts compared to *P. robinsoni* and *P. h. angusticeps*. Many of the same differences are also seen to a lesser extent among the female specimens.

1.1.4. *Papio spelaeus* This species was based on a single large male cranium encrusted in calcite matrix of unknown provenance first described by Broom (1936). Subsequent authors (Freedman, 1957; Szalay and Delson, 1979) have considered it to be of Holocene or at least nearly Holocene age and recognized its similarity to modern chacma baboons. We also recognize it as a junior synonym of *P. hamadryas ursinus*, and it will not be considered further here.

1.1.5. *Papio hamadryas botswanae* *P. h. botswanae* is currently known from a single cranium recovered from a Middle Pleistocene cave system in the !Ncumtsa (Koanaka) Hills, Botswana (Williams et al., 2012). In cranio-dental size it is smaller than most *P. h. ursinus* and *P. h. anubis* males, similar to those of *P. h. hamadryas* and *P. h. papio,* but larger than *P. h. kindae.* While within the range of cranial shape variation of extant *P. hamadryas* populations, 3D cranial geometric morphometrics demonstrated the uniqueness of this specimen relative to the extant *P. hamadryas* subspecies, with *P. h. botswanae* displaying an extremely prominent supraorbital region, wide neurocranium and a relatively short and broad muzzle for a baboon of its size. Its muzzle is moderately klinorynch, but less so than that of *P. h. ursinus*, the modern subspecies with the most klinorynch rostra (Williams et al., 2012).

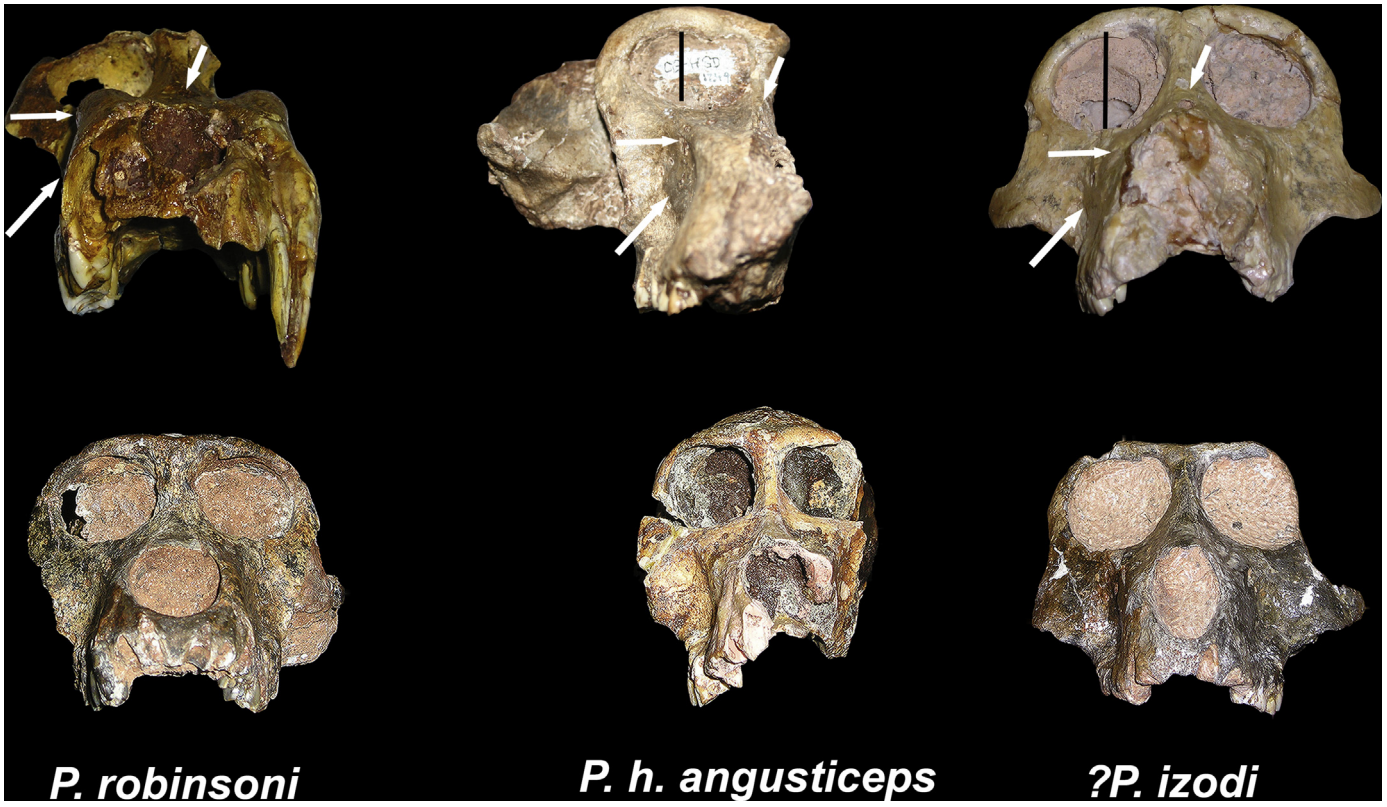

Figure 4. Major morphological differences between specimens of *P. robinsoni* (left), *P. h. angusticeps* (center), and *?P. izodi* (right) in frontal view. Top row = male specimens, bottom row = female specimens. *P. robinsoni* males represented by SK 555; *P. h. angusticeps* males represented by HGD 1249; and *?P. izodi* represented by SWP Uncatalogued Cranium from Member 2. *P. robinsoni* females represented by UCMP 56797; *P. h. angusticeps* represented by UCMP 56767; and *?P. izodi* represented by TP-10 (ex-UCMP 56605). Specimens are approximately to scale. Differences between taxa are most obvious among male specimens. In males, note the differences in orbit height/size (white/black bars), and in maxillary fossae development, maxillary ridge development, and height of the nasals relative to the maxillary ridges (white arrows). The orbits of *?P. izodi* are relatively larger than seen in *P. robinsoni* and *P. h. angusticeps*. As seen in lateral view and, again, in contrast to *P. robinsoni* and *P. h. angusticeps*, *?P. izodi* males do not possess definitive maxillary ridges or maxillary fossae. Many of the same differences are also seen to a lesser extent among the female specimens.

1.2. Goals of this study

The three fossil taxa from South Africa discussed above have been argued to be early members of the genus *Papio*. However, the morphological diagnoses of these taxa, summarized above, have not been reassessed in a number of years despite great changes to our understanding of papionin phylogeny and evolution (see above). Thus, it is possible that an updated analysis of these fossil *Papio* populations may help refine and revise our understanding of baboon evolution and taxonomy. For example, as alluded to above, Gilbert (2013) recently suggested that *?P. izodi* from Taung and Sterkfontein retains many plesiomorphic features that may require taxonomic reassignment to a genus other than *Papio*. Both *P. robinsoni* and *P. h. angusticeps,* on the other hand, have at times been considered as subspecies of the extant species (Szalay and Delson, 1979; Delson, 1988; Frost, 2007a; Gilbert et al., 2015), and both were thus claimed to represent the first appearance of the modern form. Because of their derived appearance, *P. h. angusticeps* and *P. robinsoni* have further been used as important biochronological markers for the Plio-Pleistocene sites at which they are found, and they have been suggested to co-occur at Kromdraai A and B and Cooper's A (Freedman, 1957; Delson, 1984, 1988; McKee et al., 1995; Heaton, 2006; Jablonski and Frost, 2010).

In order to test these taxonomic and distributional hypotheses, a broader and more comprehensive review of extant and fossil *Papio* material is needed. Our goals are to 1) clarify which fossil populations can be referred to any specific named taxa; 2) offer a revised morphological diagnosis of fossil *Papio* species and the genus *Papio* based on our updated hypodigms; and 3) review the resulting distribution of fossil *Papio* species and populations in the Plio-Pleistocene fossil record. This has implications for our understanding of the origins and evolution of the genus, its first appearance in the fossil record, its biogeography, its taxonomy, and the biochronology of the sites where it occurs.

2. Materials and methods

In 2012–2016, we reviewed all major Plio-Pleistocene collections containing African cercopithecoids with the explicit goal of refining the taxonomy at each site and, ultimately, providing an updated biochronological analysis relative to the landmark studies of Delson (1984, 1988) on the basis of our results. Fossil specimens examined during this study (and in some cases previously by Delson) were housed at: the Ditsong National Museum, Pretoria (TMP, formerly Transvaal Museum); the Council for Geosciences, Pretoria (CGS); the Bernard Price Institute, Johannesburg (BPI); the University of the Witswatersrand Anatomy Department, Johannesburg (UW-AD); the Evolutionary Studies Institute, Johannesburg (ESI); the Iziko South Africa Museum, Cape Town (SAM); the National Museum of Tanzania, Dar es Salaam (NMT); the National Museums of Kenya, Nairobi (KNM); the National Museum of Ethiopia, Addis Ababa (NME); the Natural History Museum, London (NHM-UK); the Museum für Naturkunde, Berlin (MB); the Bayerische Staatssammlung für Paläontologie und Geologie, München, Germany (BSPG [formerly BSM]); and the University of California Museum of Paleontology, Berkeley (UCMP).

Thus, we examined nearly all of the fossil *Papio* material that was available at the time, employing typical comparative morphological methods. Specimens were qualitatively and quantitatively evaluated for key morphological features (Freedman, 1957; Delson, 1975, 1988; Szalay and Delson, 1979; Frost, 2001a,b; Fleagle and McGraw, 2002; Gilbert, 2007, 2013). Digital calipers were used to collect standard craniometric measurements, and digital photographs were taken of the more complete specimens whenever possible. Qualitative characters were scored according to the criteria described in Gilbert (2013). Comparative measurements and reference qualitative comparisons with extant taxa were taken from specimens housed at the American Museum of Natural History, New York (AMNH) as well as from Frost (2001a), Gilbert (2013), and the PRIMO online database (http://primo.nycep.org). For the full list of samples, characters, and measurements used, see Tables 1–7 and the references therein.

Univariate and multivariate statistical analyses were performed in PAST v3.14 (Hammer et al., 2001) and SPSS v23.0.0.2 (IBM Corp.). To investigate ranges of variation in fossil *Papio* populations across fossil sites, we compared our dental measurements in the form of premolar and molar area boxplots from the upper and lower dentitions of the fossil specimens to a modest sample of a living *P. hamadryas* subspecies, *P. h. ursinus* ($n = 120–152$ depending on tooth position; see Tables 1 and 2 for summary information and Supplementary Online Material [SOM] Tables S1–S4 for a complete list of extant and fossil *Papio* specimens and measurements). *P. h. ursinus* is an appropriate comparison in this case because it is similar in size to both *P. h. angusticeps* and *P. robinsoni* (slightly larger than *P. angusticeps*, very similar in dental size to *P. robinsoni*), thereby controlling for any significant size effects, and it is found in the same geographical region as the fossil populations in question, thereby controlling for any strong latitudinal or biogeographical effects. We reasoned that if the ranges found in the fossil samples were similar to, or less than, that observed in a modern subspecies, then we have no basis for definitively recognizing multiple *Papio* taxa in the absence of more diagnostic craniodental material. We also assessed the range of variation found across fossil and extant taxa using our new classification system (i.e., *P. robinsoni*, *P. h. angusticeps*, compared to *P. h. ursinus*). If the range of variation in the fossil taxa is again comparable to that observed in *P. h. ursinus*, this would suggest that our revised classification system does not introduce excessive variation despite time-averaging and including material across multiple sites in each fossil taxon. In addition to univariate comparisons, multivariate analyses were performed in relation to the 3D geometric morphometric analysis described in more detail below.

2.1. Geometric morphometrics

To quantitatively assess the overall cranial shape of fossil *Papio* taxa we collected 3D landmarks following the protocol of Frost et al. (2003) on 24 relatively complete fossil crania (Table 3). These were superimposed with a sample of 778 extant papionins from PRIMO (Table 4) in Morpheus (Slice, 2013) by Generalized Procrustes Analysis (GPA) to remove variation due to size, position, and orientation (Rohlf and Slice, 1990). Centroid size, the square root of the sum of the squared distance of each landmark to the centroid, was used as a measure of size (Bookstein, 1991). In order to minimize the effects of taphonomic deformation and impute bilateral landmarks missing from one side, all specimens were mirrored and averaged (Gunz et al., 2009).

Principal Components Analysis (PCA) was used as a data reduction and ordination technique to explore the distribution of specimens in shape space (Neff and Marcus, 1980; Manly, 1994). To maximize the number of specimens, remaining missing landmarks were imputed by species-sex means where available. For the PCA, grand means were used to fill in any remaining landmarks. Previous studies of papionin cranial variation have demonstrated that allometry accounts for the largest share of total variance, and most of the shape differences were related to sex (e.g., Singleton, 2002; Frost et al., 2003). Therefore, following Frost et al. (2003) and Williams et al. (2012), we regressed GPA aligned coordinates against the natural log of centroid size and sex to produce adjusted landmark configurations (Frost et al., 2003). Discriminant function analysis on genera was performed on the GPA aligned coordinates with the extant papionins used as the model and fossil papionin specimens as unknowns. Cross-validation, where each known specimen was individually removed from calculation of the discriminant functions and then reclassified, was used to evaluate the reliability of the function.

2.2. Phylogenetic analysis

In addition to quantitative and qualitative craniometric comparisons, a 362 character phylogenetic analysis using parsimony, including 36 extant and fossil cercopithecoid species, was conducted in PAUP* 4.0b10 (Swofford, 2003). Relative to the previous analyses of Gilbert and colleagues (Gilbert and Rossie, 2007; Gilbert et al., 2009a, 2016a; Gilbert, 2013), the current analysis is distinct in that it considers extant species rather than genera as operational taxonomic units (OTUs), includes additional extant and fossil data from PRIMO and Frost (2001a), and includes the fossil taxon *P. robinsoni*. For full sample sizes by species, see Tables 5 and 6. In addition to the 318 craniodental characters listed in Gilbert (2013), 44 postcranial characters (22 for each sex) previously noted to be phylogenetically informative were also added to the current matrix (Table 7; see also Gilbert et al., 2016a, 2016b). The matrix used in this study is provided as a nexus file in the SOM.

Three separate analyses were performed. The first analysis, here termed "Morphology-only", constrained only the outgroup taxa (see below), thereby allowing all ingroup taxa to group freely. The second analysis, here termed "Molecular backbone *P/L/R*", incorporated the results of molecular studies, which consistently suggest a *Cercocebus/Mandrillus* (*C/M*) and *Papio/Lophocebus/Rungwecebus/Theropithecus* (*P/L/R/T*) clade among extant African papionin taxa. Within the *P/L/R/T* clade, recent evidence suggests a closer relationship among *P/L/R* (see Introduction). Therefore, we imposed three molecular backbone/scaffold constraints within the ingroup at the genus level, to construct a tree consistent with these groupings, i.e., ((*C,M*),(*T,*(*P,L,R*))). Ingroup fossil taxa and extant species within genera were then allowed to float freely among these constraints. The third analysis, "Molecular backbone *P/R*", differs from "Molecular backbone *P/L/R*" in that only a sister relationship between *Papio* and *Rungwecebus* is also enforced within *P/L/R/T*, as suggested by all nuclear DNA analyses including the kipunji (i.e., ((*C,M*),(*T,L,*(*P,R*)))). Again, ingroup fossil taxa and extant species within each genus were allowed to float freely among these constraints. In all analyses, a 10,000 replication, random addition sequence heuristic search was employed with *Victoriapithecus*, *Allenopithecus*, *Parapapio lothagamensis*, and *Macaca* constrained as successive outgroups to find the most parsimonious trees (MPTs). For clade support, a 1000 replication bootstrap procedure with replacement was conducted.

3. Results

3.1. Review of South African fossil Papio by site

Here we review the distribution of fossil *Papio* specimens at the main South African sites, following the listing of sites in Table 8 as

Table 1
Summary statistics for the upper dentition of extant and fossil Plio-Pleistocene *Papio* species in South Africa.

Taxon	P^4 BL	P^4 MD	M^1 MBL	M^1 DBL	M^1 MD	M^2 MBL	M^2 DBL	M^2 MD	M^3 MBL	M^3 DBL	M^3 MD
?Papio izodi	8.3 *n* = 10 (7.2–9.5)	6.4 *n* = 12 (5.0–7.2)	9.6 *n* = 9 (7.6–10.6)	9.2 *n* = 8 (8.8–9.9)	9.6 *n* = 13 (8,2–10.7)	11.3 *n* = 12 (9.8–12.5)	10.4 *n* = 13 (9.1–11.4)	11.6 *n* = 15 (10.8–12.9)	11.4 *n* = 11 (9.9–12.3)	9.9 *n* = 10 (8.7–10.7)	11.4 *n* = 12 (10.5–12.8)
Papio hamadryas angusticeps	8.2 *n* = 23 (6.7–9.1)	7.1 *n* = 25 (6.1–8.3)	9.5 *n* = 27 (7.4–11.0)	8.6 *n* = 28 (7.3–10.2)	10.3 *n* = 29 (8.0–12.3)	11.2 *n* = 27 (9.4–12.9)	10.0 *n* = 28 (7.8–11.6)	12.3 *n* = 30 (11.0–14.4)	11.1 *n* = 24 (8.4–12.8)	9.1 *n* = 24 (6.7–11.2)	12.2 *n* = 26 (10.0–14.4)
Papio robinsoni	9.4 *n* = 25 (8.3–10.9)	7.8 *n* = 26 (6.2–9.4)	10.5 *n* = 33 (9.0–12.1)	9.4 *n* = 29 (7.9–10.9)	10.9 *n* = 32 (8.8–13.4)	11.9 *n* = 41 (10.0–13.7)	10.8 *n* = 38 (8.9–13.2)	13.2 *n* = 42 (10.6–15.7)	12.1 *n* = 30 (10.2–14.7)	9.8 *n* = 29 (7.7–11.9)	13.2 *n* = 28 (11.1–15.5)
Papio cf. *robinsoni* Swartkrans Member 2	9.1 *n* = 1 (9.1–9.1)	7.5 *n* = 1 (7.5–7.5)	10.1 *n* = 1 (10.1–10.1)	9.1 *n* = 1 (9.1–9.1)	11.1 *n* = 1 (11.1–11.1)	11.8 *n* = 1 (11.8–11.8)	10.5 *n* = 1 (10.5–10.5)	13.4 *n* = 1 (13.4–13.4)	11.6 *n* = 1 (11.6–11.6)	9.6 *n* = 1 (9.6–9.6)	13.2 *n* = 1 (13.2–13.2)
Papio cf. *robinsoni* Kromdraai B	9.1 *n* = 2 (8.3–9.8)	8.2 *n* = 3 (7.1–9.0)	10.8 *n* = 1 (10.8–10.8)	9.7 *n* = 1 (9.7–9.7)	11.6 *n* = 1 (11.6–11.6)	12.0 *n* = 2 (11.3–12.7)	10.9 *n* = 2 (10.4–11.3)	14.0 *n* = 2 (13.1–15.0)	10.1 *n* = 2 (8.4–11.7)	7.3 *n* = 2 (5.2–9.4)	11.2 *n* = 2 (10.0–12.4)
Papionini gen. et sp. indet. Swartkrans Member 3	9.1 *n* = 1 (9.1–9.1)	7.0 *n* = 1 (7.0–7.0)	10.4 *n* = 1 (9.8–10.9)	9.2 *n* = 1 (8.8–9.5)	10.0 *n* = 1 (9.5–10.5)	11.9 *n* = 1 (11.5–12.7)	11.1 *n* = 1 (10.3–12.3)	13.1 *n* = 1 (11.7–14.2)	12.0 *n* = 1 (11.3–12.9)	10.5 *n* = 1 (9.8–11.4)	13.5 *n* = 1 (12.2–14.8)
Papionini gen. et sp. indet. Cooper's D	– – –	– – –	9.0 *n* = 3 (8.5–9.4)	8.8 *n* = 3 (8.5–9.2)	11.5 *n* = 3 (10.6–13.0)	8.8 *n* = 1 (8.8–8.8)	10.0 *n* = 1 (10.0–10.0)	14.0 *n* = 1 (14.0–14.0)	11.4 *n* = 2 (11.0–11.8)	10.0 *n* = 2 (9.7–10.2)	14.0 *n* = 2 (12.8–15.2)
Papio sp. indet. Swartkrans II	8.2 *n* = 1 (8.2–8.2)	7.0 *n* = 1 (7.0–7.0)	9.2 *n* = 1 (9.2–9.2)	8.5 *n* = 1 (8.5–8.5)	9.8 *n* = 1 (9.8–9.8)	10.0 *n* = 1 (10.0–10.0)	10.2 *n* = 1 (10.2–10.2)	12.5 *n* = 1 (12.5–12.5)	10.9 *n* = 1 (10.9–10.9)	9.9 *n* = 1 (9.9–9.9)	13.0 *n* = 1 (13.0–13.0)
Papio sp. indet. Sterkfontein Member 4/4?	9.4 *n* = 5 (8.7–10.5)	7.4 *n* = 5 (6.4–8.5)	10.9 *n* = 4 (10.6–11.6)	10.4 *n* = 4 (10.0–10.9)	10.5 *n* = 5 (10.2–10.8)	12.8 n = 6 (11.8–13.4)	12.1 *n* = 5 (11.6–12.6)	12.9 n = 6 (11.8–13.5)	12.4 *n* = 4 (11.3–13.1)	11.2 *n* = 4 (9.7–11.9)	13.3 n = 6 (11.6–14.2)
Papio hamadryas botswanae	8.2 *n* = 1 (8.2–8.2)	6.7 *n* = 1 (6.7–6.7)	9.5 *n* = 1 (9.5–9.5)	9.4 *n* = 1 (9.4–9.4)	10.5 *n* = 1 (10.5–10.5)	12.5 *n* = 1 (12.5–12.5)	– - –	12.1 *n* = 1 (12.1–12.1)	12.2 *n* = 1 (12.2–12.2)	10.1 *n* = 1 (10.1–10.1)	13.0 *n* = 1 (13.0–13.0)
Papio hamadryas ursinus	8.7 *n* = 127 (7.0–10.3)	7.9 *n* = 127 (6.1–9.8)	10.0 *n* = 152 (8.9–12.0)	9.3 *n* = 152 (8.0–11.0)	11.2 *n* = 154 (8.5–13.1)	11.9 *n* = 141 (9.5–13.7)	11.0 *n* = 139 (9.0–12.9)	13.6 *n* = 141 (10.7–15.5)	12.4 *n* = 120 (10.3–14.2)	10.7 *n* = 120 (8.2–13.1)	14.1 *n* = 122 (11.4–16.4)

Notes: For each taxon, the mean (top), sample size (middle), and range (bottom) are given for each tooth position. For individual specimen measurements, see SOM Tables S1–S4.

Table 2
Summary statistics for the lower dentition of extant and fossil Plio-Pleistocene *Papio* species in South Africa.

Taxon	P_4 BL	P_4 MD	M_1 MBL	M_1 DBL	M_1 MD	M_2 MBL	M_2 DBL	M_2 MD	M_3 MBL	M_3 DBL	M_3 MD
?Papio izodi	–	–	–	–	–	–	10.2	12.6	11.8	–	15.7
	–	–	–	–	–	–	$n = 1$	$n = 2$	$n = 1$	–	$n = 2$
	–	–	–	–	–	–	(10.2–10.2)	(11.8–13.4)	(11.8–11.8)	–	(15.5–15.8)
Papio hamadryas angusticeps	6.7	7.8	8.1	8.2	9.8	9.9	9.6	11.8	10.4	9.1	14.8
	$n = 31$	$n = 32$	$n = 34$	$n = 36$	$n = 36$	$n = 33$	$n = 32$	$n = 36$	$n = 34$	$n = 30$	$n = 32$
	(4.7–7.6)	(6.4–9.4)	(6.7–9.6)	(6.6–9.6)	(7.8–12.3)	(8.0–11.8)	(7.6–10.7)	(9.1–13.5)	(9.0–12.6)	(8.0–10.8)	(13.1–19.2)
Papio robinsoni	7.5	9.0	8.3	8.6	10.3	10.6	10.1	12.8	11.0	9.5	16.7
	$n = 26$	$n = 26$	$n = 14$	$n = 15$	$n = 18$	$n = 22$	$n = 23$	$n = 27$	$n = 25$	$n = 22$	$n = 24$
	(6.0–9.0)	(7.4–10.4)	(7.1–9.3)	(7.7–9.7)	(8.2–12.6)	(8.8–12.1)	(8.3–11.2)	(11.1–15.5)	(9.2–13.4)	(8.5–10.8)	(13.6–18.8)
Papio cf. *robinsoni* Swartkrans Member 2	7.1	9.6	–	–	–	9.6	9.6	12.7	10.5	9.2	16.4
	$n = 1$	$n = 1$	–	–	–	$n = 1$	$n = 1$	$n = 1$	$n = 2$	$n = 2$	$n = 2$
	(7.1–7.1)	(9.6–9.6)	–	–	–	(9.6–9.6)	(9.6–9.6)	(12.7–12.7)	(10.0–11.1)	(9.1–9.2)	(15.5–17.3)
Papio cf. *robinsoni* Kromdraai B	7.6	8.9	8.3	8.6	11.2	10.4	9.7	12.3	10.3	9.5	15.3
	$n = 5$	$n = 5$	$n = 7$	$n = 7$	$n = 7$	$n = 6$	$n = 5$	$n = 7$	$n = 2$	$n = 3$	$n = 3$
	(7.0–8.1)	(8.5–9.4)	(7.4–8.8)	(7.9–9.5)	(10.5–12.5)	(9.4–11.5)	(8.8–10.5)	(10.0–14.7)	(10.1–10.5)	(8.6–10.0)	(15.2–15.5)
Papionini gen. et sp. indet. Swartkrans Member 3	7.7	9.6	8.5	9.1	10.9	10.7	10.4	13.6	10.3	9.2	16.2
	$n = 4$	$n = 4$	$n = 2$	$n = 2$	$n = 2$	$n = 2$	$n = 2$	$n = 2$	$n = 6$	$n = 6$	$n = 6$
	(6.8–8.1)	(7.7–10.3)	(8.0–9.1)	(8.5–9.7)	(9.6–12.2)	(9.3–12.1)	(8.9–11.9)	(12.0–15.2)	(9.1–11.8)	(8.2–10.4)	(14.3–18.9)
Papionini gen. et sp. indet. Cooper's D	7.4	9.9	8.2	8.0	11.2	9.2	8.8	13.3	–	–	–
	$n = 2$	$n = 2$	$n = 3$	$n = 3$	$n = 3$	$n = 2$	$n = 2$	$n = 2$	–	–	–
	(7.1–7.7)	(9.5–10.3)	(7.5–9.4)	(7.2–9.1)	(10.5–12.2)	(9.1–9.2)	(8.0–9.6)	(12.0–14.6)	–	–	–
Papio sp. indet. Swartkrans II	7.4	8.7	–	–	–	11.0	10.4	12.5	11.7	10.9	18.2
	$n = 1$	$n = 1$	–	–	–	$n = 1$	$n = 1$	$n = 1$	$n = 1$	$n = 1$	$n = 1$
	(7.4–7.4)	(8.7–8.7)	–	–	–	(11.0–11.0)	(10.4–10.4)	(12.5–12.5)	(11.7–11.7)	(10.9–10.9)	(18.2–18.2)
Papio sp. indet. Sterkfontein Member 4/4?	7.3	8.0	8.8	9.3	9.8	10.5	10.6	12.5	10.5	10.0	16.5
	$n = 3$	$n = 3$	$n = 2$	$n = 3$	$n = 3$	$n = 4$	$n = 3$	$n = 4$	$n = 2$	$n = 2$	$n = 3$
	(6.7–7.6)	(7.3–8.9)	(8.5–9.1)	(9.2–9.4)	(9.0–10.3)	(10.0–11.0)	(9.6–11.2)	(11.4–13.2)	(10.1–10.9)	(9.4–10.5)	(15.9–17.1)
Papio hamadryas botswanae	–	–	7.3	7.9	9.6	9.7	9.4	11.4	9.4	8.1	13.6
	–	–	$n = 1$	$n = 1$	$n = 1$	$n = 1$	$n = 1$	$n = 1$	$n = 1$	$n = 1$	$n = 1$
	–	–	(7.3–7.3)	(7.9–7.9)	(9.6–9.6)	(9.7–9.7)	(9.4–9.4)	(11.4–11.4)	(9.4–9.4)	(8.1–8.1)	(13.6–13.6)
Papio hamadryas ursinus	7.0	8.9	8.2	8.6	10.7	10.4	9.9	13.1	11.3	10.2	16.9
	$n = 127$	$n = 127$	$n = 151$	$n = 152$	$n = 154$	$n = 140$	$n = 138$	$n = 140$	$n = 122$	$n = 121$	$n = 123$
	(5.7–8.0)	(7.0–10.6)	(6.4–9.4)	(6.8–9.9)	(8.0–12.4)	(8.7–12.5)	(7.9–11.6)	(10.1–15.3)	(9.2–13.0)	(8.1–11.6)	(14.3–19.4)

Notes: For each taxon, the mean (top), sample size (middle), and range (bottom) are given for each tooth position. For individual specimen measurements, see SOM Tables S1–S4.

Table 3
Fossil specimens included in a 3D Geometric Morphometric Analysis of *Papio* cranial shape with DFA results.

Taxon	Institution	Specimen#	Sex	Site	DFA result
P. h. angusticeps	UW-AD	GV 4040	Female	Gladysvale	*Papio* (100%)
P. h. angusticeps	TMP	KA 194	Female	Kromdraai A	*Papio* (63%) *Parapapio* (37%)
P. h. angusticeps	TMP	CO 135a	Female	Coopers A	*Papio* (99%) *Mandrillus* (1%)
P. h. angusticeps	TMP	CO 101	Female	Coopers A	*Papio* (92%) *Dinopithecus* (6%) *Mandrillus* (2%)
P. h. angusticeps	UCMP	56767	Female	Bolt's Farm Pit 6	*Papio* (54%) *Theropithecus* (46%)
P. h. angusticeps	TMP	CO 100	Male	Coopers A	–
P. h. angusticeps	TMP	HGD 600	Male	Haasgat	–
P. h. angusticeps	TMP	HGD 606	Male	Haasgat	–
P. h. botswanae	BNMM	FC 346	Male	!Ncumtsa	–
P. robinsoni	TMP	SK 562	Female	Swartkrans Mb. 1	*Papio* (100%)
P. robinsoni	UCMP	56797	Female	Bolt's Farm Pit 23	*Papio* (84%) *Theropithecus* (16%)
P. robinsoni	TMP	SK 560	Male	Swartkrans Mb. 1	–
P. robinsoni	TMP	SK 555	Male	Swartkrans Mb. 1	–
P. robinsoni	BPI	M3147	Unknown	Skurweberg	*Papio* (100%)
?Papio izodi	UW-AD	TP 11	Female	Taung	*Procercocebus* (62%) *Papio* (36%) *Parapapio* (1%) *Theropithecus* (1%)
?Papio izodi	UW-AD	TP 10	Female	Taung	*Papio* (71%) *Parapapio* (22%) *Procercocebus* (6%)
?Papio izodi	UW-AD	TP 4	Female	Taung	*Papio* (51%) *Procercocebus* (43%) *Parapapio* (5%)
?Papio izodi	TMP	STS 262	Female	Taung	*Soromandrillus* (60%) *Papio* (25%) *Macaca* (14%)
?Papio izodi	TMP	T 13	Female	Taung	*Soromandrillus* (100%)
?Papio izodi	UW-AD	TP 12	Male	Taung	–
?Papio izodi	UW-AD	T89-11-1	Male	Taung	–
?Papio izodi	TMP	T 10	Male	Taung	–
?Papio izodi	UWMA	SWP 29	Female	Sterkfontein Member 4	–
Papio sp. indet	TMP	SK II 25	Female	Swartkrans II	–

Notes: DFA Result column indicates taxon that the individual specimen was classified to along with the posterior probability of that classification in parentheses. - indicates that the specimen could not be included in the DFA analysis due to its incompleteness.

Table 4
Extant sample included in a 3D Geometric Morphometric Analysis of *Papio* cranial shape.

Taxon	Females	Males	Both
Papio hamadryas anubis	59	124	183
Papio hamadryas cynocephalus	9	25	34
Papio hamadryas hamadryas	4	30	34
Papio hamadryas kindae	22	19	41
Papio hamadryas papio	1	16	17
Papio hamadryas ursinus	82	116	198
Cercocebus agilis	9	10	19
Cercocebus atys	3	3	6
Cercocebus torquatus	11	20	31
Lophocebus albigena	20	30	50
Mandrillus sphinx	14	27	41
Mandrillus leucophaeus	18	36	54
Macaca sylvanus	13	15	28
Theropithecus gelada	13	29	42
Totals	**278**	**500**	**778**

closely as possible for ease of reference, where the different sites are organized by the species present. In each case, we briefly note the most important specimens upon which our species identifications for that site are based (see also Figs. 2–4; SOM Figs. S1–S4).

3.1.1. Sterkfontein Member 2 Although still formally unpublished, *?P. izodi* has been previously recognized at Sterkfontein Member 2 by Pickering et al. (2004) and Heaton (2006). We had the opportunity to study some of the Member 2 material in 2009 (CCG, access courtesy of R. Clarke) and 2012 (CCG and SRF, courtesy of R. Clarke), and we confirm this identification here. Among the cercopithecoid material from Member 2 are at least four partial crania that unambiguously document the presence of *?P. izodi* (Table 8; SOM Fig. S1; Heaton, 2006: Figs. 4–7). These partial crania, particularly the females, are so similar to the type series from Taung as to leave no doubt to their taxonomic affinity (SOM Fig. S1). Thus, these crania display relatively large orbits, relatively large teeth, moderate to absent maxillary ridges, moderately-developed to absent maxillary fossae, and a relatively shorter and broader rostrum compared to other *Papio* species. In addition, the anteorbital drop in these specimens is variably developed. A more detailed analysis of these specimens awaits their formal description and introduction into the literature.

3.1.2. Sterkfontein Member 4 *?P. izodi* has previously been documented at Sterkfontein Member 4 by Eisenhart (1974), Delson (1984, 1988), and McKee (1993) in the form of a subadult female specimen, STS 262. Because fossils deriving from the Sterkfontein Type Site (STS) can be of uncertain provenience (although generally assumed to be derived from Member 4), it is also important to note that we recognize at least one more secure specimen, SWP 29a+b, a subadult partial face and mandible of a female from Member 4, as *?P. izodi* on the basis of its apparent anteorbital drop, relatively large orbits, relatively large teeth, and relatively short, rounded rostrum with no maxillary ridges and weakly excavated fossae.

Table 5
Sample sizes for extant taxa included in cladistic analysis.

Taxon	Quantitative character sample size (Mean, Median, Mode, Range)	Qualitative character sample size (Mean, Median, Mode, Range)
Allenopithecus nigroviridis Males	4.8, 5, 5, 0–5	5.9, 6, 6, 0–7
Allenopithecus nigroviridis Females	4.8, 5, 5, 0–7	6.4, 7, 7, 0–7
Cercocebus agilis Males	10.0, 8, 0, 0–23	14.2, 16, 16, 0–16
Cercocebus agilis Females	6.6, 8, 3, 0–13	11.5, 13, 13, 0–13
Cercocebus atys Males	5.6, 4, 11, 0–12	1.9, 2, 2, 0–4
Cercocebus atys Females	9.1, 5, 0, 0–21	1.8, 2, 2, 0–2
Cercocebus chrysogaster Males	3.3, 0, 0, 0–9	5.6, 6, 6, 0–6
Cercocebus chrysogaster Females	2.3, 0, 0, 0–6	3.6, 4, 4, 0–4
Cercocebus torquatus Males	16.5, 20, 20, 0–32	30.9, 32, 33, 0–35
Cercocebus torquatus Females	13.1, 16, 18, 0–18	12.9, 14, 15, 0–16
Lophocebus albigena Males	18.1, 18, 18, 0–32	29.5, 31, 32, 0–33
Lophocebus albigena Females	15.6, 17, 17, 0–36	30.1, 35, 36, 0–36
Lophocebus aterrimus Males	1.5, 1, 1, 0–29	26.9, 29, 29, 0–29
Lophocebus aterrimus Females	2.2, 2, 2, 0–22	19.7, 22, 22, 0–22
Macaca sp. Males	20.5, 19, 20, 6–79	72.5, 78, 79, 0–80
Macaca sp. Females	19.0, 18, 19, 0–73	60.3, 68, 73, 0–74
Mandrillus leucophaeus Males	24.1, 25.5, 31, 0–35	13.6, 15, 15, 0–17
Mandrillus leucophaeus Females	14.6, 17, 18, 0–20	17.5, 20, 20, 0–21
Mandrillus sphinx Males	6.7, 6, 6, 4–18	11.4, 12, 12, 0–14
Mandrillus sphinx Females	2.9, 2, 2, 0–15	7.9, 9, 9, 0–10
Papio hamadryas anubis Males	9.0, 8, 7, 0–39	33.8, 36, 39, 0–39
Papio hamadryas anubis Females	8.9, 10, 11, 2–17	13.5, 16, 17, 0–17
Papio hamadryas cynocephalus Males	11.0, 13, 13, 0–17	13.7, 15, 15, 0–15
Papio hamadryas cynocephalus Females	6.9, 8, 9, 0–11	5.2, 6, 6, 0–6
Papio hamadryas hamadryas Males	1.2, 1, 0, 0–13	12.1, 13, 13, 0–13
Papio hamadryas hamadryas Females	0.5, 0, 0, 0–2	1.4, 2, 2, 0–2
Papio hamadryas kindae Males	4.3, 6, 0, 0–13	11.1, 13, 13, 0–13
Papio hamadryas kindae Females	4.0, 6, 0, 0–17	13.8, 15, 17, 0–17
Papio hamadryas papio Males	1.6, 1, 1, 0–10	9.4, 10, 10, 0–10
Papio hamadryas papio Females	0.0, 0, 0, 0–1	0.9, 1, 1, 0–1
Papio hamadryas ursinus Males	3.1, 4, 0, 0–36	32, 34.5, 36, 0–37
Papio hamadryas ursinus Females	2.1, 3, 3, 0–11	8.1, 9, 11, 0–11
Theropithecus gelada Males	17.7, 19, 21, 0–22	16.6, 17, 17, 0–17
Theropithecus gelada Females	16.9, 20, 21, 0–22	5.4, 6, 6, 0–6
Males average	**9, 9, 9, 1–25**	**20, 22, 22, 0–23**
Females average	**8, 8, 8, 0–18**	**13, 15, 15, 0–16**

Notes: Sample sizes are listed for specimens identifiable to sex used in character analysis. For each taxon, measurements and qualitative character state assignments were made, supplemented with additional data from the major sources listed in Tables 6–8. For a full list of characters and character states, see Gilbert (2013), Gilbert et al. (2016a,b), and Table 7.

A limited number of specimens assumed to be from Member 4 are consistent with more derived *Papio* taxa such as *P. robinsoni* and *P. h. angusticeps*, but require more complete and diagnostic material to be certain. SWP 1290 and SWP 1230 are maxillae displaying definitive maxillary fossae inconsistent with *Parapapio* and *?P. izodi*. The coordinates given for each of these specimens correspond to Member 4 according to Kuman and Clarke (2000), but the UW-AD catalog lists them as from Member 5, leading to an uncertain provenience. STS 387a is a right maxillary fragment with a clear and well-defined maxillary fossa, also consistent with derived *Papio* taxa, but neither *Parapapio* nor typical *?P. izodi*. Tooth length is also within the range of *P. robinsoni* and *P. h. angusticeps* (see boxplots Figs. 5–9). STS 358 is a large male partial mandible, highly crushed and distorted. It appears to have a shallow, but clear, corpus fossa, again more consistent with derived *Papio* taxa than *Parapapio* or *?P. izodi*. Because these last two specimens derive from the old STS collections, their exact provenience is not entirely secure.

Two specimens are more securely placed in Member 4 but are less diagnostic as to (sub)species. SWP 31 (STW 31) is a female partial face from Member 4 that has been previously identified as *P. robinsoni* (SOM Fig. S4; see also Eisenhart, 1974: Figs. 323-324; Delson, 1984, 1988). The right maxilla shows a moderately excavated but well-defined maxillary fossa, beginning at about M^1 and extending posteriorly to the zygoma, which it invades very slightly. The fossa is not as deep as those of some *P. robinsoni* and *P. h. angusticeps* specimens, but there is considerable distortion due to superioinferior plastic deformation. An anteorbital drop appears to be present as well, but it is hard to be certain given distortion. The teeth of SWP 31 are large and the malar height is taller than those of female *?P. izodi* specimens, closer to that seen in females of extant *Papio*. This specimen is perhaps most similar to *P. robinsoni* females. Although larger than most, it is, however, within the range for females of *?P. izodi* and *P. h. angusticeps* as well.

SWP 35 (STW 35) is a small fragment of a left maxilla from Member 4 preserving a P^4 and a small area of the lateral wall of the rostrum (SOM Fig. S4; see also Eisenhart, 1974: Figs 321–322). It shows a clear fossa over the M^1 partial alveolus that is more extensive than any observed in *?P. izodi* or *Parapapio* (SOM Fig. S4). Furthermore, the P^4 is considerably larger than the known *?P. izodi* range (see measurements in SOM Table S3). Given its fragmentary nature, we conservatively assign this fossil to *Papio* sp. indet., along with the other specimens listed above.

It should also be noted that at least three Member 4 specimens (SWP 1180, SWP 1217, and SWP 1348) previously cataloged as *P. robinsoni* are more properly identified as Papionini gen. et sp. indet. due to their lack of diagnostic morphology (e.g., no facial fossae, maxillary ridges, or anteorbital drop is preserved; therefore, they could be either *Papio* or *Parapapio*).

In summary, at Sterkfontein Member 4, *?P. izodi* is clearly present. In addition, there is a second more derived *Papio* taxon present, but it is unclear whether this is *P. robinsoni*, *P. h. angusticeps*, or another derived form. While two of these specimens are known to be from Member 4, others of these more derived specimens could be from either Member 4 or Member 5.

Table 6
Sample for fossil taxa included in cladistic analysis.

Fossil Taxon/OTU	Sample Size (Males, Females)	Key specimens	Source
Dinopithecus ingens	(4, 7)	SB 7, SK 401, SK 542a, SK 546, SK 548, SK 553, SK 554, SK 574, SK 599, SK 600, SK 603	Freedman, 1957; Gilbert, 2013; this study
Gorgopithecus major	(6, 4)	KA 150, KA 153, KA 154, KA 192, KA 524/676, KA 605, KA 944, KA 1148, SK 604a, OLD 1962/S.196, FLK NNI 1011	Freedman, 1957; Gilbert et al., 2016a; this study
Lophocebus sp. nov.	(6, 8)	KNM-ER 594, KNM-ER 595, KNM-ER 827, KNM-ER 898, KNM-ER 965, KNM-ER 1661, KNM-ER 3090, KNM-ER 6014, KNM-ER 6063, KNM-ER 18922, KNM-ER 40476, KNM-ER 44260, KNM-ER 44262, KNM-ER 44317	Jablonski et al., 2008; Gilbert, 2013; this study
Papio hamadryas angusticeps	(9, 9)	CO 100, CO 101, CO 102, CO 115/103, CO 134B/D, CO 135A, KA 156, KA 161, KA 165, KA 166, KA 167C, KA 168, KA 188, KA 194, KB 94, GV 4040, UW 88-886, UCMP 56767	Freedman, 1957; McKee and Keyser, 1994; Gilbert et al., 2015; this study
?Papio izodi	(3, 9)	SAM 11728, SWP Un 2, T13, T89-11-1, TP4/M681/AD946, TP7/M684/AD992, TP10, TP11, TP12, UCMP 125854, UCMP 125855, UCMP 125856	Freedman, 1957; Freedman, 1961; Freedman, 1965; Heaton, 2006; Gilbert, 2013; this study
Papio robinsoni	(8, 15)	SK 406, SK 407, SK 408, SK 409, SK 416, SK 421, SK 549, SK 555, SK 557, SK 558, SK 560, SK 562, SK 565, SK 566, SK 571B, SK 602, SK 3211B, SB 2, M3147, UCMP 56797, UCMP 56786, BF 38	Freedman, 1957; Freedman, 1965; Freedman and Brain, 1977; this study
Soromandrillus quadratirostris	(4, 5)	NME-USNO, NME Omo 47-1970-2008, NME L 4-13b NME Omo 42-1972-1, NME Omo L-185-6, NME Omo 75N (71)-C2, DGUNL LEBA02, DGUNL LEBA03, DGUNL LEBA06	Iwamoto, 1982; Eck, 1977; Eck and Jablonski, 1984; Delson and Dean, 1993; Gilbert et al., 2009b; Gilbert, 2013; this study
Parapapio ado	(2,4)	BMNH M14940, EP 1579/98, LAET 74-242/243/244, LAET 75-483, LAET 75-1209, LAET 78-5269, MB MA 42444/42445/42458	Leakey and Delson, 1987; Harrison, 2011; this study
Parapapio broomi	(18, 17)	M202/MP2, M211/MP11, M2961, M2962/MP76, M2978/MP92, M3037, M3067, STS 254, STS 255, STS 258, STS 264, STS 267, STS 297, STS 331, STS 332, STS 335, STS 337, STS 338, STS 339, STS 360, STS 363, STS 378A, STS 379, STS 390A, STS 393, STS 396A, STS 397, STS 409, STS 411A/B, STS 469, STS 534, STS 542, STS 562, STS 564, BF 43	Freedman, 1957; Freedman, 1960; Maier, 1970; Freedman and Stenhouse, 1972; Eisenhart, 1974; Gilbert, 2013; this study
Parapapio jonesi	(4, 12)	AL 363-15, AL 363-1, M215/MP15, M218/MP18, M3051/MP 165, STS 250, STS 284, STS 313, STS 355, STS 372, STS 547, STS 565, SWP (STW) 27, SWP 389, SWP 1728, SWP 2947	Freedman, 1957; Freedman, 1960; Maier, 1970; Freedman and Stenhouse, 1972; Eisenhart, 1974; Freedman, 1976; Frost and Delson, 2002; Gilbert, 2013; this study
"Parapapio" lothagamensis	(5, 2)	KNM-LT 419, KNM-LT 448, KNM-LT 449, KNM-LT 23065, KNM-LT 23091, KNM-LT 24111, KNM-LT 24136	Leakey et al., 2003; this study
Parapapio whitei	(5, 5)	M3072, MP221, MP223, STS 259, STS 266, STS 352, STS 359, STS 374, STS 389, STS 563	Freedman, 1957; Maier, 1970; Freedman, 1976; Freedman and Stenhouse, 1972; Eisenhart, 1974; Gilbert, 2013; this study
Pliopapio alemui	(4, 6)	AME-VP-1/64, ARA-VP 1007, ARA-VP 1723, ARA-VP 1/73, ARA-VP 1/133, ARA-VP 1/563, ARA-VP 1/1006, ARA-VP 1/2553, ARA-VP 6/437, ARA-VP 6/933	Frost, 2001b; Frost et al., 2009; Gilbert, 2013; this study
Procercocebus antiquus	(5, 14)	SAM 4850, SAM 5356, SAM 5364, M3078, M3079, T11, T14, T17, T18, T20, T25, T21, T89-154, T88-17, TP8, TP9, TP13, UCMP 56624, UCMP 56653, UCMP 56694, UCMP 56821/125956	Gilbert, 2007; Gilbert, 2013; this study
Theropithecus baringensis	(2, 0)	KNM-BC 2, KNM-BC 1647	Leakey, 1969; Delson and Dean, 1993; Eck and Jablonski, 1984; this study
Theropithecus brumpti	(12, 6)	NME L17-45, NME 32-154, NME L32-155, NME L122-34, NME L338Y-2257, NME L345-3, NME L345-287, NME L576-8, KNM-TH 46700, KNM-WT 16749, KNM-WT 16806, KNM-WT 16808, KNM-WT 16828, KNM-WT 16888, KNM-WT 17571, KNM-WT 17555, KNM-WT 17560, KNM-WT 39368CX	Eck and Jablonski, 1987; Harris et al., 1988; Jablonski et al., 2008; Gilbert et al., 2011b; this study
Theropithecus oswaldi darti	(12, 6)	M2974, M3073, MP44, MP217, MP222, NME AL 58-23, NME AL 134-5, NME AL 142-19, NME AL 144-1, AL 153-14, NME AL 163-11, NME AL 186-17, NME AL 187-10, NME AL 196-3, NME AL 205-1, NME AL 208-10, NME AL 321-12, NME AL 416-2	Eck, 1993; Eck and Jablonski, 1987; Freedman, 1957; Maier, 1970; Maier, 1972; this study
Victoriapithecus macinnesi	(4, 2)	KNM-MB 18993, KNM-MB 21027, KNM-MB 27876, KNM-MB 29100, KNM-MB 29158, KNM-MB 31281	Benefit, 1987; Benefit, 1993; Benefit and McCrossin, 1991; Benefit and McCrossin, 1997; this study

Notes: Sample sizes are listed for key specimens, identifiable to sex, used in character analysis. Measurements and character state assignments were made and supplemented with additional data from the major sources listed for each taxon.

Table 7
Postcranial characters added to the Gilbert (2013) morphological character matrix.

	Character description	Reference
A1	**Vertebral Number**: quantitative; modal number of thoracic and lumbar vertebrae	Williams (2012)
S1	**Scapular Index**: quantitative; Max. height × 100/Max. length	Fleagle and McGraw (2002)
H1	**Deltoid Plane Width**: quantitative; deltoid plane width x 100/humeral head width	Fleagle and McGraw (2002)
H2	**Brachialis Flange Width**: quantitative; Max width of the brachialis flange × 100/Geometric Mean	Gilbert et al. (2016a)
H3	**Supinator Crest Length**: qualitative; supinator crest height; 0 = not extended, 1 = polymorphic, 2 = extended	Fleagle and McGraw (2002)
H4	**Distal Articulation Breadth**: quantitative; anterior articular width x 100/biepicondylar width	Fleagle and McGraw (2002)
H5	**Medial Trochlear Lip**: qualitative; 0 = normal, 1 = polymorphic, 2 = prominent	Fleagle and McGraw (2002)
H6	**Olecranon Fossa Width:** quantitative; olecranon fossa breadth × 100/Geometric Mean	Gilbert et al. (2016a)
H7	**Lateral Margin of Olecranon Fossa:** qualitative; 0 = normal, 1 = prominent	Fleagle and McGraw (2002)
H8	**Olecranon Fossa Depth:** qualitative; 0 = normal, 1 = polymorphic, 2 = deep	Gilbert et al. (2016a)
H9	**Olecranon Fossa Shape:** qualitative; 0 = rounded, 1 = polymorphic, 2 = triangular	Gilbert et al. (2016a)
H10	**Distal AP Depth**: quantitative**;** max AP depth of distal articulation × 100/Gmean	Gilbert et al. (2016a)
H11	**Medial Epicondyle Orientation**: qualitative; 0= < 45°, 1 = 45-60°, 2= > 60°	Harrison (1989) Frost and Delson (2002)
U1	**Coronoid Width**: quantitative; coronoid width × 100/articular notch width	Fleagle and McGraw (2002) Harrison (1989) Guthrie (2011)
U2	**Interosseous Crest:** qualitative; 0 = strong, 1 = weak	Fleagle and McGraw (2002)
R1	**Radial Shaft Shape**: qualitative; 0 = triangular, 1 = rounded	Fleagle and McGraw (2002)
MC1	**Relative MC I Length**: quantitative; 0 = short, 1 = intermediate, 2 = long compared to MC II-V	Harrison (1989) Frost and Delson (2002) Guthrie (2011)
I1	**Ilium Breadth**: quantitative; ilium min. width × 100/max. acetabular diameter	Fleagle and McGraw (2002)
I2	**Gluteal Tuberosity**: qualitative; 0 = prominent, 1 = weak	Fleagle and McGraw (2002)
F1	**Patellar Groove, Medial Lip**: qualitative; 0 = weak/round, 1 = moderate	Fleagle and McGraw (2002)
F2	**Patellar Groove, Lateral Lip**: qualitative; 0 = weak, 1 = moderate, 2 = strong/sharp	Fleagle and McGraw (2002)
T1	**Tibial Compression**: quantitative; mid AP diameter × 100/mid ML diameter	Fleagle and McGraw (2002)

Notes: Samples for extant taxa as given in the references listed. For any given character where character states were consistent among extant species within sampled genera, the genus average was used for any unsampled extant species within a given genus. For available postcranial characters, *Allenopithecus* was scored on the basis of 3 males (1 adult, 2 subadults with most epiphyses fused) and 1 female. Fossil taxa sampled include adult *T. darti, T. brumpti, Pp. jonesi, Pr. antiquus, P. izodi, Pp. ado*, "*Pp*". *lothagamensis*, and *Victoriapithecus*. All postcranial characters were treated as ordered.

3.1.3. Taung The type series of *?P. izodi* documents this taxon at Taung. The best specimens are listed in Table 8.

3.1.4. Malapa UW-88-886 establishes *P. h. angusticeps* as the only non-hominin primate at the site, with a date range of ca. 2.4–2.0 Ma (see Gilbert et al., 2015).

3.1.5. Haasgat McKee and Keyser (1994) and Adams (2012) recognized *P. h. angusticeps* at Haasgat, as we do here. Many specimens show the diagnostic morphology of *P. h. angusticeps*, including deep maxillary and mandibular corpus fossae, marked maxillary ridges, and rostra that are narrower and less flattened than in most *Papio* (see also SOM Fig. S2). In addition, they are also smaller, on average, than *P. robinsoni*. See McKee and Keyser (1994: Figs. 2–4) and Adams (2012: Fig. 3) for more complete descriptions. The best specimens exhibiting clear and diagnostic morphology are listed in Table 8.

3.1.6. Kromdraai A Previous analyses have suggested that both *P. robinsoni* and *P. h. angusticeps* are found at Kromdraai A (Freedman, 1957; Delson, 1984, 1988; McKee et al., 1995; Heaton, 2006). *P. h. angusticeps* is clearly established by the type specimen KA 194, a partial female cranium (Broom, 1940; SOM Fig. S2). However, while studying the entire Kromdraai A sample in 2012, we noticed that there are no specimens preserving diagnostic features unique to *P. robinsoni* and/or exclusive of *P. h. angusticeps*. The small number of *P. robinsoni* specimens previously recognized by Freedman (1957) and Delson (1984, 1988) were diagnosed based on their general *Papio* features and large size compared to the rest of the sample. In fact, at all sites where *P. h. angusticeps* and *P. robinsoni* have been previously argued to co-occur, we were struck by the observation that only one of the two taxa is ever represented by relatively complete cranial material, while the other is typically recognized on the basis of fragmentary fossils judged to be too large (*P. robinsoni*) or too small (*P. h. angusticeps*) to fit with the better preserved specimens. In the absence of more definitive evidence, we recognize only one variable *Papio* species at Kromdraai A, *P. h. angusticeps* (see also metric analysis below, Figs. 5–9).

3.1.7. Cooper's A This sample includes Cooper's A-E in the old collection at the Ditsong National Museum, and these are all equivalent to Cooper's A in the new system (C. Steininger, pers. comm.). The bulk of this material was collected from dump heaps at a limestone mine, making exact provenience uncertain (Folinsbee and Reisz, 2013; C. Steininger, pers. comm.). In any case, the predominant papionin taxon present among the Cooper's A collection is *P. h. angusticeps*, which is represented by a number of good cranial specimens preserving features such as well-defined and deep maxillary fossae, well-defined maxillary ridges, and small premolars (Table 8; Figs. 2–3; SOM Fig. S2). While both Freedman (1957) and Delson (1984, 1988) again recognized some fragmentary specimens at Cooper's A as *P. robinsoni*, we feel they are all comfortably accommodated within a single population

Table 8
Diagnostic specimens establishing the presence of *Papio* taxa by site.

Taxon	Site	Diagnostic/Best specimen(s)	Brief description(s)	Reference
?P. izodi	Sterkfontein Member 2	SWP 2948	Subadult female partial cranium	Heaton (2006)
		SWP 2953	Partial cranium missing most of rostrum; sex unknown	Heaton (2006)
		SWP Uncatalogued	Male partial cranium	Heaton (2006)
		SWP 2946	Female partial cranium	Heaton (2006)
	Sterkfontein Member 4	SWP 29a+b	Subadult female partial face and mandible	Heaton (2006)
		STS 262	Subadult female partial cranium	Eisenhart (1974); Delson (1984, 1988); McKee (1993)
	Taung	UW-AD 922/TP-7	Female partial cranium with dentition (TYPE)	Gear (1926); Jones (1937); Freedman (1957)
		SAM 11728	Female partial cranium with dentition	Freedman (1961)
		SAM 5357	Cranial endocast with partial mandible and dentition	Freedman (1957)
		TP-10/UCMP 56605	Female partial cranium with dentition	Freedman (1961)
		TP-4/AD 946	Female partial face with mandible and dentition	Freedman (1957)
		TP-12/UCMP 56652	Male partial cranium with dentition	Freedman (1965)
		T89-11-1	Male partial cranium with dentition	this study
		UCMP 125856	Male partial cranium with dentition	Delson (1988); Gilbert (2013)
		T13	?Female cranium with dentition	Freedman (1957)
		T10	Subadult cranium with dentition	Freedman (1957); this study
		UCMP 125854	Female partial cranium with dentition	Delson (1988); Gilbert (2013)
		UCMP 125855	Female partial cranium with dentition	Delson (1988); Gilbert (2013)
?Papio cf. izodi	Gladysvale	GV 4340	Female partial cranium, no dentition	Berger et al. (1993); this study
P. h. angusticeps	Malapa	UW-88-886	Male partial cranium	Gilbert et al. (2015)
	Haasgat	HGD 1249	Male partial right face with dention	McKee and Keyser (1994); Adams (2012)
		HGD 600	Male muzzle with dentition	McKee and Keyser (1994); Adams (2012)
		HGD 605	Partial maxilla with dentition	McKee and Keyser (1994); Adams (2012)
		HGD 603	Left male maxilla with dentition	McKee and Keyser (1994); Adams (2012)
		HGD 606	Male maxilla with dentition	McKee and Keyser (1994); Adams (2012)
		HGD 644	Male left maxilla with dentition	McKee and Keyser (1994); Adams (2012)
		HGD 601	Subadult female partial cranium with dentition	McKee and Keyser (1994); Adams (2012)
		HGD 1246	Female partial mandible with dentition	McKee and Keyser (1994); Adams (2012)
		HGD 1243	Female partial mandible with dentition	McKee and Keyser (1994); Adams (2012)
		HGD 618	Male partial mandible with dentition	McKee and Keyser (1994); Adams (2012)
		HGD 615	Female partial mandible with dentition	McKee and Keyser (1994); Adams (2012)
		HGD 626	Female partial mandible with dentition	McKee and Keyser (1994); Adams (2012)
	Kromdraai A	KA 194	Female partial cranium with dentition (TYPE)	Broom (1940); Freedman (1957)
	Cooper's A	CO 100	Partial male cranium with dentition	Freedman (1957)
		CO 101	Partial female cranium with dentition	Freedman (1957)
		CO 103/115	Male mandible with dentition	Freedman (1957)
		CO 134B-D	Subadult male partial maxilla and mandible with dentition	Freedman (1957); this study
		CO 135	Partial female cranium with dentition	Freedman (1957)
		CO 102	Partial muzzle with dentition	Freedman (1957)
	Gladysvale	GV 4040	Partial female cranium with dentition	this study
	Bolt's Farm Pit 6	UCMP 56767	Female partial cranium with dentition	Freedman (1965); this study
		UCMP 56766	Male crushed muzzle with dentition	Freedman (1965); this study
		UCMP 56768	Male partial mandible with dentition	Freedman (1965); this study
		UCMP 56772	Male partial mandible with dentition	Freedman (1965); this study
		UCMP 56769	?Female partial mandible with dentition	Freedman (1965); this study
		UCMP 177639	?Male partial mandible with dentition	this study
		UCMP 56771	Female partial mandible with dentition	Freedman (1965); this study
P. robinsoni	Drimolen Main Quarry	DN 2160	Male partial cranium with dentition	Adams et al. (2016); this study
		DN 541	Male crushed face with dentition	Adams et al. (2016); this study
		DN 403	Male palate with dentition	Adams et al. (2016); this study
		DN 528	Male right face and muzzle with dentition	Adams et al. (2016); this study
		DN 363	?Female crushed partial cranium with dentition	Adams et al. (2016); this study
		DN 2344	Female partial crushed cranium with dentition	Adams et al. (2016); this study
		DN 2162	Male mandibular corpus with dentition	Adams et al. (2016); this study
		DN 2345	Female partial mandible with dentition	Adams et al. (2016); this study
		DN 1158	Right mandibular fragment with dentition	Adams et al. (2016); this study
		DN 1109	Left mandibular fragment with dentition	Adams et al. (2016); this study
	Swartkrans Member 1	SK 555	Male muzzle with dentition (TYPE)	Freedman (1957)
		SK 560	Male muzzle with dentition	Freedman (1957)
		SK 602	Male crushed face with dentition	Freedman (1957)
		SK 14006	Crushed face with M3	Freedman and Brain (1977)
		SK 557	Female partial cranium with dentition	Freedman (1957)
		SK 558	Female partial cranium with dentition	Freedman (1957)
		SK 562	Female maxilla and muzzle with dentition	Freedman (1957)
		SK 566	Female compressed muzzle with dentition	Freedman (1957)
		SK 14083	Male left mandibular corpus and ramus with dentition	Freedman and Brain (1977)

(*continued on next page*)

Table 8 (*continued*)

Taxon	Site	Diagnostic/Best specimen(s)	Brief description(s)	Reference
		SK 406	Male partial mandible with dentition	Freedman (1957)
		SK 408	Male partial mandible with dentition	Freedman (1957)
		SK 407	Female mandibular corpus with dentition	Freedman (1957)
		SK 421	Female partial mandible with dentition	Freedman (1957)
		SK 571a	Female partial mandible with dentition	Freedman (1957)
		SK 14156	Female partial mandible with dentition	Freedman and Brain (1977)
	Skurweburg	SB 2	Crushed male partial cranium	Freedman (1957)
		M3147	Partial muzzle with dentition	this study
	Bolt's Farm Pit 23	BF 38	Male muzzle and palate with dentition	Freedman (1965); this study
		UCMP 56797	Female partial cranium with dentition	Freedman (1965); this study
Papio cf. robinsoni	Swartkrans Member 2	SKX 814	Subadult female palate and partial muzzle with dentition	Delson (1988); this study
	Kromdraai B	KB 1456	Subadult female palate with dentition	Delson (1988); this study
		KB 5230	Female partial mandible with dentition	Delson (1988); this study
		KA 196/KB 94	Mandibular fragment with dentition	Freedman (1957); this study
		KA 197/KB 104	Mandibular fragment with dentition	Freedman (1957); this study
	Bolt's Farm Pit 10?	Uncatalogued	Partial maxilla with dentition	this study
Papio sp. indet.	Swartkrans II	SK II 25	Partial female cranium with dentition	Freedman (1957); this study
		SK II 26	Partial male mandible with dentition	Freedman (1957); this study
	Sterkfontein Member 4	SWP 31	Female partial face dentition	Eisenhart (1974); this study
		SWP 35	Maxillary fragment with P4	Eisenhart (1974); this study
	Sterkfontein Member 4 or 5	STS 387a	Maxillary fragment with dentition	Eisenhart (1974); this study
		STS 358	Male partial (crushed) mandible with dentition	Eisenhart (1974); this study
		SWP 1290	Partial maxilla with dentition	this study
		SWP 1230	?Female maxilla with dentition	Heaton (2006); this study
	Sterkfontein Member 5	SWP 1232	Male partial mandible with dentition	this study
	Sterkfontein Member 6	SWP 1012	Female partial mandible with dentition	this study

Notes: "Reference" column lists other references which discuss the specimen in question. If the specimen in question has been reassigned to a different taxon in this study, the original reference is given in addition to "this study". If the specimen in question was not directly mentioned by the original reference (only the taxon), the original reference is also given in addition to "this study". Finally, specimens formally assigned to a taxon for a first time in this study are listed as "this study".

(Figs. 5–9). There is no relatively complete cranial material that is diagnostically *P. robinsoni* at Cooper's A, in contrast to the material found at Swartkrans and Skurweberg.

3.1.8. Gladysvale *P. h. angusticeps* is represented at Gladysvale by GV 4040, a female partial cranium with partial dentition. Interestingly, there is also a possible female partial cranium (GV 4340) with large orbits, slight maxillary fossae, a possible anteorbital drop, and slight to absent maxillary ridges; these features are most consistent with *?P. izodi* (see also Berger, 1993; Berger et al., 1993). However, the specimen lacks any dentition and is not complete enough to be certain (we consider it to be cf. *?P. izodi* here). Furthermore, the time averaging and geological complexity present between the various internal and external deposits at Gladysvale make it impossible to determine whether GV 4040 and GV 4340 come from the same level or whether they represent two different depositional events at the site (see also Berger and Tobias, 1994; Lacruz et al., 2002; Pickering et al., 2007).

3.1.9. Bolt's Farm Pit 6 Following Freedman (1965), Delson (1984, 1988) previously recognized only *P. robinsoni* at Bolt's Farm Pit 6 and Pit 23. While we concur with this assessment of Pit 23, at Pit 6 we find the *Papio* material more consistent with the features diagnostic for *P. h. angusticeps* and we re-assign the *Papio* material present at this site to that subspecies. There are a number of good specimens of *P. h. angusticeps* present at Pit 6, including: UCMP 56767, a female cranium very similar to KA 194 with narrow muzzle, deep maxillary fossae invading the infraorbital plate, relatively small orbits, peaked nasals well above the muzzle dorsum, maxillae that do not meet in the midline, and well-defined maxillary ridges (better developed than seen in *P. robinsoni* UCMP 56797 from Pit 23; see Figs. 2–4); UCMP 56766, a male crushed muzzle/rostrum with very deep and well-defined maxillary fossae invading the infraorbital plate, a muzzle which appears to have probably been narrower than that of *P. robinsoni*, and a P^4 that is not noticeably large (see Figs. 5, 7; SOM Tables S3–S4); UCMP 56768, a male partial mandible with P_4 qualitatively small, mandibular corpus fossae clearly present under P_4/M_1 contact and deep on left hand side; and UCMP 56772, a male partial mandible with partial dentition and very deep mandibular corpus fossa under P_4/M_1 on the left side. Other diagnostic specimens of *P. h. angusticeps* from Pit 6 are listed in Table 8. In addition, UCMP 56771 is a female complete mandibular dentition incompletely prepared from surrounding matrix and consistent in size with *P. h. angusticeps* but with no mandibular morphology preserved. Given that there is no evidence of dental variation beyond that expected in a single population of modern *P. h. ursinus*, we again recognize only one *Papio* taxon at Bolt's Farm Pit 6, *P. h. angusticeps*.

3.1.10. Drimolen Main Quarry *P. robinsoni* is reported at Drimolen Main Quarry by Keyser (2000) and subsequently confirmed by Adams et al. (2016) and our own observations here (access courtesy of C. Menter). While the specimens await formal description and publication, they display characteristic *P. robinsoni* features such as large size, a definitive anteorbital drop, a squared-off "boxy" rostrum, qualitatively large premolars, and weak-to-moderately developed maxillary and mandibular fossae (SOM Fig. S3). They seem to differ from the Swartkrans and Skurweberg

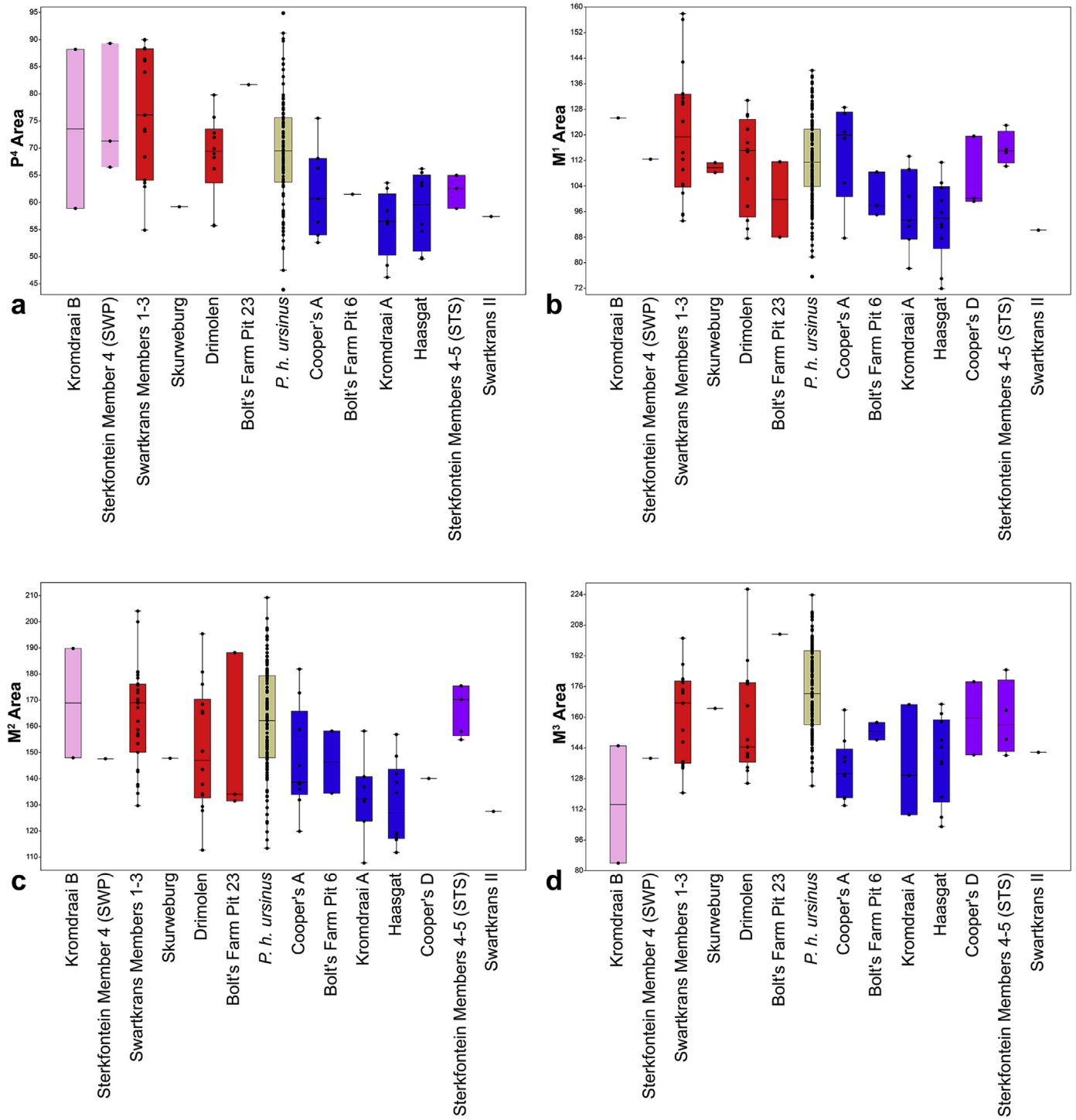

Figure 5. Boxplots illustrating dental size ranges (expressed as tooth area = maximum mesiodistal length x maximum buccolingual width) for upper P^4s and upper molars among Plio-Pleistocene South African sites and a sample of extant *P. h. ursinus* specimens. Pink indicates those populations designated as *P.* cf. *robinsoni*, red indicates those populations designated as *P. robinsoni*, blue indicates those populations designated as *P. h. angusticeps*, purple indicates those populations designated as *Papio* sp. indet., and gold indicates extant *P. h. ursinus*. For samples by tooth position, see Tables 1 and 2 and SOM Tables S1–S4.

populations in that the maxillae do not seem to contact in the midline on the rostrum, but only two specimens are really assessable for this feature (DN 2160, 541) and so it is possible that this feature is present at Drimolen Main Quarry, just in lower frequency. The most definitive specimens are listed in Table 8.

3.1.11. Swartkrans Member 1 The type specimen of *P. robinsoni* Freedman, 1957 (SK 555) derives from Swartkrans Member 1, along with several other good specimens that help define the morphological features of the species (Figs. 2–4; SOM Fig. S3). The best specimens are listed in Table 8.

3.1.12. Skurweberg *P. robinsoni* is clearly documented at Skurweberg by the male crushed partial cranium SB 2, and the partial face and muzzle of unknown sex, M3147. Both specimens display a flattened muzzle dorsum, clear maxillary ridges (more rounded in

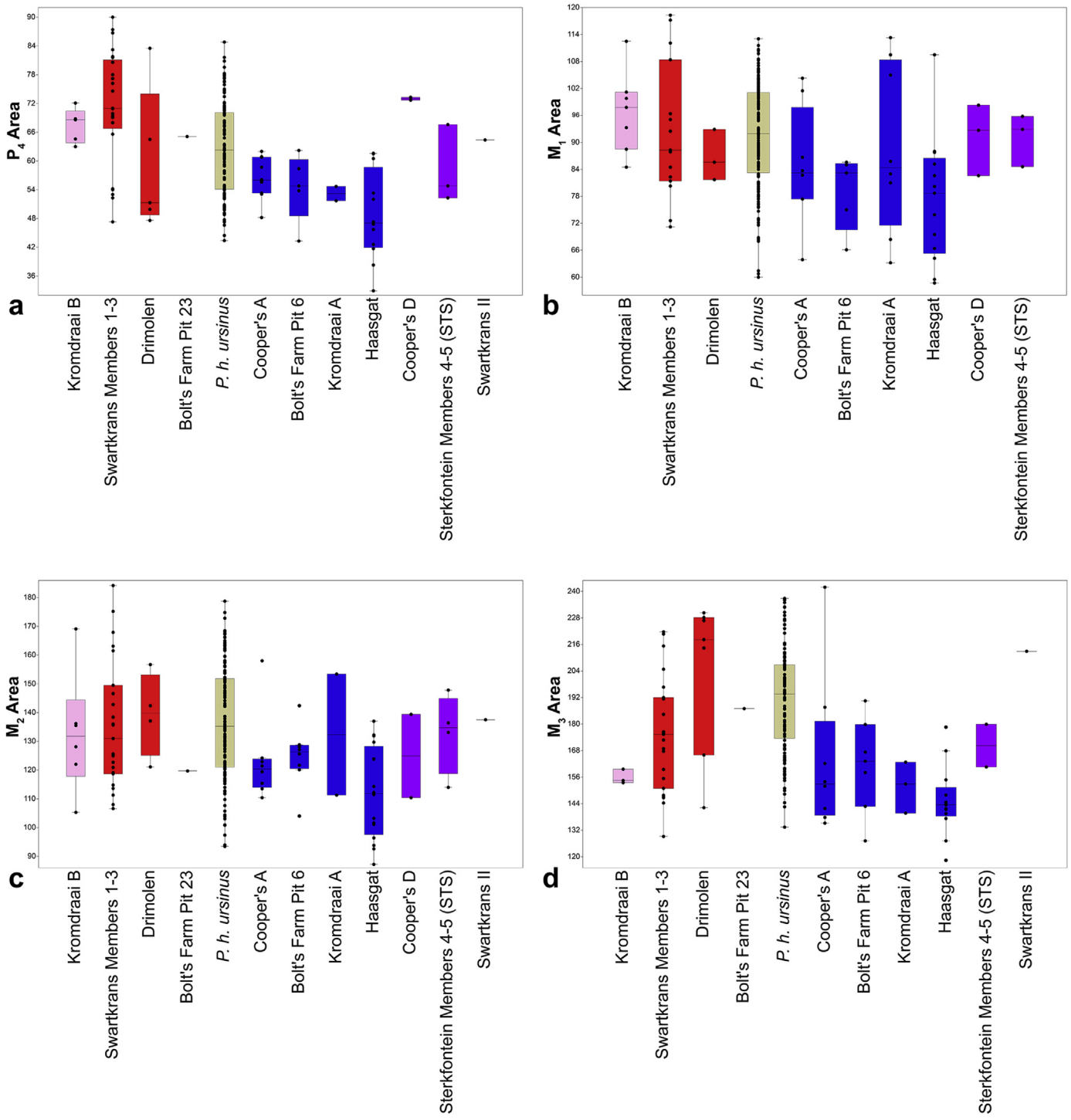

Figure 6. Boxplots illustrating dental size ranges (expressed as tooth area = maximum mesiodistal length x maximum buccolingual width) for lower P_4s and lower molars among Plio-Pleistocene South African sites and a sample of extant *P. h. ursinus* specimens. Pink indicates those populations designated as *P.* cf. *robinsoni*, red indicates those populations designated as *P. robinsoni*, blue indicates those populations designated as *P. h. angusticeps*, purple indicates those populations designated as *Papio* sp. indet., and gold indicates extant *P. h. ursinus*. For samples by tooth position, see Tables 1 and 2 and SOM Tables S1–S4.

SB 2, sharper in 3147), clear maxillary fossae that are not as deep as those of *P. h. angusticeps,* and maxillae that override the nasals and meet in the midline.

3.1.13. Bolt's Farm Pit 23 *P. robinsoni* is present at Bolt's Farm Pit 23 based on the presence of BF 38 (adult male muzzle and palate preserving partial dentition) and UCMP 56797 (adult female partial cranium with partial dentition), as previously noted by Freedman (1976) and Delson (1984, 1988) (Figs. 2–4).

3.1.14. Swartkrans Member 2 A number of fragmentary specimens are present that are most consistent with *P. robinsoni*, but lack enough of the cranium and dentition to be certain. In particular, the large size and shallow-to-moderate maxillary fossa preserved in subadult female SKX 814 is a good match for SK 562 from

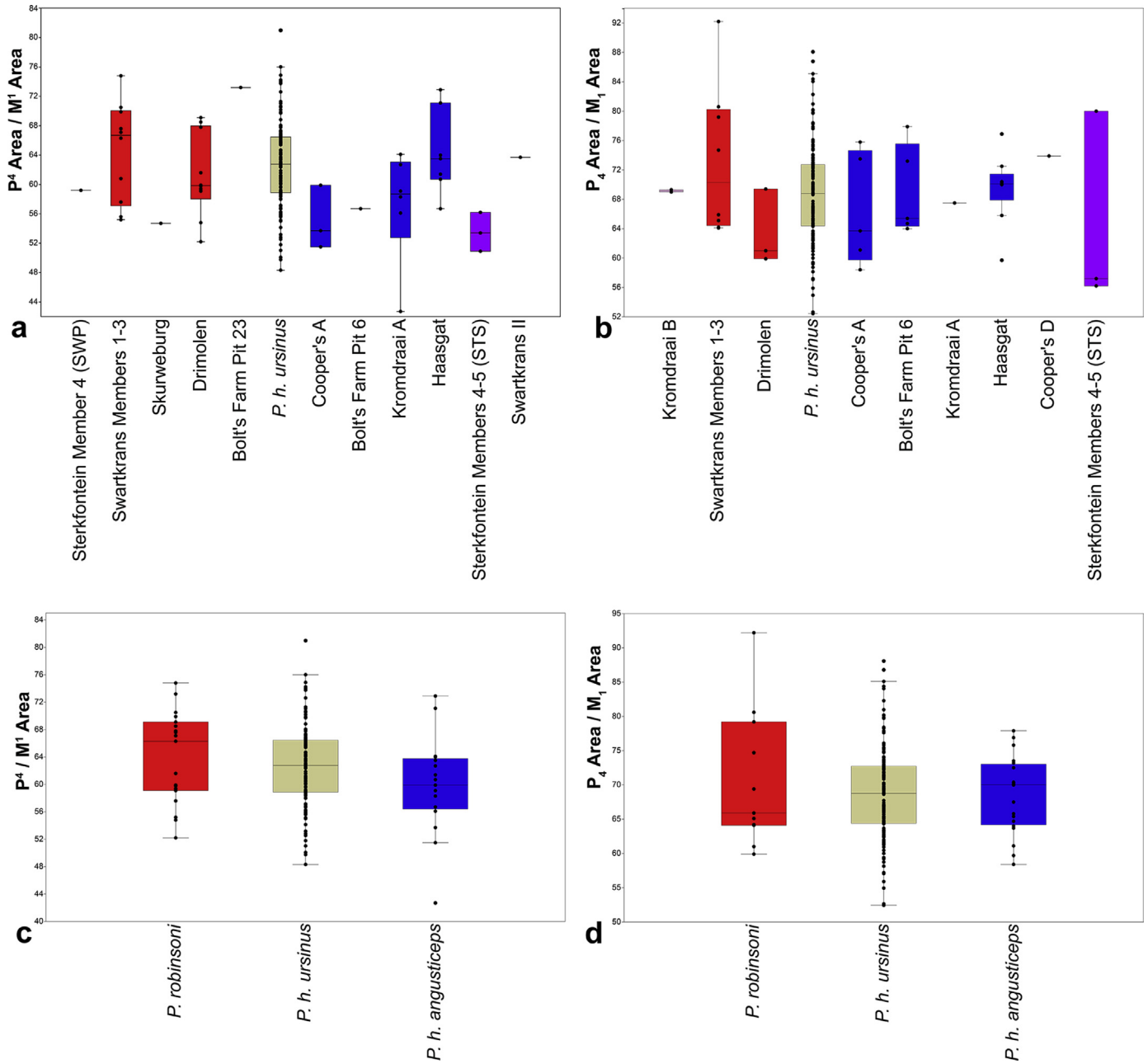

Figure 7. Boxplots illustrating dental size ranges for upper and lower P4/M1 ratios (expressed as [P4 area/M1 Area] x 100) among Plio-Pleistocene South African sites and among Plio-Pleistocene South African *Papio* taxa compared with a sample of extant *P. h. ursinus* specimens. Pink indicates those populations designated as *P.* cf. *robinsoni*, red indicates those populations designated as *P. robinsoni*, blue indicates those populations designated as *P. h. angusticeps*, purple indicates those populations designated as *Papio* sp. indet., and gold indicates extant *P. h. ursinus*. For samples by tooth position, see Tables 1 and 2 and SOM Tables S1–S4.

Member 1. Overall, the material is sufficient to suggest it is most similar to *P. robinsoni* among known papionin taxa, and we conservatively assign it to *P.* cf. *robinsoni* until more complete and definitive fossils come to light.

3.1.15. Kromdraai B Previous authors generally also recognized both *P. h. angusticeps* and *P. robinsoni* from Kromdraai B, at least tentatively (Delson, 1984, 1988; McKee et al., 1995; Heaton, 2006). There are a few specimens at Kromdraai B that are referable to the genus *Papio*, most consistent with *P. robinsoni*. KB 5416, a subadult female palate with partial dentition, is large and displays maxillary fossae that are shallow to moderate. KB 5230 is a large female mandible with shallow mandibular corpus fossae and a large P_4. KA 196 and KA 197, mandibular fragments described as "*Parapapio*" *coronatus* by Freedman (1957) but noted to be most similar to *Papio*, are considered *Papio* specimens here.[1] These specimens have since been renumbered KB 94 and KB 104, respectively, implying a revised association with KB deposits rather than those from KA. Without more definitive craniofacial material, it is not possible to assign these *Papio* specimens to any species with certainty. Overall, however, they are more consistent with *P. robinsoni* and we assign them to *P.* cf. *robinsoni* here. As with Kromdraai A, the *Papio* dental material at Kromdraai B is

[1] The holotype of *Parapapio coronatus* Broom and Robinson, 1950 - KA 195, since renumbered to KB 122 - is most likely a junior synonym of *Cercopithecoides* (Szalay and Delson, 1979; Anderson et al., 2015).

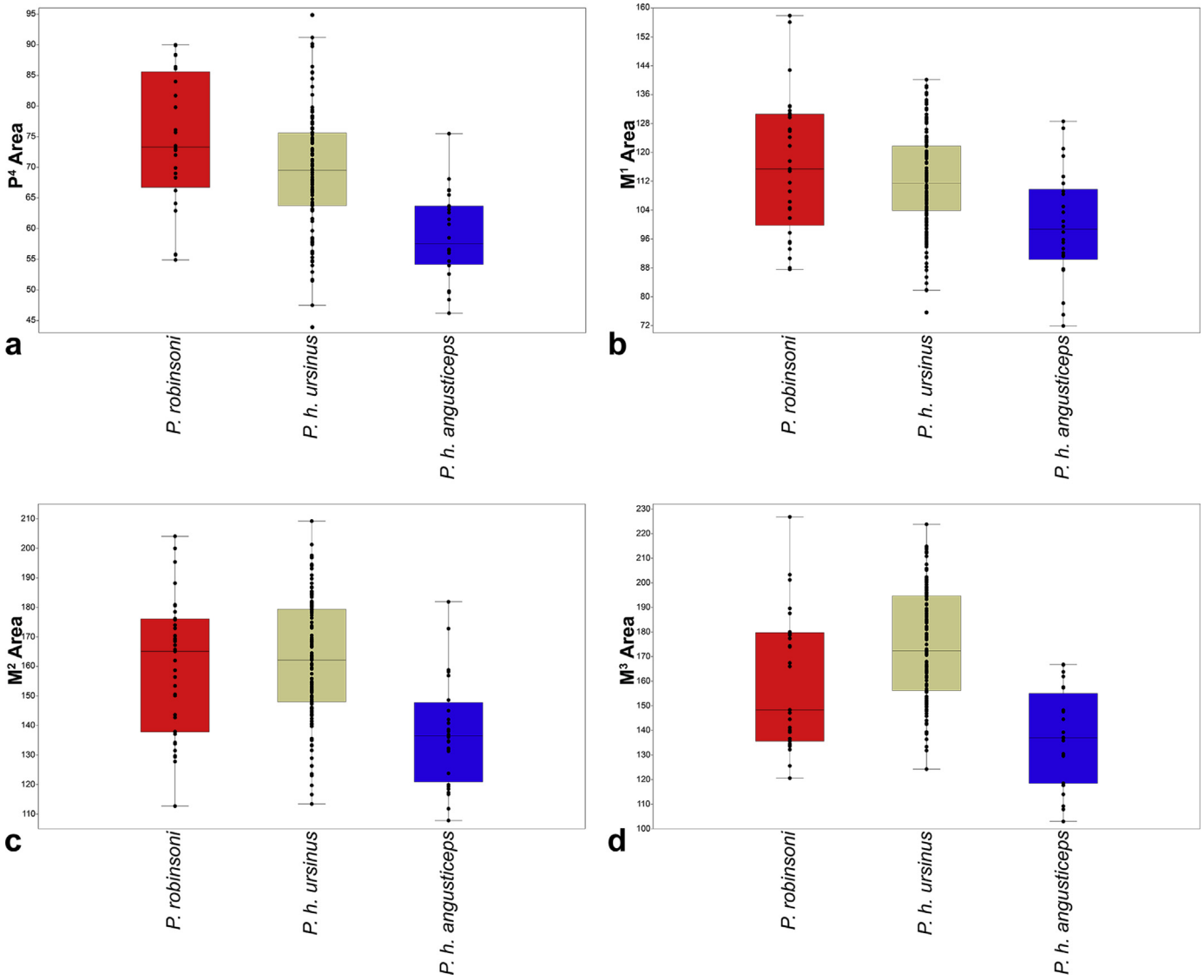

Figure 8. Boxplots illustrating dental size ranges (expressed as tooth area = maximum mesiodistal length x maximum buccolingual width) for upper P^4s and upper molars among Plio-Pleistocene South African *Papio* taxa and a sample of extant *P. h. ursinus* specimens. Red indicates those populations designated as *P. robinsoni*, blue indicates those populations designated as *P. h. angusticeps*, and gold indicates extant *P. h. ursinus*. For samples by tooth position, see Tables 1 and 2 and SOM Tables S1–S4.

consistent with a single population (Figs. 5–9), and we therefore do not find any convincing evidence at this time suggesting both *P. robinsoni* and *P. h. angusticeps* are present at Kromdraai B.

3.1.16. Bolt's Farm Pit 10? An uncatalogued right maxillary fragment with M^{2-3} that may be from Pit 10 is similar in dental size to *P. robinsoni*. The zygomatic arch is present, and its anterior face is invaded by a clear but shallow fossa, although it is hard to gauge definitively because of damage and glyptol glue. This specimen is incompatible with *Parapapio* because of the presence of the fossa and its larger size. Overall morphology is most consistent with *P. robinsoni*, and we recognize it here as *P.* cf. *robinsoni*.

3.1.17. Swartkrans II Both Freedman (1957) and Delson (1984) recorded *P. robinsoni* as present at the Swartkrans II locality on the basis of the female partial cranium SK II 25. The specimen preserves much of the left side of the face and neurocranium, parts of the right side of the face, and partial dentition. While undoubtedly a member of the genus *Papio*, the female SK II 25 is somewhat smaller than most *P. robinsoni*, it possesses a narrower muzzle, and displays smaller premolars. In fact, SK II 25 is also reminiscent of the *P. h. angusticeps* females at Cooper's A but slightly larger in size. In addition to SK II 25, the male *Papio* mandible SK II 26 displays very distinct and deep corpus fossae in contrast with the all of the *P. robinsoni* and *P.* cf. *robinsoni* mandibular material at Swartkrans Members 1-3 and Drimolen Main Quarry. Overall, the observable craniodental features are most consistent with extant *Papio* and *P. h. angusticeps*. However, the dental size of the Swartkrans II population, particularly SK II 26, is at the high end of the range of *P. h. angusticeps* and most similar to *P. robinsoni* and extant *Papio*. If SK II 26 is included in the *P. h. angusticeps* hypodigm, it would have the largest P_4 in the sample and be larger in M_3 size than all other known males except one (CO 134B/D) (Fig. 6). However, the total *P. h. angusticeps* size range would still not be larger than in extant *P. ursinus* or even *P. robinsoni* (Fig. 6). Put another way, SK II 26 would be among the largest known *P. angusticeps* individuals, but not extend the known size range of *P. h. angusticeps* in an unreasonable way. In total, this combination of size (more similar to *P. robinsoni*) and morphology (most similar to *P. h. angusticeps*) makes a definitive

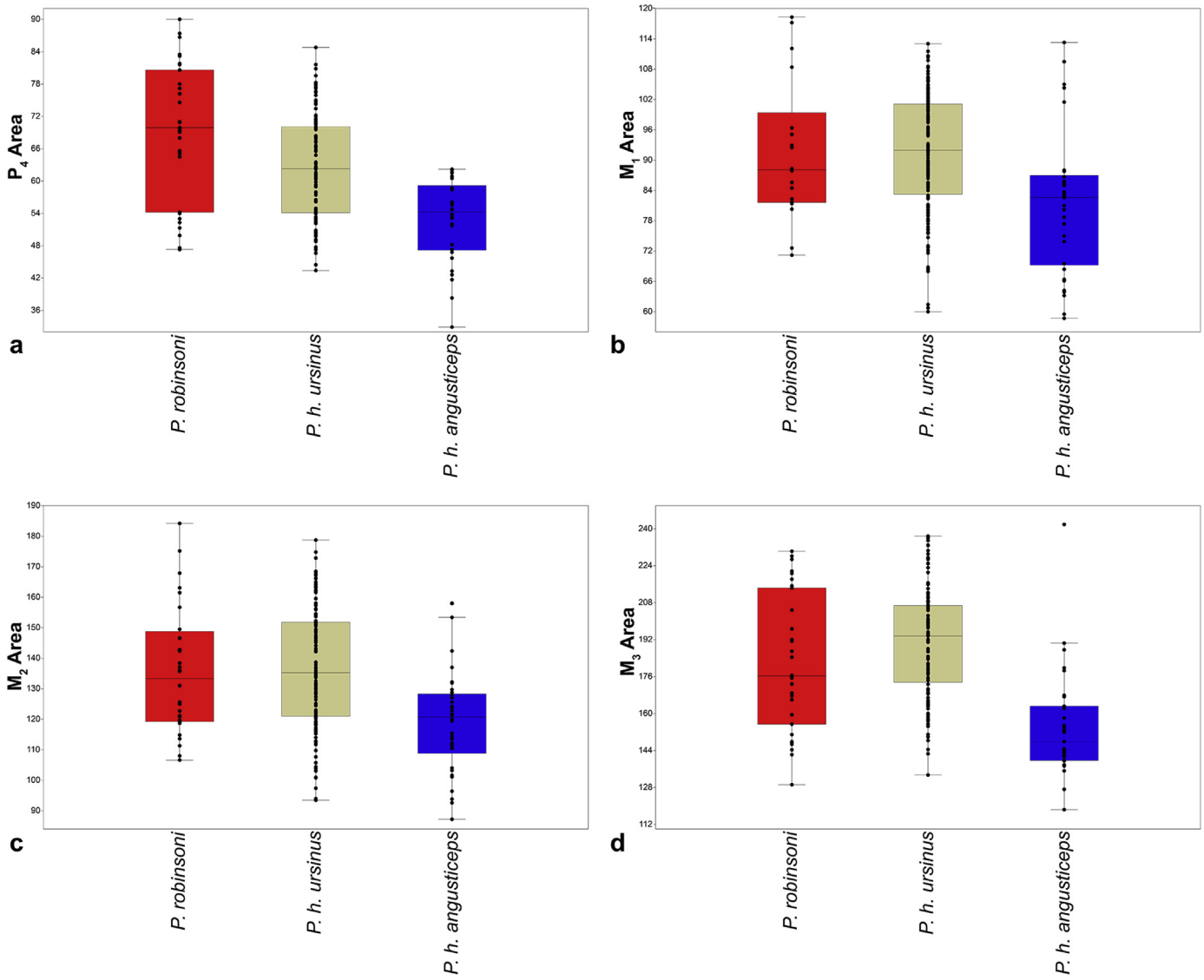

Figure 9. Boxplots illustrating dental size ranges (expressed as tooth area = maximum mesiodistal length x maximum buccolingual width) for lower P_4s and lower molars among Plio-Pleistocene South African *Papio* taxa and a sample of extant *P. h. ursinus* specimens. Red indicates those populations designated as *P. robinsoni*, blue indicates those populations designated as *P. h. angusticeps*, and gold indicates extant *P. h. ursinus*. For samples by tooth position, see Tables 1 and 2 and SOM Tables S1–S4.

species attribution difficult for the SK II series. We therefore assign this material to *Papio* sp. indet.

3.1.18. Sterkfontein Members 5 and 6 As noted above, some specimens assumed to be from Member 4 may derive from Member 5 instead (see also Heaton, 2006). There is also a male partial mandible (SWP 1232) from Member 5 displaying a long P_3 honing flange and definitive mandibular corpus fossae, typical of *Papio*. From Member 6, SWP 1012 represents a female partial mandible with deep corpus fossae below the P_3-M_1, again consistent with *Papio*. While Heaton (2006) argued that the *Papio* material from Member 5 represents *P. robinsoni*, we find none of the specimens diagnostic. Additional material is necessary to confirm which species may be present at Members 5-6. We therefore recognize these specimens as *Papio* sp. indet.

3.1.19. Swartkrans Member 3 There are a number of specimens, more fragmentary than those in Member 2, that are consistent with *P. robinsoni* in size, but potentially consistent with other *Papio* taxa or other papionin species as well. Specimens previously attributed to *P. robinsoni* from Member 3 by Delson (1988) do not preserve enough diagnostic cranial morphology to be certain. Therefore, we consider this population best allocated to Papionini gen. et sp. indet. until more complete and diagnosable material is recovered.

3.1.20. Cooper's D A small collection of isolated teeth from Cooper's D were described as cf. *Papio* sp. (Folinsbee and Reisz, 2013). Because this material is fragmentary, preserving no diagnostic features of any fossil or extant *Papio* species, and is also within the size range of *P. h. angusticeps*, *P. robinsoni*, and other papionin taxa, we conservatively assign the previously recognized *Papio* material at Cooper's D to Papionini gen. et sp. indet.

3.2. *Review of East African Plio-Pleistocene* Papio*-bearing sites*

In addition to the South African sites above, there are several in eastern Africa where *Papio* has been reported. These generally fall into two categories, middle and later Pleistocene material that is modern in overall appearance and assigned either to *Papio* sp. or one of the extant varieties (e.g., *P. hamadryas* sspp., *P. h.* cf. *anubis*, etc.), or earlier Plio-Pleistocene forms that were initially identified

as *Papio*, but subsequently allocated to other genera or are too fragmentary to identify to genus with confidence (Szalay and Delson, 1979; Jablonski, 2002; Jablonski and Frost, 2010).

3.2.1. Middle and later Pleistocene Among the more complete specimens of this group is a well-preserved partial cranium of a juvenile male (BSPG, 1931 II 26) from Bed IV or above at Olduvai that has been referred to *Papio* sp. and *P.* cf. *hamadryas* sspp. (Remane, 1925; Dietrich, 1942; Leakey, 1971; Szalay and Delson, 1979; Frost, 2014: Fig. 7). Even though it is a juvenile with the M^2 beginning to erupt, the specimen shows a clear anteorbital drop, maxillary fossae and ridges, and a flattened muzzle dorsum. A left maxilla with M^3 and left male mandibular symphysis with C–P_4 from Lemagrut Korongo and an M^2 in a small maxillary fragment from Laetoli (probably the Ngaloba Beds) that preserve clear facial fossae and other diagnostic features of *Papio* have been variously referred to *P.* cf. *neumanni*, *P. hamadryas* cf. *anubis,* and *Papio* sp. (Dietrich, 1942; Leakey and Delson, 1987; Harrison, 2011). A series of diagnostic facial material, including relatively complete male and female maxillae and mandibles, from Asbole in the Afar region of Ethiopia dated to 600 Ka was assigned to *P. hamadryas* ssp. indet. by Frost and Alemseged (2007). Morphologically the specimens are consistent with both *P. h. anubis* and *P. h. hamadryas*, but generally on the smaller end of the extant size range. Here we refer all this material from Olduvai, Laetoli, Lemagrut Korongo, and Asbole to *P. hamadryas* ssp. indet. Isolated teeth from the ca. 500 Ka Dawaitoli Formation of the Middle Awash, Ethiopia, and Members J – K of the Shungura Formation, Ethiopia have also been assigned to *Papio* sp. or *P. hamadarys* sspp., but are not diagnostic beyond being papionins similar in size to extant *P. hamadryas* (Eck, 1976, 1977; Kalb et al., 1982; Frost, 2001a; Frost, 2007a, 2007b). Overall, this material suggests that baboons similar to the extant varieties were widespread in eastern Africa by the Middle Pleistocene. Their relationship to *Papio* fossils from South Africa is unclear.

3.2.2. Earlier Plio-Pleistocene Several earlier Plio-Pleistocene specimens have been assigned to *Papio*, often as new species, but these have been subsequently allocated to other genera. Two partial crania and several other fragments from Olduvai Bed I originally described as cf. *Papio* sp. nov. by Leakey and Leakey (1976) have more recently been assigned to *Gorgopithecus major* (Gilbert et al., 2016a). Leakey and Leakey (1976) also tentatively allocated a maxilla and three partial mandibles from the Upper Burgi and Okote Members to cf. *Papio* sp. Frost (2001a) suggested this material could represent either a species of *Papio* or late occurring *Dinopithecus quadratirostris* (since transferred to *Soromandrillus quadratirostris* [Gilbert, 2013]), and thus left it as Papionini gen. et sp. indet. C. Jablonski et al. (2008), on the other hand, placed two of these (KNM-ER 143 and KNM-ER 144) in *Parapapio* sp. indet. A. and two (KNM-ER 141 and KNM-ER 142) in *Parapapio* sp. indet. B. A right dP^4 and distal humerus from Laetoli tentatively designated cf. *Papio* sp. by Leakey and Delson (1987) has been reallocated, along with a more recently discovered male right upper canine, to Papionini gen. et sp. indet. by Harrison (2011).

Leakey (1969) described a partial skull from the Baringo Chemeron Formation dated to 3.2 Ma as the type specimen of a new species, *Papio baringensis*. Since then, however, a number of studies have suggested that this specimen is morphologically most similar to *Theropithecus*, and it has been tentatively reassigned there by most authors (e.g., Eck and Jablonski, 1984, 1987; Delson and Dean, 1993; Frost, 2001a; Frost and Delson, 2002; Jablonski, 2002; Jablonski and Frost, 2010; Gilbert, 2013).

Finally, sizeable numbers of Plio-Pleistocene specimens from Omo (Usno Formation and Members A through G of the Shungura Formation) were previously referred to *Papio* sp. by Eck (1976, 1977). These largely consisted of isolated teeth, but more diagnostic material that spans Members D through lower G includes two female partial crania, a male rostrum, and several mandibular and maxillary fragments that clearly indicate a large long-faced papionin. Delson (1984), Delson and Dean (1993), and Frost (2001a) referred these more complete specimens along with the holotype cranium of *Papio quadratirostris* from the Usno Formation (Iwamoto, 1982), and a number of others from the Humpata Plateau in Angola, to *Dinopithecus*, but these authors also recognized *Dinopithecus* as a subgenus of *Papio*.[2] More recently, Gilbert (2013) transferred this material to a new genus, *Soromandrillus*, a decision we follow here. Other specimens from Omo Shungura not listed in the *Soromandrillus* hypodigm are best left as Papionini gen. et sp. indet. although many of the isolated teeth may well be *S. quadratirostris.*

3.3. Morphological analysis of revised hypodigms

To test the robusticity of our revised hypodigms for the named South African *Papio* taxa as well as our hypothesis that *P. robinsoni* and *P. h. angusticeps* do not co-occur at Kromdraai A or elsewhere, we conducted several descriptive statistical analyses. For comparison and in order to make the fewest possible changes relative to previous taxonomic schemes, all material previously reported as "*Papio*" for each site where *P. robinsoni, P. h. angusticeps,* or both had been argued to occur was lumped together into one population for analysis (see SOM Tables S1–S4 for a complete list of specimens and measurements). Our results are presented in Figures 5–9 and suggest that, with very few exceptions, the range of variation found at each site is no greater than that of extant *P. h. ursinus* collected in the past century or so. Likewise, when data across sites are combined into paleotaxa, the range of variation is again similar to that observed in *P. h. ursinus*.

In a few instances, outliers do exist. However, in these cases we note that other large papionins are present at the site in question, or surrounding sites, and the allocation of these specimens to *Papio* is only tentative. In other words, almost all outlier specimens are lacking in sufficiently diagnostic morphology to confirm their attribution to *Papio*, and therefore could represent other papionin taxa, such as *Gorgopithecus* or *Dinopithecus*. For example, SK 590 from Swartkrans Member 1 is a large maxillary fragment preserving a large M^1 and M^2 that metrically fall within the *Gorgopithecus* range as well as the *P. robinsoni* range. Likewise, SK 419 and SK 445 preserve large M_1-M_2 from Swartkrans Member 1 that are both within the *Gorgopithecus* range as well. KA 163 preserves a dP_4-M_1, with the M_1 being in the *Gorgopithecus* size range. HGD 660 is identified as an isolated M_1, and its measurements are within the *Gorgopithecus* size range, but it is also possible this specimen is an isolated M_2 instead. Finally, while CO 134 B/D exhibits a very large M_3, the other teeth in this subadult male mandible are not outliers and the M_3 may also be slightly larger due to the fact that it is unworn. There are other large teeth included in our sample that similarly overlap the range of multiple large papionin taxa, and as noted above, it is also possible that a few isolated teeth are mis-identified to position. In an effort to be conservative, we included as many specimens previously attributed to *Papio* as we could for each site, but it may ultimately be more reasonable to refer to some of the outlier specimens as Papionini gen. et sp. indet., particularly since some of them overlap the size ranges of *G. major* and *Dinopithecus ingens*, which are also known to co-occur with *P. robinsoni* or *P. h. angusticeps*

[2] Eck and Jablonski (1984, 1987) transferred the Usno Fm. holotype to *Theropithecus quadratirostris* and Jablonski (1994, 2002) considered the Angolan and Shungura specimens to be *T. baringensis.* We strongly disagree, as detailed in the cited publications.

(Freedman, 1957; Szalay and Delson, 1979; Delson, 1984, 1988; Jablonski, 2002; Jablonski and Frost, 2010).

Based on the above reassessment of fossil *Papio* species distributions and the revised hypodigms resulting from our study of the material, we also conducted a 3D geometric morphometric analysis of all three South African fossil *Papio* taxa relative to other papionins, particularly extant *P. hamadryas* ssp (Frost et al., 2003). As with previous analyses of papionin crania, allometry was the largest factor contributing to the shape variation in our sample with PC1 explaining 61% of total variance and being highly correlated with the natural log of centroid size ($r^2 = 0.87$). The second component accounted for 9.6% of the sample variance and largely separates male *Mandrillus* from other papionins (Fig. 10). The third component accounted for 6.0% of variance and seriated *Theropithecus, Macaca, Papio, Cercocebus* and *Mandrillus,* and *Lophocebus* from most positive to most negative (Fig. 10). Most of the fossil *Papio* specimens fell within the 95% confidence ellipse for extant *Papio*, but several of the *P. robinsoni* specimens and one *Papio* sp. (TMP SK II 25) fell somewhat outside. All but the last specimen are within the convex hull for extant *Papio*.

The discriminant function analysis was highly accurate among the model sample, with the cross-validation correctly classifying 98.9% of specimens. All of the *P. h. angusticeps* and *P. robinsoni* specimens that could be included were classified within extant *Papio* (Table 3). Only two of the *?P. izodi* specimens, however, were classified as *Papio,* whereas two were also classified as *Soromandrillus* and one as *Procercocebus* (Table 3). Interestingly, both *Soromandrillus* and *Procercocebus* retain primitive papionin craniodental morphologies in addition to the shared derived features linking them with extant *Cercocebus* and *Mandrillus* (e.g., shallow maxillary fossae, relatively shallow to absent mandibular corpus fossae, straight nasal bones/nasal profile; see Gilbert, 2007, 2013), perhaps indicating that *?P. izodi* shares primitive papionin shape retentions with these taxa as well.

Finally, we also performed a three-part 362 character cladistic analysis on all extant and fossil African papionins at the species level, including all three South African fossil *Papio* taxa, and treating all extant *Papio* species/subspecies populations as individual OTUs. In the first analysis, we enforced no topological constraints on the ingroup (i.e., Morphology-only) and recovered six most parsimonious trees (MPTs). The majority-rule consensus suggests that *P. h. angusticeps* and *P. robinsoni* are both likely to be nested within the modern *P. hamadryas* radiation (Fig. 11). However, the extant *P. hamadryas* taxa are reconstructed as a paraphyletic group in all MPTs and *P. robinsoni* is outside of the crown *P/L/T/R* clade in two of the six MPTs. Thus, *P. robinsoni* is also outside of the *P. hamadryas* + *Lophocebus* + *Rungwecebus* group (along with *P. h. papio*) in the strict consensus tree (Fig. 11; see SOM for all MPTs). *?P. izodi* is hypothesized as a stem *P/L/T/R* taxon in all MPTs, never being found within the modern *P. hamadrayas* radiation. *P. h. angusticeps* is reconstructed as the sister taxon to *P. h. kindae* in all MPTs, in support of Delson's (1984, 1988) observations. In the second analysis enforcing the ((*C,M*),(*T,*(*P,L,R*))) backbone, *?P. izodi* is again outside of the crown *P/L/T/R* clade in all trees, but *P. h. angusticeps* and *P. robinsoni* are always within the *P. hamadryas* clade, with *P. h. angusticeps* reconstructed as the sister taxon to a *P. robinsoni*+*P. h. hamadryas* clade at the base of the *P. hamadryas* radiation (Fig. 12; see SOM for all 14 MPTs). In the third analysis, enforcing the ((*C,M*),(*T,L,*(*P,R*))) backbone, *P. h. angusticeps* and *P. robinsoni* are again always within the *P. hamadryas* clade, in the same relative positions as in the second analysis (Fig. 13). *?P. izodi* is again never found within the crown *P/L/T/R* clade, instead being reconstructed as a late-occurring stem *P/L/T/R* taxon (Fig. 12; see SOM for all 12 MPTs). Among all analyses, bootstrap support for any clades within the larger *P/L/T/R* clade was low, except in the cases of *Theropithecus* and extant *Lophocebus* (Figs. 11–13).

In total, our results suggest that, of the four widely recognized fossil *Papio* taxa in the southern African Plio-Pleistocene fossil record, *?P. izodi* appears the most morphologically primitive and distinct from the extant population, *P. robinsoni* specimens are most often within the modern range of morphological variation, but also sometimes on the periphery or just outside the range of variation seen in extant populations, and *P. h. angusticeps* as well as *P. h. botswanae* are always included within the extant range of morphological variation. Based on these results, we offer revised diagnoses of these fossil species as well as the genus *Papio* below.

4. Systematic paleontology

Class MAMMALIA Linnaeus, 1758.
Order PRIMATES Linnaeus, 1758.
Infraorder CATARRHINI E. Geoffroy, 1812
Superfamily CERCOPITHECOIDEA Gray, 1821
Family CERCOPITHECIDAE Gray, 1821
Subfamily CERCOPITHECINAE Gray, 1821
Tribe PAPIONINI Burnett, 1828

Papio Erxleben, 1777
(= or including: *Cercopithecus* Erxleben, 1777, in part. *Cynocephalus* Geoffroy and Cuvier, 1795 (not of Boddaert, 1768). *Simia (Chaeropithecus)* Gervais, 1839; Senechal, 1839. *Choeropithecus* Blainville, 1839. *Hamadryas* Lesson, 1840 (not of Hübner, 1806). *Mandrillus* Milne-Edwards, 1841 (not of Ritgen, 1824). *Cercopithecus* Linnaeus, 1758: Peters, 1853, in part. *Choiropithecus* Reichenbach, 1862. *Theropithecus* I. Geoffroy, 1843: Reichenbach, 1863, in part (fide Napier, 1981, p. 80). *Comopithecus* Allen, 1925. *Parapapio* Jones, 1937: Broom, 1940, in part; Freedman, 1957, in part. *Papio (Chaeropithecus)* Gervais, 1839: Ellerman, Morrison–Scott and Heyman, 1953; Szalay and Delson, 1979, in part.)
Type species: *Papio hamadryas* (Linnaeus, 1758).[3]
Other included species: *?P. izodi* Gear, 1926, *P. robinsoni* Freedman, 1957.

Generic diagnosis: This diagnosis is modified from those of Freedman (1957), Szalay and Delson (1979) and Frost (2007a) on the basis of our above results. *Papio* is a genus of medium to large sized papionin monkeys that is most obviously

[3] The authorship and type species of *Papio* are part of a complicated history, most of which was laid out by Delson and Napier (1976, 1977). In brief, Linnaeus (1758) named *Simia hamadryas* with reference to "Alp. aegypt. 248″, and *Simia sphinx* citing a number of images of a short-tailed robust monkey (either a mandrill or a drill). In 1766 (12th edition), Linnaeus named *Simia cynocephalus* with reference to Brisson and to Jonstonus (1650, Fig. 59). Buffon (1766) discussed several "baboons", with illustrations of the "grand papion", interpreted as the Guinea baboon of reddish-brown color; and the greenish-yellow "petit papion", probably an olive baboon. He also discussed the mandrill, with illustrations of both male and female individuals.

Müller (1773) used the name *Papio* at the generic level for *S. sphinx* Linnaeus, now defined as the mandrill (lectotype designated by Delson and Napier, 1976). Then Erxleben (1777) used *Papio* for several Linnaean species including *Simia sphinx*, for which he mentioned both mandrills and savannah baboons (such as the two papions of Buffon); his description was of a Guinea baboon with dark-reddish fur. Desmarest (1820) named *Cynocephalus papio* for the Guinea baboon (*Cynocephalus* Geoffroy and Cuvier, 1795, for baboons is preoccupied by *Cynocephalus* Boddaert, 1768 for colugos). Delson and Napier (1976) petitioned the International Commission for Zoological Nomenclature to decide whether to use *Papio* for mandrills or baboons, and the ICZN decided for the latter alternative, upholding common usage over absolute priority (International Commission for Zoological Nomenclature, 1982).

Therefore, the type species of *Papio* Erxleben, 1777 is *P.* (ex-*C.*) *papio* (Desmarest, 1820), if all baboon varieties are considered as full species. If they are considered subspecies, as we do here, the senior synonym and nomen becomes *P.* (ex-*S.*) *hamadryas* (Linnaeus, 1758), as is usually indicated.

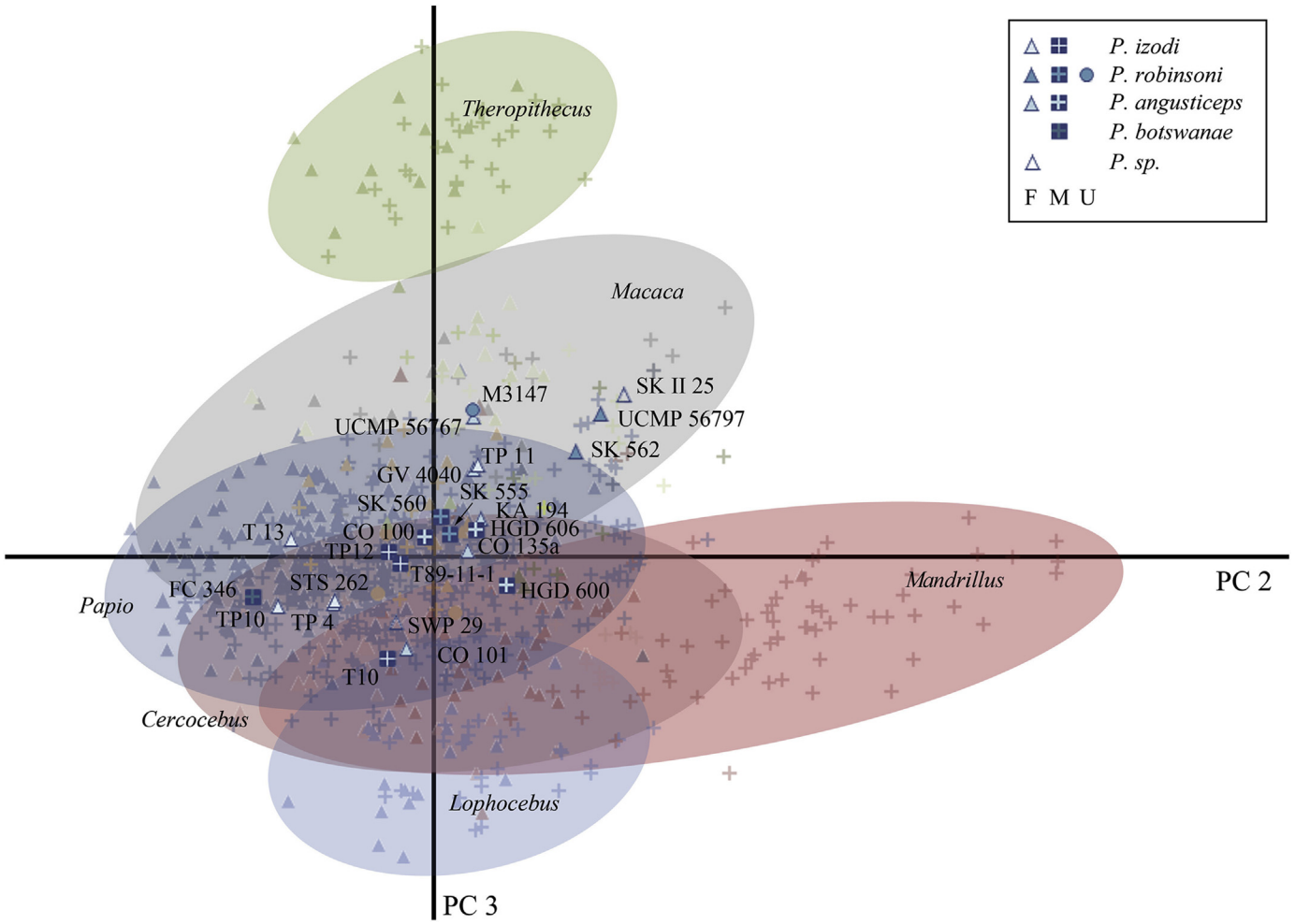

Figure 10. PCA of 3D GM analysis. Plot of PC 2 vs. PC 3 with *Papio* fossils shown and labeled (PC 1 excluded do to its strong correlation with centroid size). 95% confidence ellipses are shown for extant genera; from top to bottom: green = *Theropithecus*, gray = *Macaca*, blue = *Papio*, pink = *Cercocebus*, red = *Mandrillus*, light blue = *Lophocebus*. Note that several of the *P. robinsoni* specimens and one *Papio* sp. (TMP SK II 25) fall somewhat outside of the 95% confidence ellipse for extant *Papio*, but only SK II 25 is completely outside the convex hull for extant *Papio*. See also results of Discriminant Functions Analysis (DFA) in Table 3.

distinguished from other large papionins such as *Mandrillus, Soromandrillus, Theropithecus, Dinopithecus, Gorgopithecus*, and *Paradolichopithecus* by the combination of definitive maxillary fossae, mandibular corpus fossae, a flattened to slightly "tented" muzzle dorsum with relatively vertical sides in both males and females, and definitive maxillary ridges, especially in males. It possesses a marked anteorbital drop, which is distinct from *Parapapio, Lophocebus, Rungwecebus, Cercocebus, Procercocebus*, and most *Macaca*. Glabella and the supraorbital region is more prominent than in most papionins, but less so than in *Theropithecus*. The "squared" or slightly "tented" muzzle in cross-section is different from *T. (Theropithecus), Parapapio, Pliopapio, Gorgopithecus, Paradolichopithecus, Macaca* (other than the Sulawesi species), *Lophocebus*, *Procercocebus*, and *Cercocebus*, but shared with *T. (Omopithecus), Dinopithecus, Mandrillus*, and *Soromandrillus*. The cranial vault commonly lacks a sagittal crest, or if one is present, it is found only in the occipital region near inion. The temporal lines are typically "pinched" (converging medially along the margin of the supraorbital torus and then taking a sharp turn posteriorly; see Gilbert, 2007), particularly in males, and inion is usually inferiorly directed, unlike in *Mandrillus, Soromandrillus, Cercocebus*, and *Procercocebus*. The molars are more straight sided and the crowns less flaring than those of *Mandrillus, Lophocebus*, and *Cercocebus*, but more sloping than those of *Theropithecus*. The P4 is not typically enlarged relative to the M1 as it is in *Mandrillus*, some *Soromandrillus*, and *Cercocebus*. The incisors are relatively large compared to the molars (which is typical of many papionins), but larger than those of *Parapapio, Paradolichopithecus*, and *Theropithecus* and smaller than those of *Lophocebus* and *Cercocebus*. The postcranium is known only for the extant species and is more terrestrially adapted than other cercopithecids besides *Theropithecus*. Unlike *Theropithecus*, the hand of *Papio* does not display noticeable lengthening of manual digit ray I or shortening of manual digital ray II.

Papio hamadryas (Linnaeus, 1758).
(=: *Simia hamadryas* Linnaeus, 1758; *Simia cynamolgus* Linnaeus, 1758; *Cynocephalus wagleri* Agassiz, 1828; *Cynoscephalus hamadrias* Rüppell, 1835 (lapsus); *Hamadryas chaeropithecus* Lesson, 1840; *Theropithecus nedjo* Reichenbach, 1863 (fide Napier, 1981, p. 80); *Hamadryas aegyptiaca* Gray, 1870; *Papio arabicus* Thomas, 1899; *Papio brockmanni* Elliot, 1909; *Papio hamadryas abissinicus* Roth, 1965; *Papio hamadryas sudanensis* Roth, 1965. Including [synonyms of other subspecies, indicated as a, c, p, k, u]: *Simia cynocephalus* Linnaeus, 1766 (*Papio cyanocephalus*: Smithers, 1966; lapsus); *Simia sphinx* Erxleben, 1777 (not of Linnaeus, 1758) [p]; *Simia porcaria* Boddaert, 1787 (not of Brünnich,

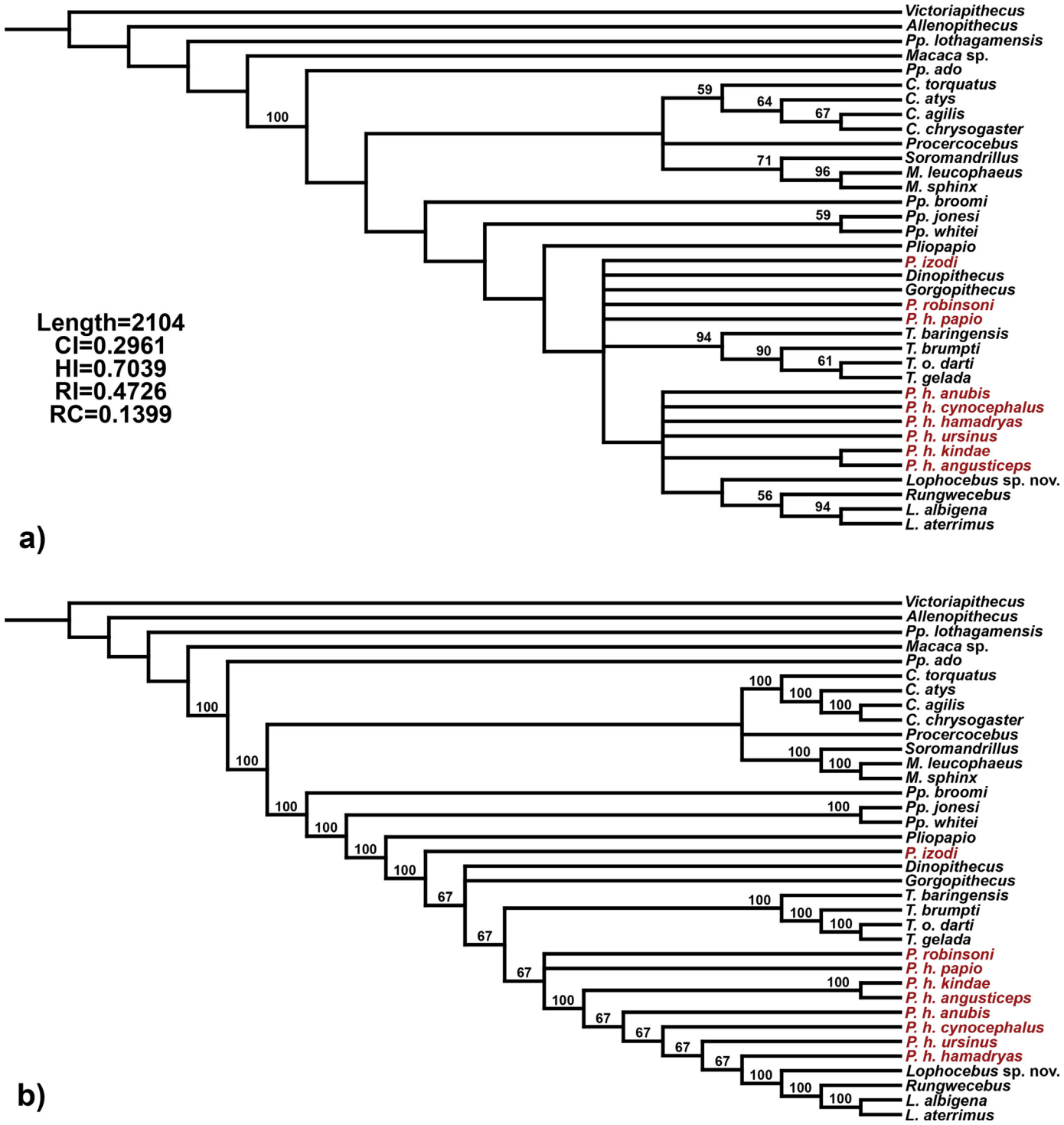

Figure 11. a) Strict consensus tree from the morphology-only analysis. Numbers above branches indicate bootstrap support over 50% for any clades. b) Majority-rule consensus tree from this analysis. Numbers above branches represent the percentage of MPTs in which a given clade is found. For matrix and individual MPTs, see SOM.

1782) (*Papio porcarius* E. Geoffroy, 1812; emendation) [u]; *Simia (Cercopithecus) hamadryas ursinus* Kerr, 1792; *Simia (Papio) variegata* Kerr, 1792 [suppressed by ICZN 1970, may be *sphinx* Linnaeus, 1758 or *cynocephalus* Linnaeus, 1766]; *Simia basiliscus* Schreber, 1800 [c]; *Simia sublutea* Shaw, 1800 [c]; *Simia sphingiola* Hermann, 1804 [u]; *Papio comatus* E. Geoffroy, 1812 [u]; *Cynocephalus papio* Desmarest, 1820; *Cynocephalus babouin* Desmarest, 1820 [c] (*Cynocephalus babuin*: Jardine, 1833; *Papio babuini*: Roth, 1965; lapsi); *Cynocephalus antiquorum* Schinz, 1821 [c]; *Cynocephalus capensis* Smith, 1826 [u]; *Simia anubis* Lesson, 1827; *Cynocephalus thoth* Ogilby, 1838 [c] (*Papio toth*: Matschie, 1898; lapsus); *Cynocephalus olivaceus* I. Geoffroy, 1851 [p]; *Papio rubescens* Temminck, 1853 [p]; *Cercopithecus ochraceus* Peters, 1853 [c] (*P. cynocephalus ochraeus*: Roth, 1965; lapsus?); *Cercopithecus flavidus* Peters, 1853 [c]; *Cynocephalus choras* Ogilby, 1838 [a]; *Cynocephalus doguera* Pucheran and Schimper, 1856 [a]; *Cynocephalus langheldi* Matschie, 1892 [c]; *Papio thoth ibeanus* Thomas, 1893 [c]; *Papio pruinosos* Thomas,

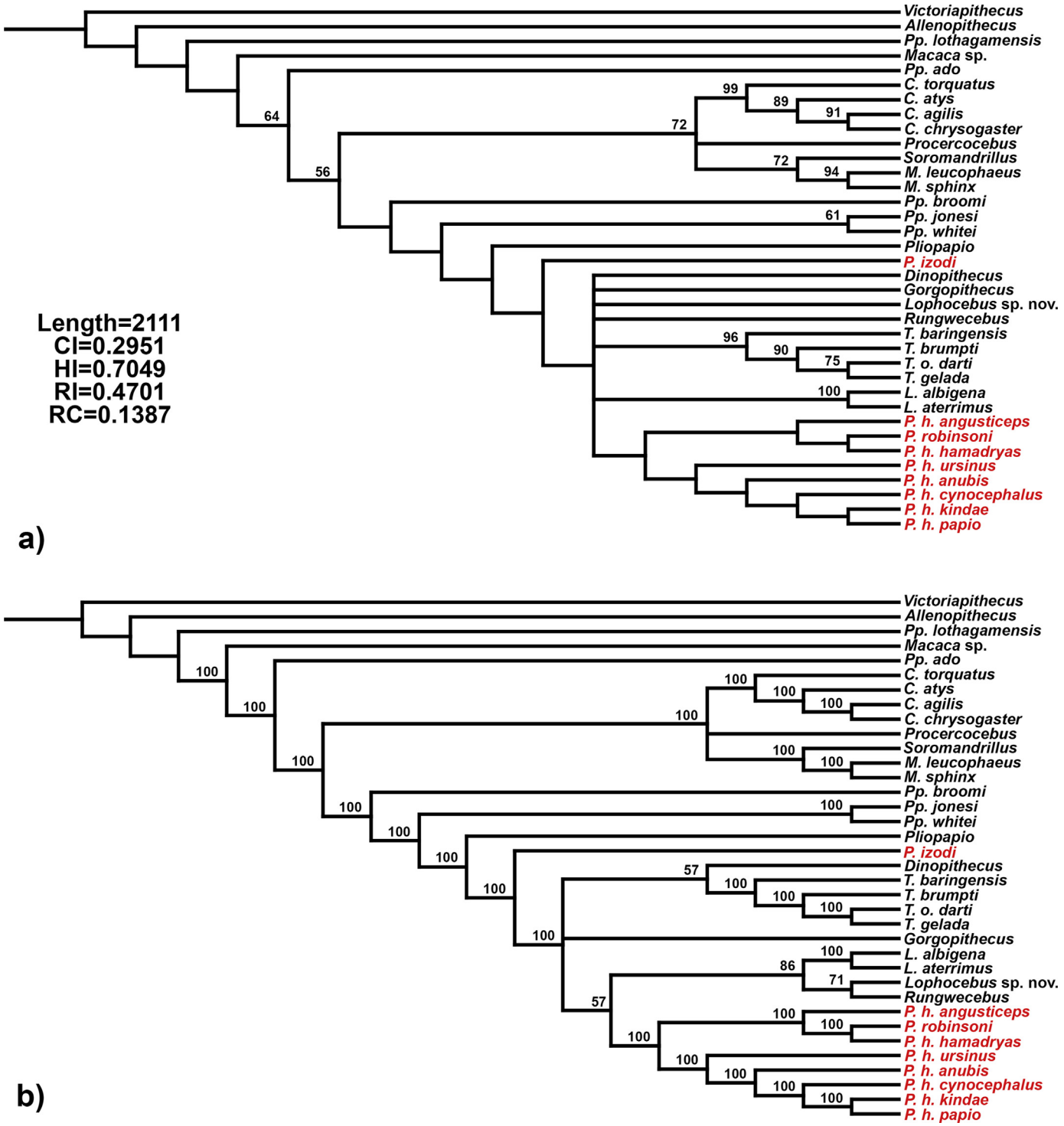

Figure 12. a) Strict consensus tree from the (*Papio, Lophocebus, Rungwecebus*) [((*C,M*),(*T,*(*P,L,R*)))] molecular backbone analysis. Numbers above branches indicate bootstrap support over 50% for any clades. b) Majority-rule consensus tree from this analysis. Numbers above branches represent the percentage of MPTs in which a given clade is found. For matrix and individual MPTs, see SOM.

1897 [a]; *Papio neumanni* Matschie, 1897 [a]; *Papio heuglini* Matschie, 1898 [a]; *Papio yokoensis* Matschie, 1900 [a]; *Papio lydekkeri* Rothschild, 1902 [a]; *P. anubis olivaceus* de Winton, 1902 [a] (not of I. Geoffroy, 1851); *Papio furax* Elliot, 1907 [a]; *Papio strepitus* Elliot, 1907 [c]; *Papio nigeriae* Elliot, 1908 [a]; *Papio tesselatum* Elliot, 1909 [a]; *Papio porcarius griseipes* Pocock, 1911 [u]; *Papio lestes* Heller, 1913 [a]; *Papio vigilis* Heller, 1913 [a]; *Papio sylvestris* Lorenz, 1915 [a]; *Papio werneri* Wettstein, 1916 [a]; *Papio graueri* Lorenz, 1917 [a]; *Choiropithecus rhodesiae* Haagner, 1918 [c]; *P. kindae* Lönnberg, 1919; *Papio porcarius orientalis* Goldblatt, 1926 [u]; *Papio porcarius occidentalis* Goldblatt, 1926 [u]; *Cynocephalus transvaalensis* Zukowsky, 1927 [u]; *Papio cynocephalus jubilaeus* Schwarz, 1928 [c]; *Papio porcarius nigripes* Roberts, 1932 [u]; *Papio porcarius ngamiensis* Roberts, 1932 [u]; *Papio porcarius chobiensis* Roberts, 1932 [u]; *Parapapio angusticeps* Broom, 1940; *Papio comatus ruacana* Shortridge,

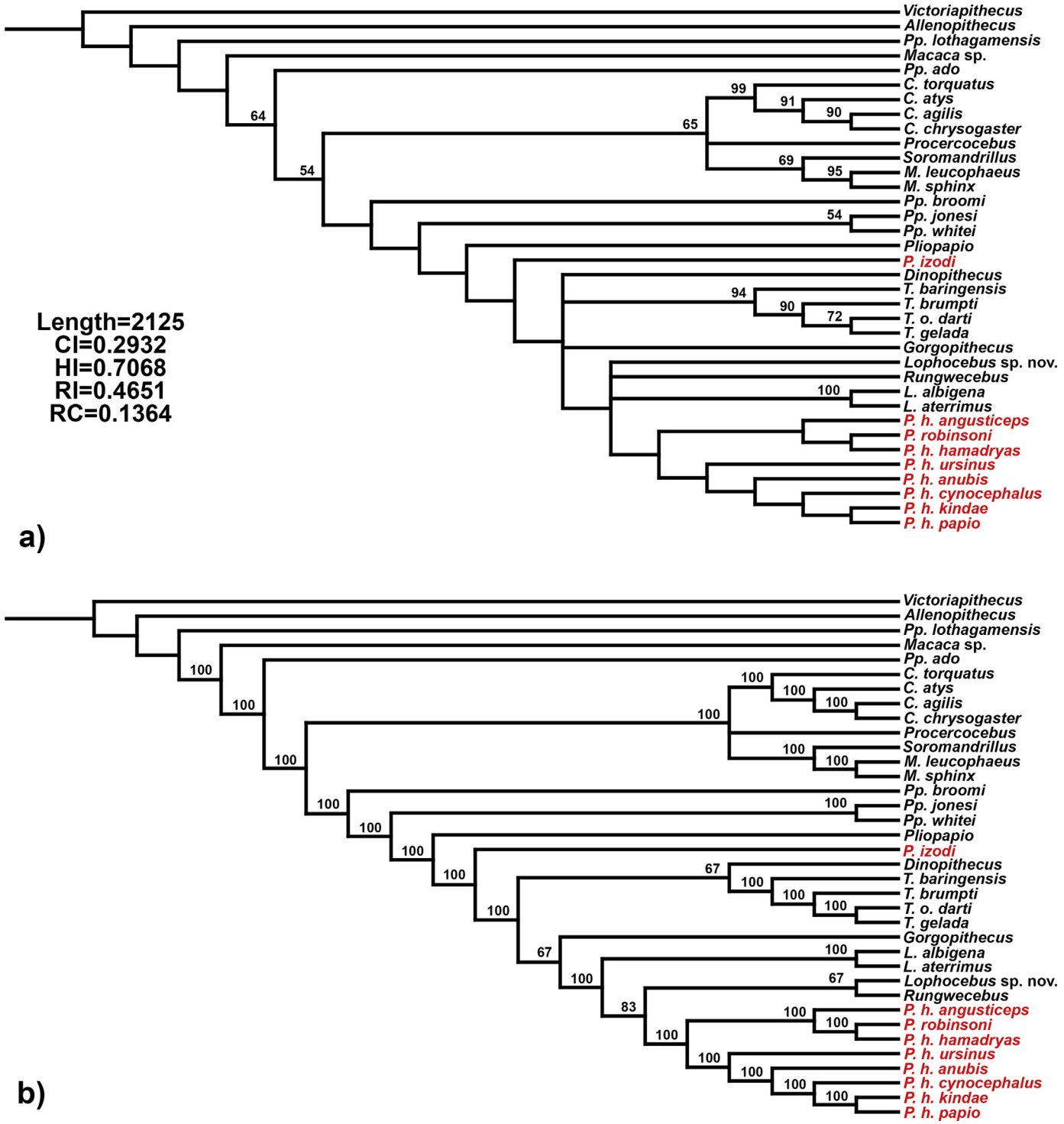

Figure 13. a) Strict consensus tree from the (*Papio, Rungwecebus*) [((*C,M*),(*T,L*,(*P,R*)))] molecular backbone analysis. Numbers above branches indicate bootstrap support over 50% for any clades. b) Majority-rule consensus tree from this analysis. Numbers above branches represent the percentage of MPTs in which a given clade is found. For matrix and individual MPTs, see SOM.

1942 [u]; *Papio ruhei* Zukowsky, 1942 [c]; *Papio angusticeps* (Broom, 1940): Freedman, 1957; *Papio doguera tibestianus* Dekeyser and Derivot, 1960 [a]; *P. ursinus chacamensis* Roth, 1965 [u] (nomen nudum); *Papio anubis niloticus* Roth, 1965 [a] (nomen nudum); *Papio izodi* Gear, 1926: Szalay and Delson, 1979, in part; *Papio hamadryas angusticeps* (Broom, 1940): Williams et al., 2012; *Papio hamadryas botswanae* Williams et al., 2012.)

Type specimen: illustration cited by Linnaeus from "Alp. aegypt. 248"

Included subspecies: *P. h. hamadryas* (Linnaeus, 1758), *P. h. cynocephalus* (Linnaeus, 1766), *P. h. ursinus* (Kerr, 1792), *P. h. papio* (Desmarest, 1820), *P. h. anubis* (Lesson, 1827), *P. h. kindae* Lönnberg, 1919; *P. h. angusticeps* (Broom, 1940), *P. h. botswanae* Williams et al., 2012.

Specific diagnosis: Differs from *?P. izodi* in the presence of deeper maxillary fossae and mandibular corpus fossae, more pronounced maxillary ridges, a definitive anteorbital drop, a relatively longer, narrower and more flattened muzzle dorsum, a relatively taller malar region, orbits and molars that are smaller relative to overall cranial size, and overall larger size (other than for *P. h. kindae*). Differs from *P. robinsoni* in that the nasals are prominent above the maxillary ridges in lateral view, the maxillary and mandibular corpus fossae are often deeper and more clearly defined, and the P^4 is smaller.

Papio robinsoni Freedman, 1957.
(= or including: *Parapapio* sp. Robinson, 1952; *Parapapio whitei* Broom, 1940: Freedman, 1957, 1976, in part; *Papio hamadryas robinsoni*: Szalay and Delson, 1979).
Type Specimen: TMP SK 555.
Specific Diagnosis:

Differs from *P. hamadryas* and *?P. izodi* in the possession of larger upper and lower P4s (on average), a flatter muzzle with the nasals positioned below the maxillary ridge in lateral view (particularly in males), shallower maxillary and mandibular corpus fossae (on average), and a high incidence of the maxillae meeting in the midline of the face before nasion. Further differs from *?P. izodi* in overall larger size, relatively smaller orbits and molars, a definitive anteorbital drop, better developed facial fossae, better developed maxillary ridges, and a relatively taller malar region.

?*Papio izodi* Gear, 1926 (new combination).
(= or including: *Papio antiquus* Haughton, 1925, in part (*Papio africanus*: Gear, 1926, lapsus: Broom, 1934; in part); *Papio izodi* Gear, 1926; *Parapapio izodi* (Gear, 1926): Broom, 1940, in part; *Parapapio antiquus* (Haughton, 1925): Broom, 1948, in part, Freedman, 1957, in part; *Papio antiquus* Haughton, 1925: Gear, 1958, in part; *Papio wellsi* Freedman, 1961; *P. whitei* Broom, 1940: Freedman, 1965, in part.
Type Specimen: UW-AD 992 lectotype (Jones, 1937).

Specific Diagnosis: Differs from *P. hamadryas* and *P. robinsoni* in possessing variably developed maxillary ridges (i.e., absent to moderately developed in males and females), variably developed maxillary fossae (absent to moderately developed in males and females), weak to absent mandibular corpus fossae (in both sexes), a relatively shorter and broader rostrum, a more weakly developed to absent anteorbial drop, a relatively short malar region, and relatively large orbits and molars. Differs further from *P. robinsoni* in smaller cranial size. Differs further from *P. hamadryas* by displaying a relatively large dentition.

5. Discussion

After consideration of the relevant morphology, we conclude that *?P. izodi* is not definitively a member of the genus *Papio* (possibly necessitating a new genus), and that *P. robinsoni* and *P. h. angusticeps* are successively derived towards extant *Papio* populations, with *P. h. angusticeps* almost certainly a member of the modern species and possibly *P. robinsoni* as well. The inclusion of *?P. izodi* within the genus *Papio* would require a morphological expansion of the genus to include features such as relatively large orbits (and molars), variable facial fossae, the expression of weak to no maxillary ridges in males and females, a short malar region, and the variable expression of an anteorbital drop (see also Gilbert, 2013; Gilbert et al., 2015). We interpret many of these features as more "primitive" and distinct compared to those expressed by modern *Papio*, and our comprehensive morphometric and cladistic analyses also support this interpretation. At the same time, *?P. izodi* is generalized enough to have potentially given rise to *Papio* sensu stricto, and it does variably express a number of cranial features consistent with the extant genus relative to the more primitive *Parapapio* species. In addition, the only known postcranial specimen attributable to *?P. izodi* from Taung (a partial humerus) also displays features consistent with extant *Papio* (Gilbert et al., 2016b). Thus, while it seems clear that *?P. izodi* is derived relative to other fossil African papionin taxa (such as *Parapapio*), it is not clear whether it is a member of the genus *Papio*, a generalized member of the crown *P/L/R/T* clade, or simply a late occurring stem *P/L/R/T* taxon.

Another taxon that has previously been included within the genus *Papio*, most often as a subgenus, is *Dinopithecus*. Our cladistic analysis, as well as those by Gilbert (2008, 2013) and Gilbert et al. (2016a), strongly suggests that *Dinopithecus* lies outside of the genus *Papio* and finds the evidence for *Dinopithecus* as a crown vs. stem member of the *P/L/R/T* clade equivocal. Similar to *?P. izodi*, *Dinopithecus* displays weak facial fossae, which we interpret as a conservative retention. It is true that what is preserved of the male cranium SK 599 looks very similar to those regions of a modern *P. hamadryas* specimen, particularly in dorsal view, but differences exist in the basicranium (see Gilbert, 2013), and there is too little morphology present to know just how similar or different the entire skull would have been. Thus, we recognize *Dinopithecus* as a separate genus from *Papio*, pending additional fossil evidence.

The other taxa discussed here are undoubtedly closely related to the modern baboon *P. hamadryas*, and therefore members of the genus *Papio*, but seemingly differ in degree in terms of their morphological similarity to the extant populations. On the basis of our analyses, we formally recognize *P. h. angusticeps* as a clear member of the modern radiation as initially suggested by Delson (1984, 1988) and supported by Frost (2007a, 2007b) and Gilbert et al. (2015) (see diagnosis above). All morphometric and cladistic analyses place the various *P. h. angusticeps* specimens within the modern *P. hamadryas* radiation, and there is little justification for its continued separation at the specific level if the BSC is being used. *P. robinsoni*, on the other hand, is slightly different from the modern taxa in terms of shape, and in the Morphology-only trees it falls outside of the rest of the modern *Papio* taxa in one-third of the MPTs (2 out of 6 trees; see SOM). However, it is classified as a member of extant *Papio* in our morphometric DFA and placed within the monophyletic *Papio* clade in all MPTs when a molecular backbone is enforced, illustrating its overall similarity to the modern taxa. Again, if a biological species concept is being used, one could probably make a good argument for placing *P. robinsoni* within the modern species (i.e., *P. h. robinsoni*), but it could be equally argued that specific rank should be maintained (*P. robinsoni*). Here we favor the latter taxonomic arrangement to reflect its possibly more primitive status compared to *P. h. angusticeps* and its consistent expression of morphological features found at much lower frequencies in modern *P. hamadryas*. However, we also admit that a taxonomic scheme recognizing *P. h. robinsoni* is almost equally compelling given the results of our analyses, and it could be argued that *P. h. ursinus* is, in some ways, just as morphologically distinct from the other *P. hamadryas* subspecies as is *P. robinsoni*. Thus, we consider both *P. robinsoni* and *P. h. robinsoni* to be acceptable and, essentially, equivalent alternatives, with one of us (ED) preferring *P. h. robinsoni*.

Our revised classification has some repercussions for our understanding of the evolution of the genus *Papio*. We find no compelling craniodental evidence to support more than one definitive fossil *Papio* taxon at any site during the Pliocene or Early Pleistocene. *P. robinsoni* and *P. h. angusticeps* do not appear to co-occur at any South African Plio-Pleistocene site, and previous recognition of both taxa at Cooper's A and Kromdraai A and B was mainly based on large or small fragmentary specimens that do not expand the range of dental size variation beyond that expected for a

single population of modern *P. h. ursinus* (Figs. 5–9), particularly when the effects of time-averaging are considered. Perhaps most convincingly, the size ranges of upper and lower P4s at each site are well within what one would expect in a modern *P. h. ursinus* population; because *P. robinsoni* has been specifically noted to possess larger premolars than other fossil *Parapapio* and *Papio* taxa (see above), one might expect to see an obvious bimodal distribution or abnormally large range if two taxa were present (Figs. 5–9).

In a few of our metric dental comparisons, there are one or two specimens that extend the range of the fossil populations significantly, usually in the larger size direction (e.g., Swartkrans M^1, Swartkrans M_1, M_2, Kromdraai A M_1, Haasgat M_1). In these cases, we again note that in an effort to be conservative, we followed previously published taxonomic IDs for *Papio* at all of the sites as much as possible (e.g., Freedman, 1957; Delson, 1984). However, particularly in the case of Swartkrans and Kromdraai A, there are other large papionins present that could account for some of the large isolated teeth and/or maxillary/mandibular fragments previously included in *Papio*, namely *G. major* and *D. ingens* (see also above). In fact, out of all specimens examined with known provenience, we excluded only two fossils from our analyses, both P_4's previously referred to *Papio* sp. (SK 434 and SKX 35315/16). We excluded them because they were larger than the known P_4 range for *G. major*, making an attribution to any specific large papionin tenuous at best. It is quite possible that other fragmentary specimens may belong to other large papionin taxa at these sites as well (some perhaps previously unrecognized, e.g., at Haasgat), so the resulting lack of significant range extension beyond that seen in extant *P. h. ursinus* even with possible taxonomic mixing and time-averaging is particularly compelling.

The lack of co-occurrence between *P. h. angusticeps* and *P. robinsoni* is a notable conclusion of this study given that these taxa have been argued to co-occur for 60 years since the landmark study by Freedman (1957) (see Table 9 for revised distribution of fossil *Papio* taxa). However, multiple hypotheses can be envisioned for why these two taxa do not co-occur. For example, the lack of co-occurrence could be due to fluctuations in climate and environment resulting in a range shift among these fossil *Papio* populations. A modern analog might be considered between adjacent *P. hamadryas* populations: if climate change resulted in the breakdown of a river or forest barrier, for instance, it is quite possible that *P. h. ursinus* and adjacent *P. h. cynocephalus* ranges might also change slightly to the north or south, respectively. Over thousands or hundreds of thousands of years and many climatic cycles, such events could happen multiple times. If some individuals were preserved as fossils during these events, in an intermediate zone of range overlap the result would be the alternation of *P. h. ursinus* and *P. h. cynocephalus* at different localities. Note that if these climatic fluctuations occurred on the level of thousands of years, this would appear as a geological instant in the fossil record, and such populations or sites would likely be indistinguishable from each other, thus accounting for differing taxa at sites of approximately the same age. Yet another hypothesis might involve range extensions with interbreeding and asymmetrical gene flow similar to what is thought to be occurring between *P. h. anubis* and *P. h. cynocephalus* populations in southern Kenya today, where *P. h. anubis* may be expanding its range into that of *P. h. cynocephalus* (Charpentier et al., 2012). Other baboon hybrid zones appear to be quite dynamic as well (Bergman et al., 2008; Jolly et al., 2011). If these populations were to be preserved as fossils, they would also preserve a chaotic pattern of occurrence. Regardless of the cause, if *P. robinsoni* and *P. h. angusticeps* really were allotaxa, it might argue for subspecific status for the former taxon as it would suggest they were ecologically exclusionary, whereas more distinct taxa might be better able to overlap.

Another interesting observation from the above morphological analyses is that, if truly reflective of the primitive condition for the genus *Papio*, the shared morphology of *P. robinsoni* and *P. h. angusticeps* suggests that *P. h. ursinus* is derived in its cranial morphology despite being consistently reconstructed as the first *P. hamadryas* subspecies to diverge from others in mitochondrial-based molecular phylogenetic analyses (Newman et al., 2004; Wildman et al., 2004; Zinner et al., 2009, 2013). *P. robinsoni* and *P. h. angusticeps* look morphometrically and qualitatively most similar to *P. h. anubis*/*P. h. hamadryas* and *P. h. cynocephalus*/*P. h. kindae*, respectively, in features such as the less klynorhynch facial orientation (Frost et al., 2003; Leigh, 2006), overall broader cranium, and less peaked maxillary ridges. In fact, the distinctive *P. h. ursinus* morphology does not appear in the fossil record until

Table 9
Distribution of fossil *Papio* taxa across Plio-Pleistocene African sites. "T" = type locality of taxon.

	Papio robinsoni	*Papio hamadryas angusticeps*	*Papio hamadryas botswanae*	*Papio hamadryas* sspp.	*?Papio izodi*	*Papio* sp. indet.	*Papionini* gen. et sp. indet.	Total# of *Papio* species present
!Ncumtsa			T					1
Asbole				X				1
Bolt's Farm Pit 10	cf.							1
Bolt's Farm Pit 23	X							1
Bolt's Farm Pit 6		X						1
Cooper's "A"		X						1
Cooper's D							X	1
Drimolen	X							1
Gladysvale		X			cf.			2
Haasgat		X						1
Kromdraai A		T						1
Kromdraai B	cf.							1
Lemagrut Korongo				X				1
Malapa		X						1
Middle Awash, Dawaitoli Fm.				cf.				1
Olduvai Bed IV or above				X				1
Skurweburg	X							1
Sterkfontein Mb. 5						X		1
Sterkfontein Mb. 2					X			1
Sterkfontein Mb. 4					X	X		2
Swartkrans II						X		1
Swartkrans Mb. 1	T							1
Swartkrans Mb. 2	cf.							1
Swartkrans Mb. 3							X	1
Taung					T			1

the late Pleistocene or Holocene (Freedman, 1965). Cladistically, *P. robinsoni* most often falls closest to *P. h. papio* or *P. h. hamadryas*, while *P. h. angusticeps* is sister to *P. h. kindae* or *P. h. hamadryas* + *P. robinsoni*, although the morphological characters uniting these taxa are unclear and *P. h. papio* and *P. h. hamadryas* represent the two extant taxa with the lowest sample sizes. Thus, some of the features uniting these taxa cladistically may be an artifact of coding issues resulting from low sample sizes and missing data as generally discussed in Gilbert (2013). Overall, the morphology of *P. robinsoni* and *P. h. angusticeps* suggest that, although *P. h. ursinus* appears to have been the first of the modern populations to diverge genetically, it does not retain the ancestral cranial morphology for extant baboons and, instead, is likely to be more derived in its cranial morphology compared to other extant *Papio* species/subspecies such as *P. h. anubis*, *P. h. cynocephalus*, and *P. h. kindae*. Based on their morphological similarity to *P. robinsoni* and *P. h. angusticeps*, we consider *P. h. anubis* and *P. h. cynocephalus*, in particular, as the extant taxa retaining the highest number of ancestral craniodental morphologies.

While we find no evidence that *P. robinsoni* and *P. h. angusticeps* co-occur at any specific site, it is possible that *?P. izodi* and an indeterminate *Papio* species both appear at Sterkfontein Member 4 (Table 9, Fig. 14). It is also possible that *P. h. angusticeps* and *?P. izodi* co-occur at Gladysvale (Table 9, Fig. 14), although the provenance of the two specimens relative to each other is unclear. Given the presence of very large and derived *Theropithecus* dentition at Gladysvale, this implies at least part of this assemblage is younger than 1.5 Ma, and possibly even Middle Pleistocene (see also Berger and Tobias, 1994; Lacruz et al., 2002; Pickering et al., 2007), whereas the last appearance for *?P. izodi* would otherwise be Sterkfontein Mb. 4 or Taung. Therefore, in the absence of more definitive evidence regarding the exact provenance of the primate specimens and the span of time represented by the different deposits at Gladysvale, it seems probable that *?P. izodi* and *P. h. angusticeps* do not co-occur.

Based on the distribution of *P. robinsoni* and *P. h. angusticeps* across South African sites (Table 9; Fig. 14), it appears that the first appearance datum (FAD) of modern baboons (*P. hamadryas* ssp.) is close to ~2 Ma and perhaps slightly before (~2.4–2.0), as evidenced

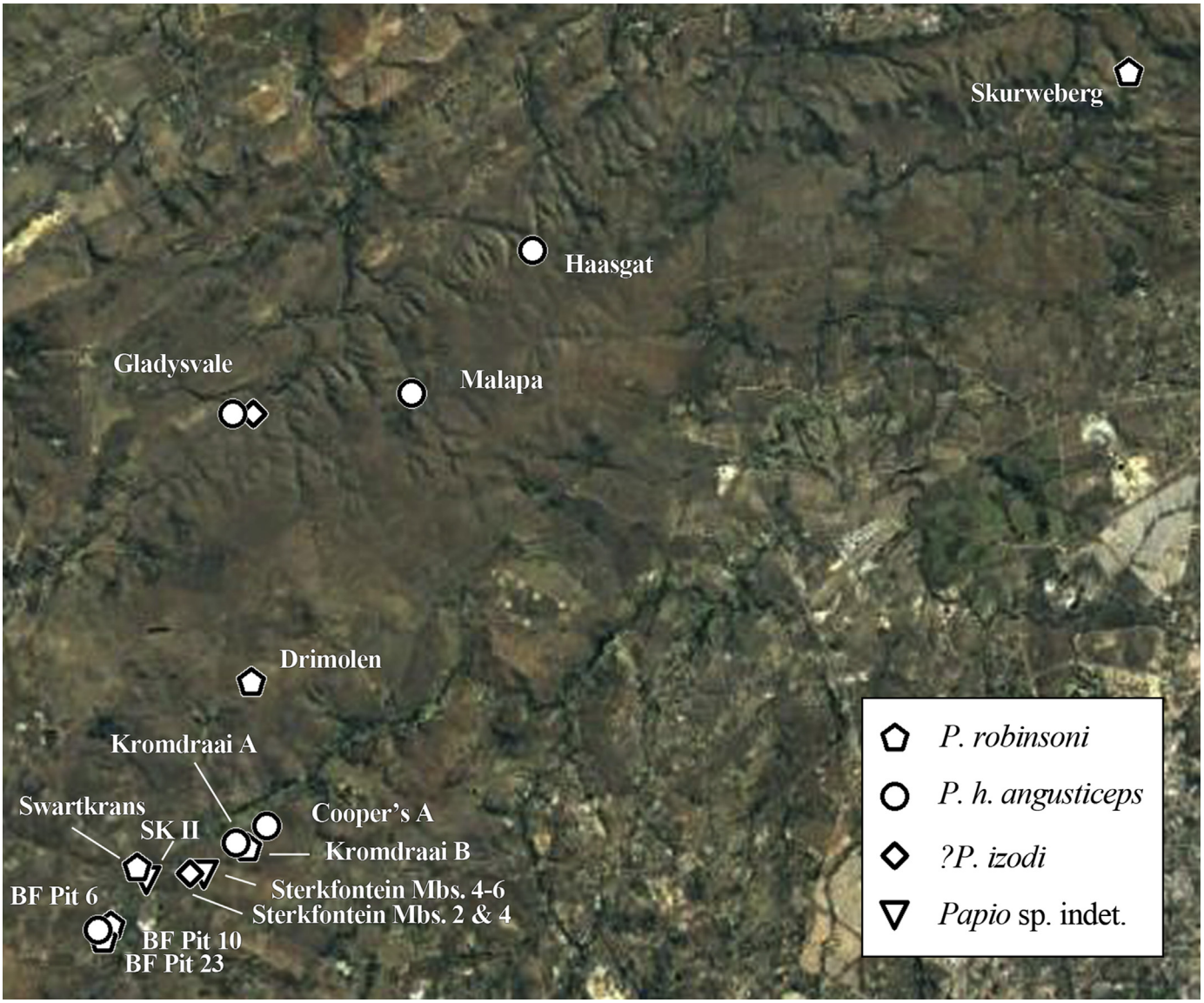

Figure 14. Map illustrating the distribution of South African fossil *Papio* taxa across sites in the Krugersdorp "Cradle of Humankind" region: circles = *P. h. angusticeps*, pentagons = *P. robinsoni*, diamonds = *?P. izodi*, and triangles = *Papio* sp. indet.

by the oldest populations of *P. h. angusticeps* at Malapa and Haasgat (Adams et al., 2013; Herries et al., 2014; Gilbert et al., 2015). A broader definition of *P. hamadryas* including *P. robinsoni* might place the FAD slightly earlier still, ~2.5–2.0 Ma if *P. robinsoni* is confirmed as the derived *Papio* species at Sterkfontein Member 4 and depending on revision to the geochronology and biochronology at other sites where *P. robinsoni* is found, such as Drimolen Main Quarry (e.g., see Adams et al., 2016) and Skurweberg. Interestingly, the FAD of both taxa overlaps the range of recent molecular clock estimates for the evolution of the extant *P. hamadryas* radiation, ~2.2–1.8 Ma (Newman et al., 2004; Wildman et al., 2004; Zinner et al., 2009, 2013), providing additional evidence that they are probably close to the origin of the modern species/subspecies (Gilbert et al., 2015). This FAD for modern *Papio* also parallels the FAD (approximately 2.0 Ma) of its close relative *Lophocebus* (at least that based on material with solid provenance) (Jablonski et al., 2008). Currently, no definitive fossil *Papio* specimens are known from eastern Africa until the Middle Pleistocene, which seems to suggest that the genus arose in southern Africa and subsequently migrated northwards.

If molecular divergence date estimates as well as the fossil record are accurate, there is good evidence to suggest that ~2.4–2.0 Ma is a reasonable FAD for the genus *Papio*, and this information may be useful in future biochronological analyses. In total, the current evidence suggests that unquestioned members of the genus *Papio* are not found in deposits much older than 2.0 million years, perhaps providing a maximum age-limit to new deposits where fossil *Papio* specimens are identified along with other fauna, such as hominins.

Acknowledgments

We thank the following people and institutions for access to specimens in their care: TMP (S. Potze), CGS (J. Hemingway, A. Kegley, J. Adams), BPI (L. Berger, B. Zipfel, B. Rubidge), UW-AD (B. Zipfel, J. Hemingway), ESI (L. Berger, C. Steininger, B. Zipfel, C. Menter, J. Heaton), SAM (R. Govender, G. Avery, K. van Willingh), NMT (COSTECH), KNM (E. Mbua, K. Manthi), NME (ARCCH, G. Senishaw, T. Getachew, Y. Asseffa, Z. Alemseged, J.-R. Boisserie, Y. Haile-Selassie, W. Kimbel, K. Reed, S. Semaw, T. White), NHMUK (R. Kruszynski), MB (T. Schossleitner, F. Bibi), UCMP (the late D.E. Savage, P. Holroyd, L. Hlusko), and AMNH (Neil Duncan, Eileen Westwig, Eleanor Hoeger). Sarah Elton and two anonymous reviewers provided helpful comments that greatly improved this manuscript. This study was generously supported by the Wenner-Gren Foundation (Research Grant #8523 and Hunt Fellowship #8928), the PSC-CUNY faculty research award program, Hunter College, the University of Oregon, and NSF 0966166 (NYCEP IGERT). This is NYCEP Morphometrics contribution number 105.

Supplementary Online Material

Supplementary online material related to this article can be found at https://doi.org/10.1016/j.jhevol.2018.04.012.

References

Adams, J.W., 2012. A revised listing of fossil mammals from the Haasgat cave system *ex situ* deposits (HGD), South Africa. Palaeontologia Electronica 15, 29A.
Adams, J.W., Kegley, A.D.T., Krigbaum, J., 2013. New faunal stable carbon isotope data from the Haasgat HGD assemblage, South Africa, including the first reported values for *Papio angusticeps* and *Cercopithecoides haasgati*. Journal of Human Evolution 64, 693–698.
Adams, J.W., Rovinsky, D.S., Herries, A.I.R., Menter, C.G., 2016. Macromammalian faunas, biochronology and palaeoecology of the early Pleistocene Main Quarry hominin-bearing deposits of the Drimolen Palaeocave System, South Africa. PeerJ 4, e1941.
Anderson, M., Frost, S.R., Gilbert, C.C., Delson, E., 2015. Cranial shape and intrageneric diversity in the genus *Cercopithecoides*. American Journal of Physical Anthropology 156(S60), 69.
Benefit, B.R., 1987. The molar morphology, natural history, and phylogenetic position of the middle Miocene monkey *Victoriapithecus*. Ph.D. Dissertation, New York University.
Benefit, B.R., 1993. The permanent dentition and phylogenetic position of *Victoriapithecus* from Maboko Island, Kenya. Journal of Human Evolution 25, 83–172.
Benefit, B.R., McCrossin, M.L., 1991. Ancestral facial morphology of Old World higher primates. Proceedings of the National Academy of Sciences of the USA 88, 5267–5271.
Benefit, B.R., McCrossin, M.L., 1997. Earliest known Old World monkey skull. Nature 388, 368–371.
Berger, L.R., 1993. A preliminary estimate of the age of the Gladysvale australopithecine site. Palaeontologia Africana 30, 51–55.
Berger, L.R., Keyser, A.W., Tobias, P.V., 1993. Brief Communication: Gladysvale: first early hominid site discovered in South Africa since 1948. American Journal of Physical Anthropology 92, 107–111.
Berger, L.R., Tobias, P.V., 1994. New discoveries at the early hominin site of Gladysvale, South Africa. South African Journal of Science 90, 223–226.
Bergman, T.J., Phillips-Conroy, J.E., Jolly, C.J., 2008. Behavioral variation and reproductive success of male baboons (*Papio anubis-Papio hamadryas*) in a hybrid social group. American Journal of Primatology 70, 136–147.
Boddaert, P., 1768. Dierkundig Mengelwerk Vol. II. Utrecht.
Bookstein, F.L., 1991. Morphometric Tools for Landmark Data: Geometry and Biology. Cambridge University Press, New York.
Broom, R., 1936. A new fossil baboon from the Transvaal. Annals of the Transvaal Museum 18, 393–396.
Broom, R., 1940. The South African Pleistocene ceropithecid apes. Annals of the Transvaal Museum 20, 89–100.
Buffon, G. L. L. de, 1766. Histoire Naturelle, Générale et Particulière, avec la Description du Cabinet du Roi, vol. 14. L'Imprimerie Royale, Paris.
Burrell, A.S., 2008. Phylogenetics and population genetics of central African baboons. Ph.D. Dissertation, New York University.
Burrell, A.S., Jolly, C.J., Tosi, A.J., Disotell, T.R., 2009. Mitochondrial evidence for the hybrid origin of the kipunji, *Rungwecebus kipunji* (Primates: Papionini). Molecular Phylogenetics and Evolution 51, 340–348.
Charpentier, M.J.E., Fontaine, M.C., Cherel, E., Renoult, J.P., Jenkins, T., Benoit, L., Barthès, N., Alberts, S.C., Tung, J., 2012. Genetic structure in a dynamic baboon hybrid zone corroborates behavioural observations in a hybrid population. Molecular Ecology 21, 715–731.
Davenport, T.R.B., Stanley, W.T., Sargis, E.J., De Luca, D.W., Mpunga, N.E., Machaga, S.J., Olson, L.E., 2006. A new genus of African monkey, *Rungwecebus*: morphology, ecology, and molecular phylogenetics. Science 312, 1378–1381.
Delson, E., 1975. Evolutionary history of the Cercopithecidae. In: Szalay, F.S. (Ed.), Approaches to Primate Paleobiology, vol. 5, pp. 167–217. Contributions to Primatology. Karger, Basel.
Delson, E., 1984. Cercopithecid biochronology of the African Plio-Pleistocene: correlation among eastern and southern hominid-bearing localities. Courier Forschungs-Institut Senckenberg 69, 199–218.
Delson, E., 1988. Chronology of South African australopith site units. In: Grine, F.E. (Ed.), Evolutionary History of the "Robust" Australopithecines. Aldine De Gruyter, New York, pp. 317–324.
Delson, E., Dean, D., 1993. Are *Papio baringensis* R. Leakey, 1969, and *P. quadratirostris* Iwamoto, 1982, species of *Papio* or *Theropithecus*? In: Jablonski, N.G. (Ed.), *Theropithecus*: The Rise and Fall of a Primate Genus. Cambridge University Press, Cambridge, pp. 157–189.
Delson, E., Napier, P.H., 1976. Request for determination of the generic names of the baboon and the mandrill (Cercopithecidae, Primates, Mammalia). Bulletin of Zoological Nomenclature 33, 46–60.
Delson, E., Napier, P.H., 1977. Comment on the request to determine the generic names of the baboon and mandrill. Bulletin of Zoological Nomenclature 33, 149.
Desmarest, A.G., 1820. Mammalogie, ou description des especes de mammifères. In: Encyclopedie Methodique. Agasse, Paris and Liège.
Dietrich, W.O., 1942. Altestquartare Saugetiere aus der sudlichen Serengeti, Deutsch-Ostafrika. Palaontographica 94, 44–75.
Disotell, T.R., 1994. Generic level relationships of the Papionini (Cercopithecoidea). American Journal of Physical Anthropology 94, 47–57.
Disotell, T.R., 2000. Molecular systematics of the Cercopithecidae. In: Whitehead, P.F., Jolly, C.J. (Eds.), Old World Monkeys. Cambridge University Press, Cambridge, pp. 29–56.
Disotell, T.R., Honeycutt, R.L., Ruvulo, M., 1992. Mitochondrial DNA phylogeny of the Old-World monkey tribe Papionini. Molecular Biology and Evolution 9, 1–13.
Eck, G.G., 1976. Cercopithecoidea from Omo Group deposits. In: Coppens, Y., Howell, F.C., Isaac, G.L., Leakey, R. (Eds.), Earliest Man and Environments in the Lake Rudolf Basin. University of Chicago Press, Chicago, pp. 332–344.
Eck, G.G., 1977. Diversity and frequency distribution of Omo Group Cercopithecoidea. Journal of Human Evolution 6, 55–63.
Eck, G.G., Jablonski, N.G., 1984. A reassessment of the taxonomic status and phyletic relationships of *Papio baringensis* and *Papio quadratirostris*. American Journal of Physical Anthropology 65, 109–134.
Eck, G.G., Jablonski, N.G., 1987. The skull of *Theropithecus brumpti* compared with those of other species of the genus *Theropithecus*. In: Coppens, Y., Howell, F.C. (Eds.), Les Faunes Plio-Pleistocenes de la Basse Vallee de l'Omo (Ethiopie), Tome

3, Cercopithecidae de la Formation Shungura. Cahiers de Paleontologie, Editions du Centre National de la Recherche Scientifique, pp. 11–122.
Eisenhart, W.L., 1974. The fossil cercopithecoids of Madapansgat and Sterkfontein. Unpublished A.B. Thesis, Harvard College.
Erxleben, J.C.P., 1777. Systema regni animalis... Classis 1, Mammalia. Weygand, Lipsiae.
Fleagle, J.G., 2013. Primate Adaptation and Evolution. Academic Press, San Diego.
Fleagle, J.G., 2014. Identifying primate species: themes and perspectives. Evolutionary Anthropology 23, 39–40.
Fleagle, J.G., McGraw, W.S., 1999. Skeletal and dental morphology supports diphyletic origin of baboons and mandrills. Proceedings of the National Academy of Sciences of the USA 96, 1157–1161.
Fleagle, J.G., McGraw, W.S., 2002. Skeletal and dental morphology of African papionins: unmasking a cryptic clade. Journal of Human Evolution 42, 267–292.
Folinsbee, K.E., Reisz, R.R., 2013. New craniodental fossils of papionin monkeys from Cooper's D, South Africa. American Journal of Physical Anthropology 151, 613–629.
Freedman, L., 1957. The fossil Cercopithecoidea of South Africa. Annals of the Transvaal Museum 23, 121–262.
Freedman, L., 1960. Some new fossil cercopithecoid specimens from Makapansgat, South Africa. Palaeontologia Africana 7, 7–45.
Freedman, L., 1961. New cercopithecoid fossils, including a new species, from Taung, Cape Province, South Africa. Annals of the South African Museum 46, 1–14.
Freedman, L., 1963. A biometric study of *Papio cynocephalus* skulls from Northern Rhodesia and Nyasaland. Journal of Mammalogy 44, 24–43.
Freedman, L., 1965. Fossil and subfossil primates from the limestone deposits at Taung, Bolt's Farm, and Witkrans, South Africa. Palaeontologia Africana 9, 19–48.
Freedman, L., 1976. South African fossil Cercopithecoidea: A re-assessment including a description of new material from Makapansgat, Sterkfontein, and Taung. Journal of Human Evolution 5, 297–310.
Freedman, L., Brain, C.K., 1977. A re-examination of the cercopithecoid fossils from Swartkrans (Mammalia: Cercopithecidae). Annals of the Transvaal Museum 30, 211–218.
Freedman, L., Stenhouse, N.S., 1972. The *Parapapio* species of Sterkfontein, Transvaal, South Africa. Palaeontologia Africana 14, 93–111.
Frost, S.R., 2001a. Fossil Cercopithecidae of the Afar Depression, Ethiopia: species systematics and comparison to the Turkana Basin. Ph.D. Dissertation, The City University of New York.
Frost, S.R., 2001b. New Early Pliocene Cercopithecidae (Mammalia: Primates) from Aramis, Middle Awash Valley, Ethiopia. American Museum Novitates 3350, 1–36.
Frost, S.R., 2007a. Fossil Cercopithecidae from the Middle Pleistocene Dawaitoli Formation, Middle Awash Valley, Afar Region, Ethiopia. American Journal of Physical Anthropology 134, 460–471.
Frost, S.R., 2007b. African Pliocene and Pleistocene cercopithecid evolution and global climatic change. In: Bobe, R., Alemseged, Z., Behrensmeyer, A.K. (Eds.), Hominin Environments in the East African Pliocene: An Assessment of the Faunal Evidence. Springer, Dordrecht, pp. 51–76.
Frost, S.R., 2014. Primates del Plio-Pleistoceno en el norte de Tanzania. In: Dominguez-Rodrigo, M., Baquedano, E. (Eds.), La Cuna de la Humanidad. Museo de la Evolución Humana, pp. 255–263. Burgos.
Frost, S.R., Alemseged, Z., 2007. Middle Pleistocene fossil Cercopithecidae from Asbole Afar Region, Ethiopia. Journal of Human Evolution 53, 227–259.
Frost, S.R., Delson, E., 2002. Fossil Cercopithecidae from the Hadar Formation and surrounding areas of the Afar Depression, Ethiopia. Journal of Human Evolution 43, 687–748.
Frost, S.R., Haile-Selassie, Y., Hlusko, L., 2009. Cercopithecidae. In: Haile-Selassie, Y., Woldegabriel, G. (Eds.), *Ardipithecus kadabba*: Late Miocene Evidence from the Middle Awash, Ethiopia. University of California Press, Berkeley, pp. 135–158.
Frost, S.R., Marcus, L.F., Bookstein, F.L., Reddy, D.P., Delson, E., 2003. Cranial allometry, phylogeography, and systematics of large-bodied papionins (Primates: Cercopithecinae) inferred from geometric morphometric analysis of landmark data. Anat Rec Part A 275A, 1048–1072.
Frost, S.R., Jablonski, N.G., Haile-Selassie, Y., 2014. Early Pliocene Cercopithecidae from Woranso-Mille (Central Afar, Ethiopia) and the origins of the *Theropithecus oswaldi* lineage. Journal of Human Evolution 76, 39–53.
Frost, S.R., Ward, C.V., Manthi, F.K., Plavcan, J.M., Cercopithecid fossils from Kanapoi, West Turkana, Kenya (2007–2015). Journal of Human Evolution. (in revision).
Gear, J.H.S., 1926. A preliminary account of the baboon remains from Taungs. South African Journal of Science 23, 731–747.
Gilbert, C.C., 2007. Craniomandibular morphology supporting the diphyletic origin of mangabeys and a new genus of the *Cercocebus/Mandrillus* clade, *Procercocebus*. Journal of Human Evolution 53, 69–102.
Gilbert, C.C., 2008. African papionin phylogenetic history and Plio-Pleistocene biogeography. Ph.D. Dissertation, Stony Brook University.
Gilbert, C.C., 2013. Cladistic analysis of extant and fossil African papionins using craniodental data. Journal of Human Evolution 64, 399–433.
Gilbert, C.C., Frost, S.F., Strait, D.S., 2009a. Allometry, sexual dimorphism, and phylogeny: a cladistic analysis of extant African papionins using craniodental data. Journal of Human Evolution 57, 298–320.
Gilbert, C.C., McGraw, W.S., Delson, E., 2009b. Plio-Pleistocene eagle predation on fossil cercopithecids from the Humpata Plateau, Southern Angola. American Journal of Physical Anthropology 139, 421–429.
Gilbert, C.C., Stanley, W.T., Olson, L.E., Davenport, T.R.B., Sargis, E.J., 2011a. Morphological systematics of the kipunji (*Rungwecebus kipunji*) and the ontogenetic development of phylogenetically informative characters in the Papionini. Journal of Human Evolution 60, 731–745.
Gilbert, C.C., Goble, E.D., Kingston, J.D., Hill, A., 2011b. Partial skeleton of *Theropithecus brumpti* (Primates, Cercopithecidae) from the Chemeron Formation of the Tugen Hills, Kenya. Journal of Human Evolution 61, 347–362.
Gilbert, C.C., Steininger, C.M., Kibii, J.M., Berger, L.R., 2015. *Papio* cranium from the hominin-bearing site of Malapa: implications for the evolution of modern baboon cranial morphology and South African Plio-Pleistocene biochronology. PLoS One 10, e0133361.
Gilbert, C.C., Frost, S.F., Delson, E., 2016a. Reassessment of Olduvai Bed I cercopithecoids: a new biochronological and biogeographical link to the South African fossil record. Journal of Human Evolution 92, 50–59.
Gilbert, C.C., Takahashi, M.Q., Delson, E., 2016b. Cercopithecoid humeri from Taung support the distinction of major papionin clades in the South African fossil record. Journal of Human Evolution 90, 88–104.
Groves, C.P., 2001. Primate Taxonomy. Smithsonian Institute Press, Washington, DC.
Groves, C.P., 2014. The species in primatology. Evolutionary Anthropology 23, 2–4.
Grubb, P., Butynski, T.M., Oates, J.F., Bearder, S.K., Disotell, T.R., Groves, C.P., Struhsaker, T.T., 2003. Assessment of the diversity of African primates. International Journal of Primatology 24, 1301–1357.
Guevara, E.E., Steiper, M.E., 2014. Molecular phylogenetic analysis of the Papionina using concatenation and species tree methods. Journal of Human Evolution 66, 18–28.
Gunz, P., Mitteroecker, P., Neubauer, S., Weber, G.W., Bookstein, F.L., 2009. Principles for the virtual reconstruction of hominin crania. Journal of Human Evolution 57, 48–62.
Guthrie, E.H., 2011. Functional morphology of the postcrainum of *Theropithecus brumpti* (Primates: Cercopithecidae). Ph.D. Dissertation, University of Oregon.
Hammer, Ø., Harper, D.A.T., Ryan, P.D., 2001. PAST: Paleontological Statistics software package for education and data analysis. Palaeontologia Electronica 4, 9.
Harris, E.E., Disotell, T.R., 1998. Nuclear gene trees and the phylogenetic relationships of the mangabeys (Primates: Papionini). Molecular Biology and Evolution 15, 892–900.
Harris, J.M., Brown, F.H., Leakey, M.G., 1988. Stratigraphy and paleontology of Pliocene and Pleistocene localities west of Lake Turkana, Kenya. Contributions in Science 399, 1–128.
Harris, J.M., Leakey, M.G., Cerling, T.E., 2003. Early Pliocene tetrapod remains from Kanapoi, Lake Turkana Basin, Kenya. In: Harris, J.M., Leakey, M.G. (Eds.), Geology and Vertebrate Paleontology of the Early Pliocene Site of Kanapoi, Northern Kenya, pp. 39–113. Contributions in Science, Number 498. Natural History Museum of Los Angeles County.
Harrison, T., 1989. New postcranial remains of *Victoriapithecus* from the middle Miocene of Kenya. Journal of Human Evolution 18, 3–54.
Harrison, T., 2011. Cercopithecids (Cercopihtecidae, Primates). In: Harrison, T. (Ed.), Paleontology and Geology of Laetoli: Human Evolution in Context, vol. 2. Fossil Hominins and the Associated Fauna. Springer, Dordrecht, pp. 83–139.
Harrison, T., Harris, E.E., 1996. Plio-Pleistocene cercopithecids from Kanam East, western Kenya. Journal of Human Evolution 30, 539–561.
Haughton, R.H., 1925. Demonstration (of Taung fossils). Transactions of the Royal Society of South Africa 12 lxviii.
Heaton, J.L., 2006. Taxonomy of the Sterkfontein fossil Cercopithecinae: the Papionini of Members 2 and 4 (Gauteng, South Africa). Ph.D. Dissertation, Indiana University.
Herries, A.I.R., Kappen, P., Kegley, A.D.T., Patterson, D., Howard, D.L., de Jonge, M.D., Potze, S., Adams, J.W., 2014. Palaeomagnetic and synchrotron analysis of >1.95 Ma fossil-bearing palaeokarst at Haasgat, South Africa. South African Journal of Science 110, 1–12.
Hill, W.C.O., 1967. Taxonomy of the baboon. In: Vagtborg, H. (Ed.), The Baboon in Medical Research, vol. 2. University of Texas Press, Austin, pp. 4–11.
International Commission for Zoological Nomenclature, 1982. Opinion 1199. *Papio* Erxleben, 1777 and *Mandrillus* Ritgen, 1824 (Mammalia, Primates): Designation of type species. Bulletin of Zoological Nomenclature 39, 15–18.
Iwamoto, M., 1982. A fossil baboon skull from the lower Omo basin, southwestern Ethiopia. Primates 23, 533–541.
Jablonski, N.G., 1994. New fossil cercopithecid remains from the Humpata Plateau, southern Angola. American Journal of Physical Anthropology 94, 435–464.
Jablonski, N.G., 2002. Fossil Old World monkeys: the late Neogene radiation. In: Hartwig, W.C. (Ed.), The Primate Fossil Record. Cambridge University Press, Cambridge, pp. 255–299.
Jablonski, N.G., Frost, S.R., 2010. Cercopithecoidea. In: Werdelin, L., Sanders, W.J. (Eds.), The Cenozoic Mammals of Africa. University of California Press, Oakland, pp. 393–428.
Jablonski, N.G., Leakey, M.G., Anton, M., 2008. Systematic paleontology of the cercopithecines. In: Jablonski, N.G., Leakey, M.G. (Eds.), Koobi Fora Research Project, vol. 6. The Fossil Monkeys. California Academy of Sciences, San Francisco, pp. 103–300.
Jolly, C.J., 1965. The origins and specialisations of the long-faced Cercopithecoidea. Ph.D. thesis, University of London.
Jolly, C.J., 1967. The evolution of the baboons. In: Vagtborg, H. (Ed.), The Baboon in Medical Research, vol. 2. University of Texas Press, Austin, pp. 23–50.
Jolly, C.J., 1993. Species, subspecies, and baboon systematics. In: Kimbel, W.H., Martin, L.B. (Eds.), Species, Species Concepts, and Primate Evolution. Plenum Press, New York, pp. 67–107.
Jolly, C.J., 2001. A proper study for mankind: Analogies from the papionin monkeys and their implications for human evolution. Yearbook of Physical Anthropology 44, 177–204.

Jolly, C.J., 2003. Cranial anatomy and baboon diversity. The Anatomical Record 275A, 1043–1047.
Jolly, C.J., 2014. A Darwinian species definition and its implications. Evolutionary Anthropology 23, 36–38.
Jolly, C.J., Brett, F.L., 1973. Genetic markers and baboon biology. Journal of Medical Primatology 2, 85–99.
Jolly, C.J., Burrell, A.S., Phillips-Conroy, J.E., Bergey, C., Rogers, J., 2011. Kinda baboons (*Papio kindae*) and grayfoot chacma baboons (*P. ursinus griseipes*) hybridize in the Kafue river valley, Zambia. American Journal of Primatology 73, 291–303.
Jones, T., Ehardt, C.L., Butynski, T.M., Davenport, T.R.B., Mpunga, N.E., Machaga, S.J., De Luca, D.W., 2005. The highland mangabey *Lophocebus kipunji*: a new species of African monkey. Science 308, 1161–1164.
Jones, T.R., 1937. A new fossil primate from Sterkfontein, Krugersdorp, Transvaal. South African Journal of Science 33, 709–728.
Jonstonus, J., 1650. Historiae Naturalis de Quadeupedibus. Ioannem Iacobi Fil, 1657 ed. Schipper, Amstelodami.
Kalb, J.E., Jolly, C.J., Tebedge, S., Mebrate, A., Smart, C., Oswald, E.B., Whitehead, P.F., Wood, C.B., Adefris, T., Rawn-Schatzinger, V., 1982. Vertebrate faunas from the Awash Group, Middle Awash Valley, Afar, Ethiopia. Journal of Vertebrate Paleontology 2, 237–258.
Keyser, A.W., 2000. The Drimolen skull: the most complete australopithecine cranium and mandible to date. South African Journal of Science 96, 189–197.
Kuman, K., Clarke, R.J., 2000. Stratigraphy, artifact industries, and hominid associations for Sterkfontein, Member 5. Journal of Human Evolution 38, 827–847.
Lacruz, R.S., Brink, J.S., Hancox, P.J., Skinner, A.R., Herries, A., Schmid, P., Berger, L.R., 2002. Palaeontology and geological context of a Middle Pleistocene faunal assemblage from the Gladysvale Cave, South Africa. Palaeontologia Africana 38, 99–114.
Leakey, M.D., 1971. Discovery of post-cranial remains of *Homo erectus* and associated artefacts in Bed IV at Olduvai Gorge, Tanzania. Nature 232, 380–383.
Leakey, M.G., Delson, E., 1987. Fossil Cercopithecidae from the Laetoli beds. In: Leakey, M.D., Harris, J.M. (Eds.), Laetoli: A Pliocene Site in Northern Tanzania. Clarendon Press, Oxford, pp. 91–107.
Leakey, M.G., Leakey, R.E.F., 1976. Further Cercopithecinae (Mammalia: Primates) from the Plio-Pleistocene of East Africa. Fossil Vertebrates of Africa 4, 121–146.
Leakey, M.G., Teaford, M.F., Ward, C.V., 2003. Cercopithecidae from Lothagam. In: Leakey, M.G., Harris, J.M. (Eds.), Lothagam: The Dawn of Humanity in Eastern Africa. Columbia University Press, New York, pp. 201–248.
Leakey, R.E.F., 1969. New Cercopithecidae from the Chemeron Beds of Lake Baringo, Kenya. Fossil Vertebrates of Africa 1, 53–69.
Leigh, S.R., 2006. Cranial ontogeny of *Papio* baboons (*Papio hamadryas*). American Journal of Physical Anthropology 130, 71–84.
Linnaeus, C., 1758. Systema naturae per regna tria naturae, secundum classes, ordines genera, species cum characteribus, differentris, synonymis, locis, tenth ed. Laurentii Salvii, Stockholm.
Linnaeus, C., 1766. Systema naturae per regna tria naturae, secundum classes, ordines genera, species cum characteribus, differentris, synonymis, locis, twelfth ed. Laurentii Salvii, Stockholm.
Louis, E.E., Lei, R., 2014. Defining species in an advanced technological landscape. Evolutionary Anthropology 23, 18–20.
Maier, W., 1970. New fossil Cercopithecoidea from the lower Pleistocene cave deposits of the Makapansgat Limeworks, South Africa. Palaeontologia Africana 13, 69–107.
Maier, W., 1972. The first complete skull of *Simopithecus darti* from Makapansgat, South Africa, and its systematic position. Journal of Human Evolution 1, 395–400.
Manly, B.F.J., 1994. Multivariate Statistical Methods: A Primer, second ed. Chapman & Hall, Boca Raton, FL.
McKee, J.K., 1993. Taxonomic and evolutionary affinities of *Papio izodi* fossils from Taung and Sterkfontein. Palaeontologia Africana 30, 43–49.
McKee, J.K., Keyser, A.W., 1994. Craniodental remains of *Papio angusticeps* from the Haasgat, South Africa. International Journal of Primatology 15, 823–841.
McKee, J.K., Thackeray, J.F., Berger, L.R., 1995. Faunal assemblage seriation of Southern African Pliocene and Pleistocene fossil deposits. American Journal of Physical Anthropology 96, 235–250.
Morris, D., 2013. Monkey. Reaktion Books Ltd., London.
Müller, P.L.S., 1773. Des Ritters Carl von Linné koniglich Schwedischen Leibartes, vollstandiges Natursystem nach der zwölften Luteinischen Ausgabe und nach Antleitung de Hollandischen Houttuynishen Werks mit einer ausfuhrlichen Erklärung, vol. 1. G. N. Raspe, Nürnberg.
Napier, P.H., 1981. Catalogue of Primates in the British Museum (Natural History) and elsewhere in the British Isles, Part II: Family Cercopithecinae, Subfamily Cercopithecinae. British Museum (Natural History), London.
Neff, W.A., Marcus, L.F., 1980. A Survey of Multivariate Methods for Systematics. American Society of Mammalogists. American Museum of Natural History, New York.
Newman, T.K., Jolly, C.J., Rogers, J., 2004. Mitochondrial phylogeny and systematics of baboons (*Papio*). American Journal of Physical Anthropology 124, 17–27.
Olson, L.E., Sargis, E.J., Stanley, W.T., Hildebrandt, K.B.P., Davenport, T.R.B., 2008. Additional molecular evidence strongly supports the distinction between the recently described African primate *Rungwecebus kipunji* (Cercopithecidae, Papionini) and *Lophocebus*. Molecular Phylogenetics and Evolution 48, 789–794.
Perelman, P., Johnson, W.E., Roos, C., Seuánez, H.N., Horvath, J.E., Moreira, M.A.M., Kessing, B., Pontius, J., Roelke, M., Rumpler, Y., Schneider, M.P.C., Silva, A., O'Brien, S.J., Pecon-Slattery, J., 2011. A Molecular phylogeny of living primates. PLoS Genetics 7, e1001342.
Pickering, R., Hancox, P.J., Lee-Thorp, J.A., Grun, R., Mortimer, G.E., McCulloch, M., Berger, L.R., 2007. Stratigraphy, U-Th chronology, and paleoenvironments at Gladysvale Cave: insights into the climatic control of South African hominin-bearing cave deposits. Journal of Human Evolution 53, 602–619.
Pickering, T.R., Clarke, R.J., Heaton, J.L., 2004. The context of Stw 573, an early hominid skull and skeleton from Sterkfontein Member 2: taphonomy and paleoenvironment. Journal of Human Evolution 46, 279–297.
Pugh, K.D., Gilbert, C.C., in press. Phylogenetic relationships of living and fossil African papionins: combined evidence from morphology and molecules. Journal of Human Evolution.
Remane, A., 1925. Der Fossile Pavian (*Papio* Sp.) von Oldoway nebst Bemerkungen über die Gattung *Simopithecus* C. W. Andrews. In: Reck, H. (Ed.), Wissenschaftliche Ergebnisse der Oldoway-Expedition 1913, vol. 2, pp. 83–90. Borntraeger, Leipzig.
Rohlf, F.J., Slice, D.E., 1990. Extensions of the Procrustes method for the optimal superimposition of landmarks. Systematic Zoology 39, 40–59.
Roberts, T., Davenport, T.R.B., Hildebrandt, K.B.P., Jones, T., Stanley, W.T., Sargis, E.J., Olson, L.E., 2010. The biogeography of introgression in the critically endangered African monkey *Rungwecebus kipunji*. Biology Letters 6, 233–237.
Rylands, A.B., Mittermeier, R.A., 2014. Primate taxonomy: species and conservation. Evolutionary Anthropology 23, 8–10.
Silcox, M.T., 2014. A pragmatic approach to the species problem from a paleontological perspective. Evolutionary Anthropology 23, 24–26.
Singleton, M., 2002. Patterns of cranial shape variation in the Papionini (Primates: Cercopithecinae). Journal of Human Evolution 42, 547–578.
Singleton, M., 2009. The phenetic affinities of *Rungwecebus kipunji*. Journal of Human Evolution 56, 25–42.
Singleton, M., McNulty, K.P., Frost, S.R., Soderberg, J., Guthrie, E., 2010. Bringing up baby: developmental simulation of the adult cranial morphology of *Rungwecebus kipunji*. The Anatomical Record 293, 388–401.
Slice, D.E., 2013. Morpheus, Java Edition. Department of Scientific Computing. The Florida State University, Tallahassee, Florida, U.S.A. Available from: http://morphlab.sc.fsu.edu/.
Springer, M.S., Meredith, R.W., Gatesy, J., Emerlin, C.A., Park, J., Rabosky, D.L., Stadler, T., Steiner, C., Ryder, O.A., Janecka, J.E., Fisher, C.A., Murphy, W.J., 2012. Macroevolutionary dynamics and historical biogeography of primate diversification inferred from a species supermatrix. PLoS One 7, e49521.
Swofford, D.L., 2003. PAUP*. Phylogenetic Analysis Using Parsimony (*and Other Methods). Version 4.10b. Sinauer Associates, Sunderland, Massachusetts.
Szalay, F.S., Delson, E., 1979. Evolutionary History of the Primates. Academic Press, New York.
Tattersall, I., 2014. Recognizing species, past and present. Evolutionary Anthropology 23, 5–7.
Thorington, R.W., Groves, C.P., 1970. An annotated classification of the Cercopithecoidea. In: Napier, J.R., Napier, P.H. (Eds.), Old World Monkeys: Evolution, Systematics, and Behavior. Academic Press, New York, pp. 629–647.
Tosi, A.J., Morales, J.C., Melnick, D.J., 1999. Y-chromosome phylogeny of the macaques (Cercopithecidae: *Macaca*). American Journal of Physical Anthropology 28(Suppl), 266.
Tosi, A.J., Disotell, T.R., Morales, J.C., Melnick, D.J., 2003. Cercopithecine Y-chromosome data provide a test of competing morphological evolutionary hypotheses. Molecular Phylogenetics and Evolution 27, 510–521.
Tung, J., Barreiro, L.B., 2017. The contribution of admixture to primate evolution. Current Opinion in Genetics and Development 47, 61–68.
Wildman, D.E., Bergman, T.J., al-Aghbari, A., Sterner, K.N., Newman, T.K., Phillips-Conroy, J.E., Jolly, C.J., 2004. Mitochondrial evidence for the origin of hamadryas baboons. Molecular Phylogenetics and Evolution 32, 287–296.
Williams, B.A., Ross, C.F., Frost, S.R., Waddle, D.M., Gabadirwe, M., Brooks, G.A., 2012. Fossil *Papio* cranium from !Ncumtsa (Koanaka) Western Ngamiland, Botswana. American Journal of Physical Anthropology 149, 1–17.
Williams, S.A., 2012. Variation in anthropoid vertebral formulae: implications for homology and homoplasy in hominoid evolution. Journal of Experimental Zoology Part B 318, 134–147.
Yoder, A.D., 2014. Gene flow happens. Evolutionary Anthropology 23, 15–17.
Zimmerman, E., Radespiel, U., 2014. Species concepts, diversity, and evolution in primates: lessons to be learned from mouse lemurs. Evolutionary Anthropology 23, 11–14.
Zinner, D., Arnold, M.L., Roos, C., 2009. Is the new primate genus *Rungwecebus* a baboon? PLoS One 4, e4859.
Zinner, D., Buba, U., Nash, S., Roos, C., 2011. Pan-African voyagers: the phylogeography of baboons. In: Sommer, V., Ross, C. (Eds.), Primates of Gashaka: Socioecology and Conservation in Nigeria's Biodiversity Hotspot. Springer, New York, pp. 319–358.
Zinner, D., Roos, C., 2014. So what is a species anyway? A primatological perspective. Evolutionary Anthropology 23, 21–23.
Zinner, D., Wertheimer, J., Liedigk, R., Groeneveld, L.F., Roos, C., 2013. Baboon phylogeny as inferred from complete mitochondrial genomes. American Journal of Physical Anthropology 150, 133–140.
Zinner, D., Chuma, I.S., Knauf, S., Roos, C., 2018. Inverted intergeneric introgression between critically endangered kipunjis and yellow baboons in two disjunct populations. Biology Letters 14, 20170729.